Identification and functional characterization of hypoxia-induced endoplasmic reticulum stress regulating lncRNA (HypERlnc) in pericytes

Bischoff F.C., Werner A., John D., Boeckel J.-N., Melissari M.-T., Grote P., Glaser S.F., Demolli S., Uchida S., Michalik K.M., Meder B., Katus H.A., Haas J., Chen W., Pullamsetti S.S., Seeger W., Zeiher A.M., Dimmeler S., Zehendner C.M.

Circulation Research
2017 AUG 04 ; 121(4): 368-375
2017 JUN 13 (first published online)
doi: 10.1161/CIRCRESAHA.116.310531

Publisher: American Heart Association

SHORT COMMUNICATION

Identification and Functional Characterization of Hypoxia-Induced Endoplasmic Reticulum Stress Regulating lncRNA (HypERlnc) in Pericytes

Florian C Bischoff[1,2,4], Astrid Werner[1,2], David John[1,4], Jes-Niels Boeckel[3,4], Maria-Theodora Melissari[1], Phillip Grote[1], Simone F Glaser[1,2], Shemsi Demolli[1,4], Shizuka Uchida[1,4,5], Katharina M Michalik[1], Benjamin Meder[3,4], Hugo A Katus[3,4], Jan Haas[3,4], Wei Chen[4,6,7], Soni S Pullamsetti[8,9], Werner Seeger[8,9], Andreas M Zeiher[2,4], Stefanie Dimmeler[1,4], Christoph M Zehendner[1,2,4]

[1]Institute for Cardiovascular Regeneration, Centre of Molecular Medicine, Goethe University Frankfurt am Main, Germany; [2]ZIM III, Department of Cardiology, Goethe University, Frankfurt am Main, Germany; [3]Department of Internal Medicine III, University of Heidelberg, Germany [4]DZHK (Deutsches Zentrum für Herz-Kreislaufforschung); [5] Cardiovascular Innovation Institute, University of Louisville, Louisville, Kentucky, United States; [6]Laboratory for Novel sequencing technology, Functional and Medical Genomics, Berlin Institute for Medical Systems Biology, Max-Delbrück-Centrum für Molekulare Medizin, Berlin, Germany; [7]Department of Biology, Southern University of Science and Technology, Shenzhen, China; [8]Max Planck Institute for Heart and Lung Research, Department of Lung Development and Remodeling, member of the German Center for Lung Research (DZL), Bad Nauheim, Germany; [9]Department of Internal Medicine, Universities of Giessen and Marburg Lung Center (UGMLC), member of the DZL, Justus Liebig University, Giessen, Germany.

Running title: lncRNA HypERlnc Regulates Pericyte Function

Subject Terms:

Basic Science Research
Smooth Muscle Proliferation and Differentiation
Vascular Biology
Translational Studies
Ischemia

Address correspondence to:

Dr. Stefanie Dimmeler
Theodor Stern Kai 7
60590 Frankfurt am Main
Phone: ±49-69-6301-6667
Fax: ±49-69-6301-83462
dimmeler@em.uni-frankfurt.de

Christoph M. Zehendner
Theodor Stern Kai 7
60590 Frankfurt am Main
Phone: ±49-69-6301-6667
Fax: ±49-69-6301-83462
Christoph.Zehendner@gmail.com

This manuscript was sent to Brian H. Annex, Consulting Editor, for review by expert referees, editorial decision, and final disposition.

In May 2017, the average time from submission to first decision for all original research papers submitted to *Circulation Research* was 12.28 days.

ABSTRACT

***Rationale*:** Pericytes are essential for vessel maturation and endothelial barrier function. Long non-coding RNAs (lncRNAs) regulate many cellular functions, but their role in pericyte biology remains unexplored.

***Objective*:** Here we investigate the effect of Hypoxia-Induced Endoplasmic Reticulum Stress Regulating lncRNA (HypERlnc, also known as ENSG00000262454) on pericyte function in vitro and its regulation in human heart failure and idiopathic pulmonary arterial hypertension.

***Methods and Results*:** RNA sequencing in human primary pericytes (hPCs) identified hypoxia regulated lncRNAs, including HypERlnc. Silencing of HypERlnc decreased cell viability, proliferation and resulted in pericyte de-differentiation, which went along with increased endothelial permeability in co-cultures consisting of hPC and human coronary microvascular endothelial cells. Consistently, Cas9-based transcriptional activation of HypERlnc was associated with increased expression of pericyte marker genes. Moreover, HypERlnc knockdown reduced endothelial-hPC recruitment in matrigel assays ($P<0.05$). Mechanistically, transcription factor reporter arrays demonstrated that endoplasmic reticulum stress related transcription factors were prominently activated upon HypERlnc knockdown, which was confirmed via immunoblotting for the endoplasmic reticulum stress markers IRE1α ($P<0.001$), ATF6 ($P<0.01$) and soluble BiP ($P<0.001$). Kyoto encyclopedia of genes and gene ontology pathway analyses of RNA sequencing experiments following HypERlnc knockdown indicate a role in cardiovascular disease states. Indeed, HypERlnc expression was significantly reduced in human cardiac tissue from heart failure patients ($P<0.05$, $n=19$) compared to controls. In addition, HypERlnc expression significantly correlated with pericyte markers in human lungs derived from patients diagnosed with idiopathic pulmonary arterial hypertension and from donor lungs ($n=14$).

***Conclusion*:** Here we show that HypERlnc regulates human pericyte function and the endoplasmic reticulum stress response. In addition, RNA sequencing analyses in conjunction with reduced expression of HypERlnc in heart failure and correlation with pericyte markers in idiopathic pulmonary arterial hypertension indicate a role of HypERlnc in human cardiopulmonary disease.

Keywords:
Pericytes, long non-coding RNAs, cardiac disease, pulmonary heart disease, ER stress, cardiovascular disease, vascular biology.

Nonstandard Abbreviations and Acronyms:

ARV	Arrhythmogenic right ventricular cardiomyopathy
DTT	Dithiothreitol
ER	Endoplasmic reticulum
FPKM	Frames per kilobases mapped per million
GO	Gene ontology
HCMEC	Human coronary microvascular endothelial cells
HF	Heart Failure
hPC	Human pericytes
HUVEC	Human umbilical vein endothelial cells
HypERlnc	Hypoxia-Induced Endoplasmic Reticulum Stress Regulating lncRNA
IPAH	Idiopathic pulmonary arterial hypertension
KEGG	Kyoto Encyclopedia of Genes
lncRNA	Long non-coding RNA
poly A	Polyadenylated
PDGF	Platelet-derived growth factor
PDGFRβ	Platelet-derived growth factor receptor β
RNA-FISH	RNA-fluorescent in situ hybridization
RNA-seq	RNA sequencing
RT-qPCR	Reverse transcription quantitative polymerase chain reaction
Stauro	Staurosporine
TF	Transcription factor
UPR	Unfolded protein response
VSMC	Vascular smooth muscle cells

INTRODUCTION

Pericytes are perivascular mural cells that contribute to endothelial maturation and vessel stability at the level of the microvasculature[1]. Pericyte recruitment towards the vessel wall is mainly driven by the platelet-derived growth factor (PDGF) signaling axis[1,2]. In vivo, a block of PDGF signaling results in pericyte death and impaired pericyte recruitment towards endothelial cells resulting in endothelial dysfunction, including endothelial barrier breakdown[3]. These events facilitate extravasation of macromolecules with subsequent inflammation and organ remodeling. In organ injury and fibrotic disease, pericytes may hyper-proliferate and contribute to wound healing and organ remodeling[4,5]. Despite their important role within the cardiovascular system and various disease states such as idiopathic pulmonary arterial hypertension (IPAH)[6], molecular mechanisms that control human pericyte (hPC) survival and differentiation are poorly understood.

Long non-coding RNAs (lncRNAs) represent a large proportion of the non-coding transcriptome[7] and act by various mechanisms that affect transcriptional and epigenetic control of gene expression. In addition, it is well documented that lncRNAs can regulate posttranscriptional processes such as splicing[8]. Previous studies have shown a regulatory role of lncRNAs in endothelial and smooth muscle cells. For example lncRNA MALAT1 has been shown to regulate endothelial cell function[9] whereas lncRNA SENCR has been demonstrated to stabilize the smooth muscle cell contractile phenotype[10]. Recent experimental work has outlined the importance of lncRNAs in modulating clinically relevant processes such as cholesterol synthesis[11] and cardiac hypertrophy[12], making them promising molecular targets in cardiovascular disease. However, the contribution of lncRNAs to hPC function is yet unclear.

Here we show that the previously uncharacterized Hypoxia-Induced Endoplasmic Reticulum Stress Regulating lncRNA (HypERlnc) controls hPC function and propose a role for HypERlnc in disease states such as human heart failure (HF) and idiopathic pulmonary arterial hypertension.

METHODS

Please see online supplement.

RESULTS

Characterization of human pericytes.

RNA sequencing (RNA-seq) of hPC in normoxic and hypoxic conditions demonstrates robust expression of pericyte markers (e.g. PDGFRβ and NG2), which was confirmed by immunoblotting (Online Figure I). In addition, hPC formed functional intercellular junctions as indicated by intercellular dye transfer live cell imaging experiments with HUVEC (Online Figure II), suggesting that the cells in the present study are indeed pericytes[13].

HypERlnc is induced by hypoxia and is expressed in the nucleus and cytosol of human pericytes.

In order to detect regulatory lncRNAs in hPC, they were subjected to 24 hours of hypoxia followed by RNA-seq. Along with known hypoxia regulated transcripts (e.g. H19 and MIR210HG[14] (Figure 1A), we found that lncRNA HypERlnc was upregulated by hypoxia which was validated by RT-qPCR (Figure 1B). Figure 1C demonstrates HypERlnc read coverage under normoxic and hypoxic conditions. Average cycle threshold values for HypERlnc under normoxia were 25.5 and 24.8 under hypoxic conditions, documenting robust expression of the transcript.

Gene expression pattern analyses demonstrate that HypERlnc is expressed in most human organ systems (Online Figure III). Given that not all lncRNAs own poly A tails[15], RT-qPCR in poly A^+ enriched RNA fractions was conducted. Here we found that HypERlnc is polyadenylated (Figure 1D). Since lncRNA function is dependent on subcellular localization, we performed RNA-fluorescent in situ hybridization (RNA-FISH), demonstrating that HypERlnc is present in the nucleus as well as in the cytosol of the cell (Figure 1E). Furthermore, RT-qPCR in cytosolic and nuclear fractions indicates that HypERlnc is enriched in the nucleus under both normoxic and hypoxic conditions (Figure 1F).

To evaluate whether HypERlnc is conserved in mice, we performed RNA-seq in primary mouse brain pericytes under normoxic and hypoxic conditions. As the conservation across species is sparse for lncRNAs[21], we only found 13 commonly annotated lncRNAs in human and mouse pericytes (Online Figure IVA-C). However, we found a robust read coverage at the locus that is conserved between the neighboring genes MKL2 and PARN. Murine HypERlnc expression was validated by RT-PCR, suggesting that a murine HypERlnc orthologue is expressed in mouse pericytes (Online Figure IVD-F).

HypERlnc knockdown results in pericyte de-differentiation and loss of pericyte function.

LNA GapmeR mediated HypERlnc knockdown (Figure 2A) resulted in a downregulation of the pericyte markers PDGFRβ, αSMA, Desmin, and NG2 (Figure 2B-E), which was confirmed using siRNAs directed against HypERlnc (Online Figure V). Likewise, in HypERlnc gain of function experiments using

RNA guided gene activation, the expression of HypERlnc significantly correlated with the expressions of respective pericyte markers, pointing towards an important role of HypERlnc in pericyte differentiation (Figure 2F-J). Since pericyte differentiation is important for proper pericyte function, we hypothesized that HypERlnc knockdown impairs the capability of pericytes to induce endothelial barrier function. HypERlnc knockdown in hPC in a co-culture model of hPC and human coronary microvascular endothelial cells (HCMEC) significantly increased permeability for macromolecules compared to control (Figure 3A,B). Next, we studied the impact of HypERlnc knockdown on pericyte recruitment towards endothelial cells because endothelial pericyte recruitment is known to be required for proper endothelial barrier function[3]. Upon HypERlnc silencing, hPC recruitment towards HCMEC was significantly reduced in matrigel co-culture assays (Figure 3C,D). To address whether impairment of pericyte differentiation and recruitment was associated with a loss of viable pericytes or altered pericyte proliferation, we analyzed cell viability and proliferation following HypERlnc knockdown. Here we found a significant reduction in hPC viability (Figure 3E, Online Figure VIA) and Ki67 staining (Figure 3F-G). We did not detect enhanced apoptosis, autophagy and necrosis upon HypERlnc knockdown (Figure 3H, Online Figure VIB-E).

HypERlnc knockdown induces ER stress.

Since HypERlnc is also present in the nucleus, we tested the hypothesis that HypERlnc regulates transcription factor (TF) activity, which is a known molecular mechanism of lncRNAs[8]. Using TF activity luciferase reporter assays upon HypERlnc knockdown, we found increased activity of CBF/NF-Y/YY1 and ATF6 (Figure 4A); both of which are known to be involved in the cellular ER Stress response pathway[16,17]. Induction of ER stress was confirmed by enhanced expression of ER stress markers such as IRE1α, soluble BiP and ATF6 (50kDa) following HypERlnc knockdown at protein level (Figure 4B-D, Online Figure VII). Interestingly, induction of ER stress significantly lowered HypERlnc levels and induced pericyte de-differentiation, indicating a regulatory feedback role between the ER stress response and HypERlnc expression that affects pericyte function (Online Figure VII).

HypERlnc expression in cardiopulmonary disease.

To determine the impact of HypERlnc on gene regulatory pathways, we performed RNA-seq in hPC upon HypERlnc knockdown with subsequent analyses of Gene Ontology (GO) (**Online Figure VIII,** Online Table V) and Kyoto Encyclopedia of Genes (KEGG) terms. Strikingly, KEGG analysis revealed that genes involved in several cardiovascular disease states and in vascular smooth muscle cell (VSMC) contractility are significantly upregulated (Figure 4E, Online Table VI).

Cardiac disease states, including heart failure, are known to go along with enhanced ER stress[18]. In order to address the question whether HypERlnc is regulated in human cardiovascular disease, we measured HypERlnc expression in the left ventricular myocardium of patients diagnosed with heart failure. HypERlnc was significantly reduced compared to healthy controls (Figure 4F,G), corroborating a role of HypERlnc in human cardiovascular disease. We additionally addressed whether HypERlnc is associated with pericyte marker expression in disease states that go along with altered pericyte and VSMC function such as IPAH[6]. While there was no significant difference in HypERlnc levels between healthy donors and IPAH lungs, we found that HypERlnc significantly correlates with pericyte markers in healthy and diseased human lungs (Online Figure IX).

DISCUSSION

Here we characterize the expression and function of HypERlnc in human pericytes and demonstrate that HypERlnc is de-regulated in human heart failure and correlates with pericyte marker expression in human lung disease. We show that hypoxia-regulated HypERlnc exerts biologically relevant functions in pericytes by modulating pericyte differentiation, proliferation and recruitment towards endothelial cells. Mechanistically, loss of HypERlnc resulted in enhanced ER stress. Interestingly, ER stress has been proposed to play a major role in cardiovascular pathology and ageing[18–20]. For example, it has recently been shown that the histone deacetylase sirtuin 1 is cardioprotective by reducing ER stress in cardiac myocytes, thereby inhibiting apoptosis[20]. Moreover, it has been documented that pharmacological inhibition of ER stress in hypertensive mice reduces cardiac injury and results in improved endothelium-dependent relaxation in the aorta[21]. So far, only few lncRNAs have been shown to be associated with the unfolded protein response (UPR)[22–24]. Kato et al. recently demonstrated that lnc-MGC, which is induced by ER stress, is upregulated in a mouse model of diabetic nephropathy[22]. In addition, some studies have shown that lncRNAs influence the UPR. Overexpression of lncRNA MEG3 has been documented to induce ER stress markers (e.g. IRE1α) and also induces apoptosis in human hepatoma cells[23], whereas gain of function of lncRNA TUG1 partly blocked ER stress pathways and was organ protective in a model of cold-induced liver injury in mice[24]. ER stress affects multiple cellular processes and may result in adaptive or pro-apoptotic pathways[16]. We found a significant upregulation of IRE1α that is known to affect both respective pathways in the UPR and is an ER stress sensor in all eukaryotic cells[25].

However, we were not able to detect enhanced apoptosis, autophagy and necrosis in human pericytes following HypERlnc knockdown using LNA GapmeRs as well as siRNAs. Human pericytes demonstrated cellular de-differentiation in HypERlnc loss of function experiments, which is one of the known physiological effects of UPR[26].

These results point towards an adaptive UPR response in pericytes following HypERlnc knockdown. This observation is particularly of importance since we silenced HypERlnc using LNA GapmeRs, which may cause apoptosis due to unspecific off-target effects[27]. Since we did not observe enhanced apoptosis in our experimental setting, we conclude that enhanced ER stress is not caused by a non-specific toxic effect of LNA GapmeRs. In addition, an induction of ER stress resulted in downregulation of HypERlnc and pericyte de-differentiation, indicating a regulatory feedback loop between ER stress level and HypERlnc expression. We argue that the cellular mechanism for the observed loss of cell viability following HypERlnc knockdown is mediated by a decrease in proliferation. We found that HypERlnc loss significantly downregulates the PDGFRβ which is a tyrosine kinase receptor that is crucial for pericyte proliferation and recruitment[1,2].

However, we are aware that the exact mechanism by which HypERlnc loss mediates enhanced ER stress is currently unknown and will need further mechanistic investigation.

With regard to our data on impairment of pericyte proliferation and recruitment towards endothelial cells as well as impaired coronary endothelial barrier function upon HypERlnc knockdown, recent experimental data from myocardial infarction in mice have shown that FOXO4 dependent coronary endothelial barrier breakdown facilitates the migration of inflammatory cells into the myocardial parenchyma, thereby fostering tissue injury[28]. LncRNAs in pericytes may therefore be of clinical relevance in cardiac injury. Moreover, our data on ER stress as well as GO and KEGG analyses upon HypERlnc knockdown and reduced expression of HypERlnc in human heart failure samples corroborate a potential role of HypERlnc in cardiac disease. Furthermore, the clinical relevance of HypERlnc is supported by our findings that HypERlnc significantly correlates with pericyte marker expression in disease states that go along with altered pericyte and VSMC function such as IPAH[6]. Further in vivo studies would be desirable to dissect HypERlnc function in disease models such as myocardial infarction or transaortic constriction.

However, lncRNA conservation across species is sparse. Particularly the gene loci of mouse lncRNA orthologues lack sequence homology, which makes it difficult to draw a conclusion from mouse data towards human cells and vice versa. Our RNA-seq analyses from mouse pericytes demonstrate a potential mouse orthologue. It will be interesting to develop silencing strategies and study the role of murine HypERlnc in vivo.

In conclusion, our results outline that HypERlnc significantly regulates human pericyte function and may have a role in human cardiopulmonary disease.

ACKNOWLEDGMENTS
We thank Natascha Wilker and Ariane Fischer for excellent technical assistance.

SOURCES OF FUNDING
CMZ: Goethe University Startup Grant, ECCPS (DFG), LOEWE Center for Cell and Gene Therapy (State of Hessen), and the German Center for Cardiovascular Research (DZHK). FB: DFG scholarship (SFB834). SU: LOEWE Center for Cell and Gene Therapy (State of Hessen), DFG (UC 67/2-1; SFB834), and the German Center for Cardiovascular Research (DZHK). SD: ERC grant "Angiolnc" and SFB903 (DFG).

DISCLOSURES
AMZ, CMZ, SD applied for patents related to lncRNAs in pericytes.

REFERENCES

1. Lindahl P. Pericyte Loss and Microaneurysm Formation in PDGF-B-Deficient Mice. *Science*. 1997;277:242–245.
2. Bjarnegård M, Enge M, Norlin J, Gustafsdottir S, Fredriksson S, Abramsson A, Takemoto M, Gustafsson E, Fässler R, Betsholtz C. Endothelium-specific ablation of PDGFB leads to pericyte loss and glomerular, cardiac and placental abnormalities. *Development*. 2004;131:1847.
3. Armulik A, Genové G, Mäe M, Nisancioglu MH, Wallgard E, Niaudet C, He L, Norlin J, Lindblom P, Strittmatter K, Johansson BR, Betsholtz C. Pericytes regulate the blood–brain barrier. *Nature*. 2010;468:557–561.
4. Goritz C, Dias DO, Tomilin N, Barbacid M, Shupliakov O, Frisen J. A Pericyte Origin of Spinal Cord Scar Tissue. *Science*. 2011;333:238–242.
5. Zehendner CM, Sebastiani A, Hugonnet A, Bischoff F, Luhmann HJ, Thal SC. Traumatic brain injury results in rapid pericyte loss followed by reactive pericytosis in the cerebral cortex. *Sci Rep*. 2015;5:13497.
6. Ricard N, Tu L, Le Hiress M, Huertas A, Phan C, Thuillet R, Sattler C, Fadel E, Seferian A, Montani D, Dorfmüller P, Humbert M, Guignabert C. Increased pericyte coverage mediated by endothelial-derived fibroblast growth factor-2 and interleukin-6 is a source of smooth muscle-like cells in pulmonary hypertension. *Circulation*. 2014;129:1586–1597.
7. Uchida S, Dimmeler S. Long Noncoding RNAs in Cardiovascular Diseases. *Circ Res*. 2015;116:737–750.
8. Boon RA, Jaé N, Holdt L, Dimmeler S. Long Noncoding RNAs: From Clinical Genetics to Therapeutic Targets? *J Am Coll Cardiol*. 2016;67:1214–1226.
9. Michalik KM, You X, Manavski Y, Doddaballapur A, Zörnig M, Braun T, John D, Ponomareva Y, Chen W, Uchida S, Boon RA, Dimmeler S. Long noncoding RNA MALAT1 regulates endothelial cell function and vessel growth. *Circ Res*. 2014;114:1389–1397.

10. Bell RD, Long X, Lin M, Bergmann JH, Nanda V, Cowan SL, Zhou Q, Han Y, Spector DL, Zheng D, Miano JM. Identification and initial functional characterization of a human vascular cell-enriched long noncoding RNA. *Arterioscler Thromb Vasc Biol*. 2014;34:1249–1259.
11. Sallam T, Jones MC, Gilliland T, Zhang L, Wu X, Eskin A, Sandhu J, Casero D, Vallim TQ de A, Hong C, Katz M, Lee R, Whitelegge J, Tontonoz P. Feedback modulation of cholesterol metabolism by the lipid-responsive non-coding RNA LeXis. *Nature*. 2016;534:124–128.
12. Viereck J, Kumarswamy R, Foinquinos A, Xiao K, Avramopoulos P, Kunz M, Dittrich M, Maetzig T, Zimmer K, Remke J, Just A, Fendrich J, Scherf K, Bolesani E, Schambach A, Weidemann F, Zweigerdt R, de Windt LJ, Engelhardt S, Dandekar T, Batkai S, Thum T. Long noncoding RNA Chast promotes cardiac remodeling. *Sci Transl Med*. 2016;8:326ra22.
13. Nees S, Weiss DR, Senftl A, Knott M, Forch S, Schnurr M, Weyrich P, Juchem G. Isolation, bulk cultivation, and characterization of coronary microvascular pericytes: the second most frequent myocardial cell type in vitro. *AJP Heart Circ Physiol*. 2011;302:H69–H84.
14. Lin J, Zhang X, Xue C, Zhang H, Shashaty MGS, Gosai SJ, Meyer N, Grazioli A, Hinkle C, Caughey J, Li W, Susztak K, Gregory BD, Li M, Reilly MP. The long noncoding RNA landscape in hypoxic and inflammatory renal epithelial injury. *Am J Physiol Renal Physiol*. 2015;309:F901–913.
15. Yang L, Duff MO, Graveley BR, Carmichael GG, Chen L-L. Genomewide characterization of non-polyadenylated RNAs. *Genome Biol*. 2011;12:R16.
16. Minamino T, Komuro I, Kitakaze M. Endoplasmic Reticulum Stress As a Therapeutic Target in Cardiovascular Disease. *Circ Res*. 2010;107:1071–1082.
17. Baumeister P, Luo S, Skarnes WC, Sui G, Seto E, Shi Y, Lee AS. Endoplasmic reticulum stress induction of the Grp78/BiP promoter: activating mechanisms mediated by YY1 and its interactive chromatin modifiers. *Mol Cell Biol*. 2005;25:4529–4540.
18. Okada K -i. Prolonged Endoplasmic Reticulum Stress in Hypertrophic and Failing Heart After Aortic Constriction: Possible Contribution of Endoplasmic Reticulum Stress to Cardiac Myocyte Apoptosis. *Circulation*. 2004;110:705–712.
19. Battson ML, Lee DM, Gentile CL. Endoplasmic reticulum stress and the development of endothelial dysfunction. *Am J Physiol - Heart Circ Physiol*. 2017;312:H355–H367.
20. Prola A, Silva JPD, Guilbert A, Lecru L, Piquereau J, Ribeiro M, Mateo P, Gressette M, Fortin D, Boursier C, Gallerne C, Caillard A, Samuel J-L, François H, Sinclair DA, Eid P, Ventura-Clapier R, Garnier A, Lemaire C. SIRT1 protects the heart from ER stress-induced cell death through eIF2α deacetylation. *Cell Death Differ*. 2017;24:343–356.
21. Kassan M, Galan M, Partyka M, Saifudeen Z, Henrion D, Trebak M, Matrougui K. Endoplasmic Reticulum Stress Is Involved in Cardiac Damage and Vascular Endothelial Dysfunction in Hypertensive Mice. *Arterioscler Thromb Vasc Biol*. 2012;32:1652–1661.
22. Kato M, Wang M, Chen Z, Bhatt K, Oh HJ, Lanting L, Deshpande S, Jia Y, Lai JYC, O'Connor CL, Wu Y, Hodgin JB, Nelson RG, Bitzer M, Natarajan R. An endoplasmic reticulum stress-regulated lncRNA hosting a microRNA megacluster induces early features of diabetic nephropathy. *Nat Commun*. 2016;7:12864.
23. Chen R-P, Huang Z-L, Liu L-X, Xiang M-Q, Li G-P, Feng J-L, Liu B, Wu L-F. Involvement of endoplasmic reticulum stress and p53 in lncRNA MEG3-induced human hepatoma HepG2 cell apoptosis. *Oncol Rep*. 2016;36:1649–1657.
24. Su S, Liu J, He K, Zhang M, Feng C, Peng F, Li B, Xia X. Overexpression of the long noncoding RNA TUG1 protects against cold-induced injury of mouse livers by inhibiting apoptosis and inflammation. *FEBS J*. 2016;283:1261–1274.
25. Bertolotti A, Zhang Y, Hendershot LM, Harding HP, Ron D. Dynamic interaction of BiP and ER stress transducers in the unfolded-protein response. *Nat Cell Biol*. 2000;2:326–332.
26. Tsang KY, Chan D, Bateman JF, Cheah KSE. In vivo cellular adaptation to ER stress: survival strategies with double-edged consequences. *J Cell Sci*. 2010;123:2145–2154.

27. Swayze EE, Siwkowski AM, Wancewicz EV, Migawa MT, Wyrzykiewicz TK, Hung G, Monia BP, Bennett a. CF. Antisense oligonucleotides containing locked nucleic acid improve potency but cause significant hepatotoxicity in animals. *Nucleic Acids Res*. 2006;35:687–700.
28. Zhu M, Goetsch SC, Wang Z, Luo R, Hill JA, Schneider J, Morris SM, Liu Z-P. FoxO4 Promotes Early Inflammatory Response Upon Myocardial Infarction via Endothelial Arg1Novelty and Significance. *Circ Res*. 2015;117:967–977.

FIGURE LEGENDS

Figure 1: Identification and characterization of HypERlnc in pericytes. A, RNA sequencing demonstrates significant upregulation of HypERlnc and the known hypoxia regulated transcripts H19 and MIR210HG. **B**, Upregulation of HypERlnc was verified using RT-qPCR. **C**, HypERlnc read coverage under normoxic and hypoxic conditions. **D**, Biochemical analyses of HypERlnc in Poly A positive and negative fractions indicate that HypERlnc is polyadenylated. circRNA cHIPK3 was used as negative control. **E**, RNA-FISH shows HypERlnc expression in the nucleus and the cytosol of cells (right panel). Oligos directed against MALAT1 were used as nuclear-localized positive controls (left panel). **F**, RT-qPCR in cellular and nuclear fractions demonstrate that HypERlnc is about 1.5-fold enriched within the nucleus of the cell and that this localization does not change under hypoxic conditions. RPLP0 (P0) was used as a cytosolic control while MALAT1 served as nuclear control. All experiments are $n \geq 3$;* $P<0.05$; ***$P<0.001$

Figure 2: HypERlnc regulates pericyte differentiation. A, HypERlnc knockdown using LNA GapmeRs. **B-E**, Loss of HypERlnc results in cellular de-differentiation as reflected by a loss of pericyte markers such as PDGFRβ, αSMA, Desmin and NG2. **F**, RNA guided gene activation strategy. **G-J**, Pericyte markers PDGFRβ, αSMA, Desmin and NG2 significantly correlate with HypERlnc expression in gain of function experiments. All experiments are $n \geq 3$; **$P<0.01$; ***$P<0.001$

Figure 3: HypERlnc knockdown impairs pericyte function. A, Assessment of endothelial barrier function in a co-culture model consisting of pericytes and human coronary microvascular endothelial cells (HCMEC). **B**, Loss of HypERlnc significantly enhances passage of macromolecular 70kDa FITC-Dextran. **C**,**D**, Silencing HypERlnc significantly reduces pericyte (in green) recruitment towards HCMEC (in red) in matrigel assays. **E**, HypERlnc knockdown decreases pericyte viability and **F**,**G**, cell proliferation. **H**, Loss of HypERlnc does not result in enhanced apoptosis, staurosporin (Stauro) was used as a positive control in a caspase 3/7 assay. All experiments are $n \geq 3$; *$P<0.05$; ***$P<0.001$

Figure 4:HypERlnc modulates the endoplasmic reticulum stress response and is regulated in human heart failure. A, Luciferase transcription factor reporter assays in HypERlnc knockdown demonstrate enhanced luciferase activity in CBF/NF-Y/YY1 and ATF6 responsive elements which are part of the ER stress response. **B**, Representative immunoblots for ER stress markers IRE1α and soluble BiP following HypERlnc knockdown and Dithiothreitol (DTT) treatment. DTT was used as a positive control for ER stress. **C**, **D**, Quantitative analyses of soluble BiP and IRE1α protein levels confirm enhanced ER stress in LNA HypERlnc treated pericytes, **E**, KEGG pathway analyses following RNA-seq in HypERlnc knockdown demonstrate that VSMC contraction related genes and several cardiomyopathies are among the top 20 upregulated pathways. **F**, HypERlnc expression was analyzed via RT-qPCR in left ventricular myocardium from patients diagnosed with heart failure (HF, n=19). **G**, HypERlnc RNA levels were significantly reduced compared with controls (n=5 patients without a known history of heart failure). All experiments are $n \geq 3$; *$P<0.05$; ***$P<0.001$

NOVELTY AND SIGNIFICANCE

What Is Known?

- Pericytes are essential perivascular cells that induce vessel maturation, stabilize endothelial barrier function and contribute to organ remodeling in pathologic conditions.

- Pericyte survival and recruitment towards endothelial cells is mainly driven by platelet-derived growth factor signaling, however molecular regulatory mechanisms that control pericyte differentiation and survival are poorly understood.

- Long non-coding RNAs (lncRNAs) represent non-coding transcripts that have been found to significantly regulate endothelial as well as smooth muscle cell function, but their role in pericyte biology remains unclear.

What New Information Does This Article Contribute?

- Here we characterize hypoxia regulated lncRNAs in pericytes and show that HypERlnc significantly regulates human pericyte function, differentiation and survival by modulating the endoplasmic reticulum (ER) stress response.

- Analyses of HypERlnc in human hearts and lungs suggest that HypERlnc may have a role in cardiopulmonary disease states such as heart failure and idiopathic pulmonary hypertension (IPAH).

Pericytes are mural cells that contribute to vessel maturation and control endothelial barrier function. Despite their pivotal role in the vascular system, knowledge is sparse on molecular regulatory mechanisms of pericyte cell biology. Here we show for the first time that a lncRNA is essential for pericyte function, survival and differentiation. Our findings on the regulation of ER stress by HypERlnc may have a broad translational impact. ER stress has been shown to be involved in various disease states, including heart failure. Our findings that HypERlnc is significantly de-regulated in human heart failure and significantly correlates with pericyte differentiation markers in human lungs, indicate that HypERlnc may have role in human cardiopulmonary disease. The identification of a HypERlnc orthologue in mouse pericytes will enable to perform translational studies that may substantiate these findings in vivo and elucidate the role of HypERlnc in cardiopulmonary disease.

FIGURE 1

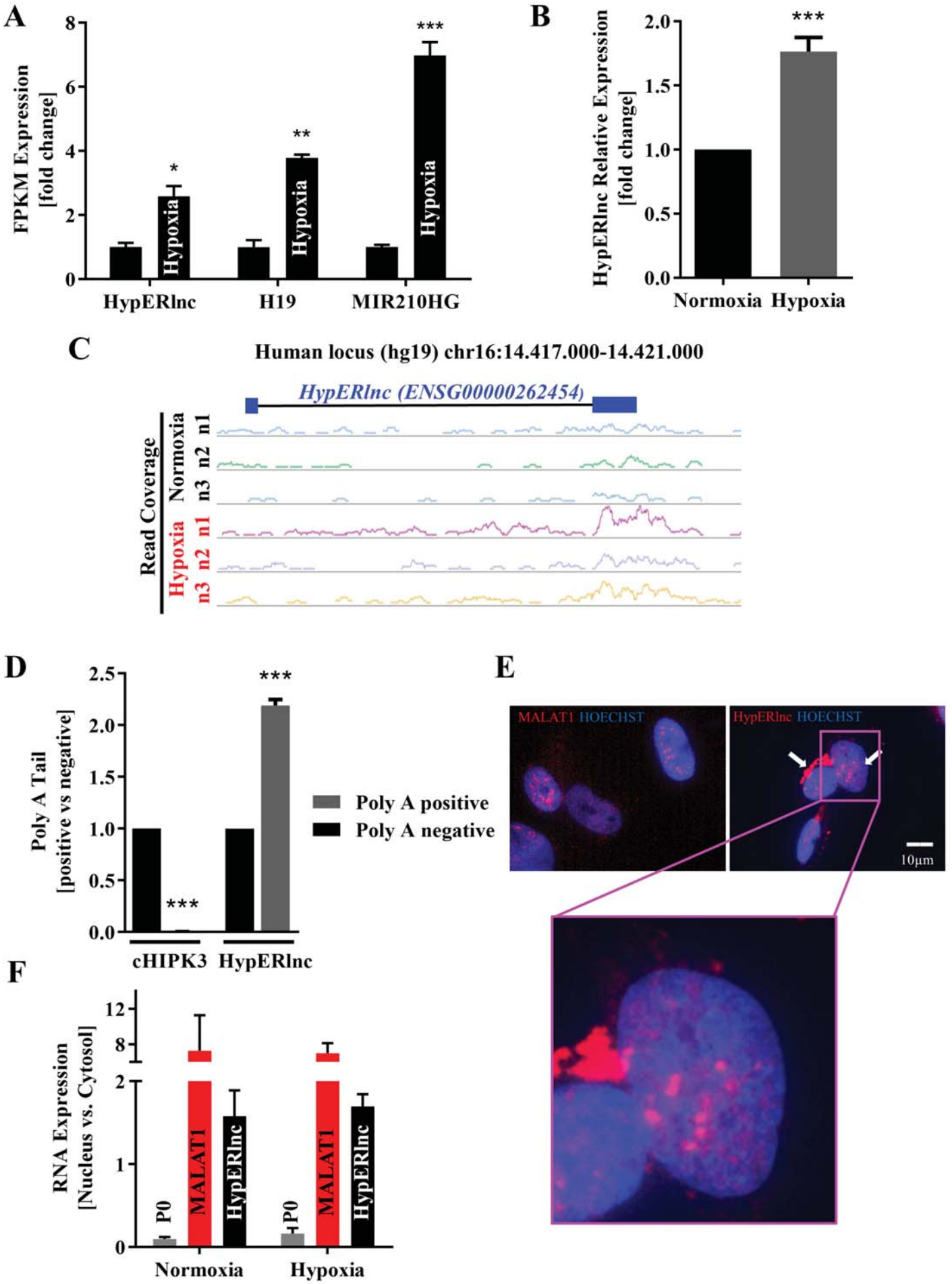
A
FPKM Expression [fold change]
Hypoxia
HypERlnc
H19
MIR210HG
B
HypERlnc Relative Expression [fold change]
Normoxia
Hypoxia
C
Human locus (hg19) chr16:14.417.000-14.421.000
HypERlnc (ENSG00000262454)
Read Coverage
Normoxia n1 n2 n3
Hypoxia n1 n2 n3
D
Poly A Tail [positive vs negative]
Poly A positive
Poly A negative
cHIPK3
HypERlnc
E
MALAT1 HOECHST
HypERlnc HOECHST
10μm
F
RNA Expression [Nucleus vs. Cytosol]
P0
MALAT1
HypERlnc
Normoxia
Hypoxia

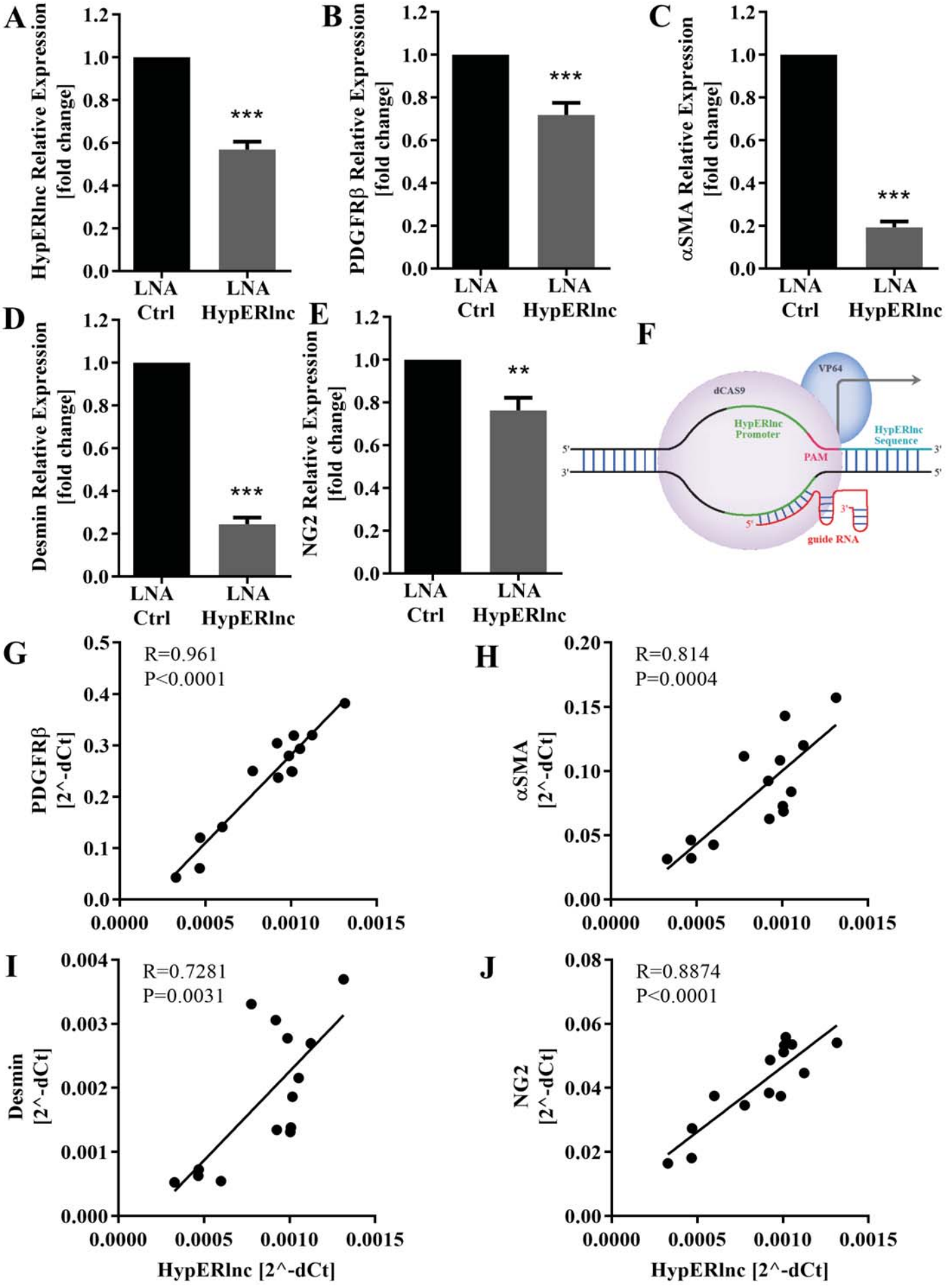
A
HypERlnc Relative Expression [fold change]
1.2
1.0
0.8
0.6
0.4
0.2
0.0
***
LNA Ctrl
LNA HypERlnc
B
PDGFRβ Relative Expression [fold change]
***
C
αSMA Relative Expression [fold change]
***
D
Desmin Relative Expression [fold change]
***
E
NG2 Relative Expression [fold change]
**
F
VP64
dCAS9
HypERlnc Promoter
HypERlnc Sequence
PAM
5'
3'
guide RNA
G
R=0.961
P<0.0001
PDGFRβ [2^-dCt]
0.5
0.4
0.3
0.2
0.1
0.0
0.0000
0.0005
0.0010
0.0015
H
R=0.814
P=0.0004
αSMA [2^-dCt]
0.20
0.15
0.10
0.05
0.00
I
R=0.7281
P=0.0031
Desmin [2^-dCt]
0.004
0.003
0.002
0.001
0.000
HypERlnc [2^-dCt]
J
R=0.8874
P<0.0001
NG2 [2^-dCt]
0.08
0.06
0.04
0.02
0.00
HypERlnc [2^-dCt]

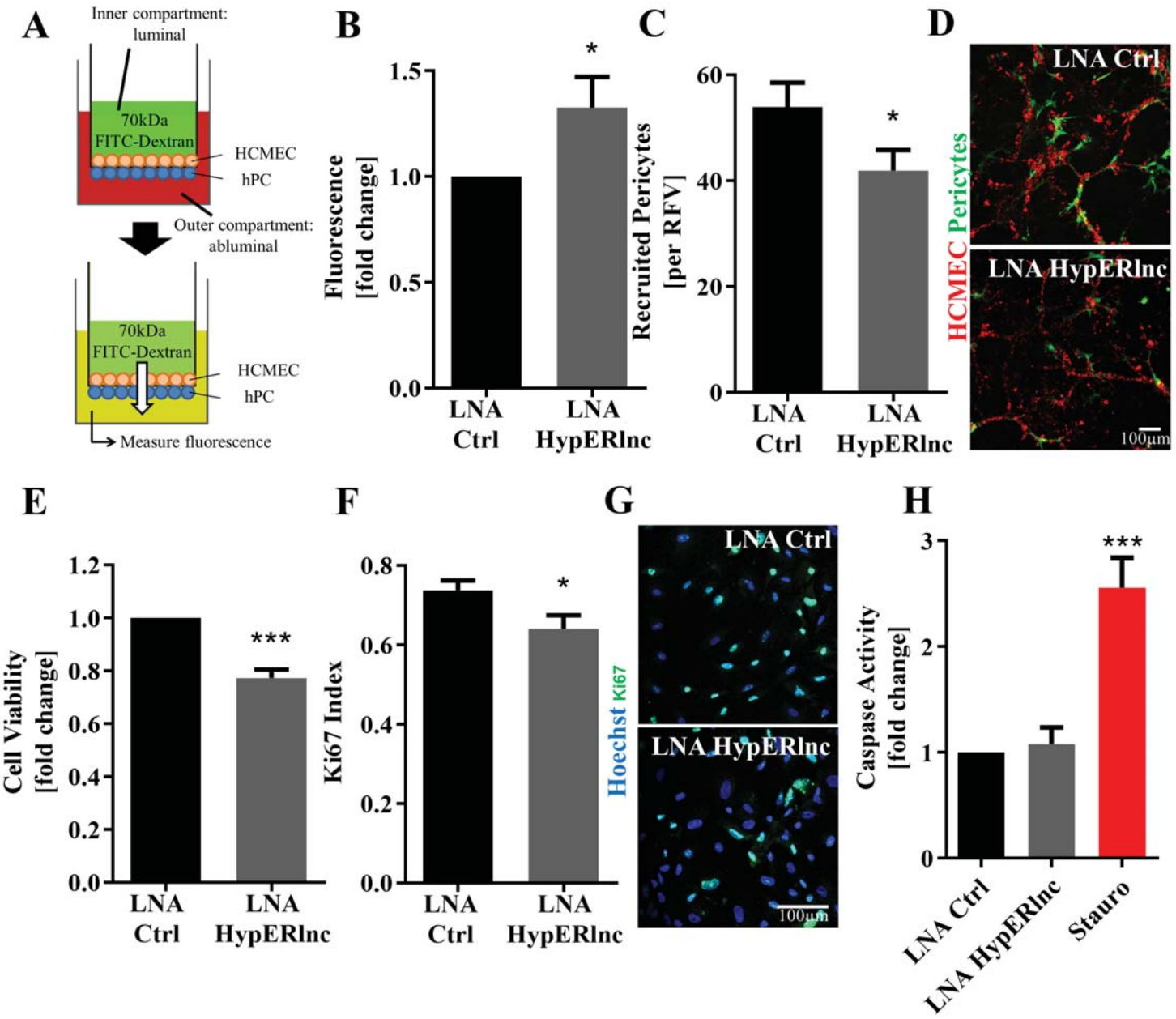
A
Inner compartment: luminal
70kDa FITC-Dextran
HCMEC
hPC
Outer compartment: abluminal
70kDa FITC-Dextran
HCMEC
hPC
Measure fluorescence
B
Fluorescence [fold change]
1.5
1.0
0.5
0.0
*
LNA Ctrl
LNA HypERlnc
C
Recruited Pericytes [per RFV]
60
40
20
0
*
LNA Ctrl
LNA HypERlnc
D
HCMEC Pericytes
LNA Ctrl
LNA HypERlnc
100µm
E
Cell Viability [fold change]
1.2
1.0
0.8
0.6
0.4
0.2
0.0
***
LNA Ctrl
LNA HypERlnc
F
Ki67 Index
0.8
0.6
0.4
0.2
0.0
*
LNA Ctrl
LNA HypERlnc
G
Hoechst Ki67
LNA Ctrl
LNA HypERlnc
100µm
H
Caspase Activity [fold change]
3
2
1
0
***
LNA Ctrl
LNA HypERlnc
Stauro

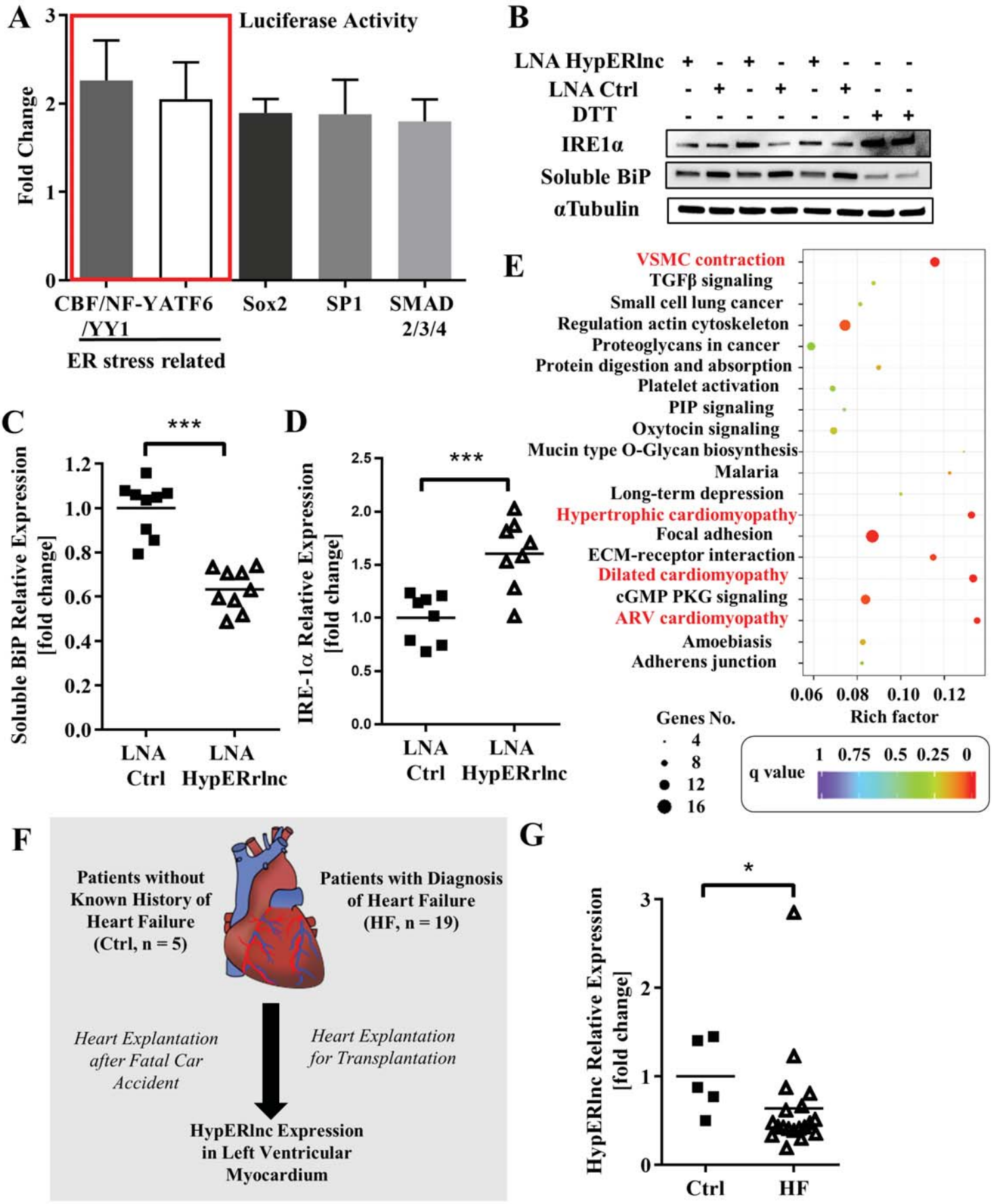
A
Luciferase Activity
Fold Change
CBF/NF-YATF6 /YY1
Sox2
SP1
SMAD 2/3/4
ER stress related
B
LNA HypERlnc
LNA Ctrl
DTT
IRE1α
Soluble BiP
αTubulin
C
Soluble BiP Relative Expression [fold change]
LNA Ctrl
LNA HypERlnc
D
IRE-1α Relative Expression [fold change]
LNA Ctrl
LNA HypERlnc
E
VSMC contraction
TGFβ signaling
Small cell lung cancer
Regulation actin cytoskeleton
Proteoglycans in cancer
Protein digestion and absorption
Platelet activation
PIP signaling
Oxytocin signaling
Mucin type O-Glycan biosynthesis
Malaria
Long-term depression
Hypertrophic cardiomyopathy
Focal adhesion
ECM-receptor interaction
Dilated cardiomyopathy
cGMP PKG signaling
ARV cardiomyopathy
Amoebiasis
Adherens junction
Rich factor
Genes No.
q value
F
Patients without Known History of Heart Failure (Ctrl, n = 5)
Patients with Diagnosis of Heart Failure (HF, n = 19)
Heart Explantation after Fatal Car Accident
Heart Explantation for Transplantation
HypERlnc Expression in Left Ventricular Myocardium
G
HypERlnc Relative Expression [fold change]
Ctrl
HF

Supplemental Material

Identification and Functional Characterization of Hypoxia-Induced Endoplasmic Reticulum Stress Regulating lncRNA (HypERlnc) in Pericytes

Florian C Bischoff[1,2,4], Astrid Werner[1,2], David John[1,4], Jes-Niels Boeckel[3,4], Maria-Theodora Melissari[1], Phillip Grote[1], Simone F Glaser[1,2], Shemsi Demolli[1,4], Shizuka Uchida[1,4,5], Katharina M Michalik[1], Benjamin Meder[3,4], Hugo A Katus[3,4], Jan Haas[3,4], Wei Chen[4,6,7], Soni S Pullamsetti[8,9], Werner Seeger[8,9], Andreas M Zeiher[2,4], Stefanie Dimmeler[1,4#], Christoph M Zehendner[1,2,4#]

# equal contribution

[1]*Institute for Cardiovascular Regeneration, Centre of Molecular Medicine, Goethe University Frankfurt am Main, Germany*
[2]*ZIM III, Department of Cardiology, Goethe University, Frankfurt am Main, Germany*
[3]*Department of Internal Medicine III, University of Heidelberg, Germany*
[4]*DZHK (Deutsches Zentrum für Herz-Kreislaufforschung)*
[5] *Cardiovascular Innovation Institute, University of Louisville, Louisville, Kentucky, United States*
[6]*Laboratory for Novel sequencing technology, Functional and Medical Genomics, Berlin Institute for Medical Systems Biology, Max-Delbrück-Centrum für Molekulare Medizin, Berlin, Germany*
[7]*Department of Biology, Southern University of Science and Technology, Shenzhen, China*
[8]*Max Planck Institute for Heart and Lung Research, Department of Lung Development and Remodeling, member of the German Center for Lung Research (DZL), Bad Nauheim, Germany*
[9]*Department of Internal Medicine, Universities of Giessen and Marburg Lung Center (UGMLC), member of the DZL, Justus Liebig University, Giessen, Germany*

Corresponding author contact:

Stefanie Dimmeler, PhD[1,4]
Theodor Stern Kai 7
60590 Frankfurt am Main
dimmeler@em.uni-frankfurt.de
Phone: ±49-69-6301-6667
Fax: ±49-69-6301-83462

Christoph M. Zehendner, MD[1,2,4]
Theodor Stern Kai 7
60590 Frankfurt am Main
Christoph.Zehendner@gmail.com
Phone: ±49-69-6301-6667
Fax: ±49-69-6301-83462

Materials and Methods:

Human pericyte cell culture

Human pericytes were acquired from ScienCell and cultured as recommended. Pericytes were used from passages 2-9. Pericytes were cultured in DMEM Glutamax completed with 10% fetal calf serum (both from Gibco, Life Technologies) and Penicillin/Streptomycin (Roche Diagnostics). The humidified atmosphere in the incubator contained 5% CO_2 and 20% O_2 at 37°C. Human coronary microvascular endothelial cells (HCMEC; passages 2-8; ScienCell) were kept in the same atmosphere and cultured in Endothelial Cell Medium (ECM; from ScienCell) containing provided supplements as recommended. For Induction of endoplasmic reticulum stress, cells were treated with Dithiothreitol (DTT; 1 mM, 1 hour; Roth) or Tunicamycin (5 µg/ml, 5 hours; Sigma-Aldrich).

Isolation of primary mouse pericytes

Primary mouse brain pericytes were isolated as documented elsewhere from adult C57Bl6 wild type mice[1] with modifications. In brief, mice were euthanized by an overdose of isoflurane followed by decapitation. Brains were quickly removed and transferred into 4°C cold DMEM (Gibco, Life Technologies). Next, olfactory bulb, cerebellum and medulla were dissected and brains were minced with a sterile scalpel. Minced brain tissue was washed once in DMEM, centrifuged for 5 min at 340 g. Medium was carefully discarded and tissue was incubated in an enzymatic digestion mixture in EBSS containing 20 units/ml Papain and 0.005 % DNAse (all from Worthington) for 70 min at 37°C. Following enzymatic digestion, brain tissue was homogenized by passing ten times through an 18 gauge needle and subsequently ten times through a 21 gauge needle. Homogenate was then mixed with 1.7-fold volume of 22% bovine serum albumin in phosphate buffered saline and centrifuged for 10 min at 3800 g. The lipid layer on top was carefully removed and cell pellet was resuspended in collagen coated 6 well plates. During the first three passages, cells were kept in ECM (ScienCell). Starting with the fourth passage, cell culture medium was switched to pericyte medium (ScienCell). Primary mouse pericytes from passage 7-12 were used for experimental manipulation. For validation of murine HypERlnc by reverse transcription PCR, RNA from primary mouse pericytes was isolated using an RNeasy Mini Kit (Qiagen) as recommended including DNA digestion. RNA was reversely transcribed as documented below.

Induction of hypoxia

Cells were kept in pre-equilibrated culture medium in a hypoxic incubator (Labotect) with humidified atmosphere at 5% CO_2, 1% O_2, 37°C. Pericytes were subjected to hypoxia for 24 hours. Hypoxia was verified with measurement of culture medium pO_2 levels with a hypoxia sensing probe (Oxford Optronix) as described elsewhere[2–4]. Additionally, VEGFA Induction was verified via RT-qPCR and only samples with 2-fold upregulation or higher were used for further analysis.

RNA sequencing in human and murine pericytes

Ribosomal RNA depleted total RNA isolated from human pericytes was analyzed via RNA deep sequencing. The RNeasy Mini Kit (Qiagen) was used to isolate RNA as recommended including DNA digestion. RNA degradation and contamination was monitored on 1% agarose gels and RNA purity determined with a NanoPhotometer® spectrophotometer (IMPLEN). RNA concentration was measured using Qubit® RNA Assay Kit in Qubit® 2.0 Fluorometer (Life Technologies). RNA quality was checked with a RNA Nano 6000 Assay Kit of the Agilent Bioanalyzer 2100 system (Agilent Technologies). Isolated RNA was fragmented and primed for cDNA synthesis. Libraries were created using a Scriptseq v2 (mouse samples, Illumina, SSV21124) or NEBNext® Ultra™ Directional RNA Library Prep Kit (human samples, Illumina) according to the manufacturer's instructions.
A HiSeq flow cell (Illumina) was used for sequencing. Based on the NONCODE database (noncode.org) lncRNA annotation was performed. RNA-seq of murine pericytes and human pericytes treated with LNA Control or LNA HypERlnc were carried out by Novogene. The uploaded data is accessible on the GEO database when published (with GEO ID: GSE92888).

GO and KEGG enrichment analyses

Gene Ontology (GO) enrichment analysis of differentially expressed genes was done using GOseq R package, in which gene length bias was corrected. GO terms with corrected P value <0.05 were considered significantly enriched by differential expressed genes. KEGG is a database resource for understanding high-level functions and utilities of the biological system, such as the cell, the organism and the ecosystem, from molecular level information, especially large scale molecular datasets generated by genome sequencing and other high-throughput experimental technologies (http://www.genome.jp/kegg/). KOBAS software was used to test the statistical enrichment of differential expression genes or lncRNA target genes in KEGG pathways.

RNA isolation and reverse transcription quantitative PCR (RT-qPCR)

To isolate total RNA from cell cultures RNeasy Mini Kit (Qiagen) was used as recommended including DNA digestion. Fractionation of RNA for nuclear and cytosolic fractions was performed as described elsewhere[5]. RNA concentration was measured using a NanoDrop 2000 Spectrophotometer (Thermo Fisher Scientific) and transcribed to cDNA using MulV reverse transcriptase (Life Technologies) and random hexamer primers (Thermo Fisher Scientific) in 40 µl reaction volume. Transcribed cDNA was used with fast SYBR Green (Applied Biosystems) in RT-qPCR performed by a Viia7 Real-Time PCR System (Thermo Fisher Scientific). CT values were normalized against ribosomal RPLP0 (P0) and relative gene expression was determined through the formula: $2^{-\Delta CT}$ ($\Delta CT=CT_{Target}-CT_{Control}$). The sequences of used primers are given in Online Table III.

Transfection

Cells were transfected after reaching a confluency of 60-80% using Opti-MEM Medium, Lipofectamine RNAiMAX (both from Life technologies) and 50 nmol/l of LNA GapmeR (Exiqon), siRNA or gRNA blocks. LNA GapmeR control A, scrambled siRNA or transfection medium free of gRNA blocks were used as control for transfection experiments. After 4 hours transfection medium was exchanged to the appropriate cell culture medium. 48 hours upon transfection cells were used for experimental manipulation.

LNA GapmeR sequences were as follows:

LNA HypERlnc: 5'-CTTGGCTGGCGGAAGG-3'

LNA Ctrl: 5'-AACACGTCTATACGC-3'

siRNA sequences directed against HypERlnc were from Sigma-Aldrich ((i)sense: 5'-ACAGCCCUUGUAACUGAUA-3'; antisense: 5'-UAUCAGUUACAAGGGCUGU-3'; (ii) sense: 5'-AGCCCUUGUAACUGAUAAC-3'; antisense: 5'-GUUAUCAGUUACAAGGGCU-3'). siRNA controls were transfected with siRNA targeting firefly luciferase as documented elsewhere[6] (from Sigma-Aldrich, sense: 5'-CGUACGCGGAAUACUUCGA-3'; antisense: 5'-UCGAAGUAUUCCGCGUACG-3').

RNA guided gene activation

A constitutive dCas9-VP64 lentiviral expression vector carrying a puromycin resistancy (addgene Plasmid #50918, http://www.addgene.org/50918/; kindly provided by Fatma Kok) was used to transduce human pericytes. To verify transduction, pericytes were kept in Pericyte Medium (ScienCell, #1201) containing provided supplements and 1 µg/ml puromycin for at least 6 days to select for successfully transduced pericytes. To achieve overexpression of HypERlnc by RNA guided gene activation, guide RNAs (gRNAs) were designed bearing the antisense sequence to the probable HypERlnc promoter region. gRNAs were designed with the gRNA design toll by the Zhang lab (http://crispr.mit.edu/). gRNA blocks constitutively expressing particular gRNA sequences were bought from IDT and amplified as endorsed by IDT via PCR. Afterwards, pericytes were transfected with the amplification product. Multiple gRNA blocks targeting different promoter region segments were used as described previously[7]. gRNA block combination and target sequences of gRNAs are shown in Online Table IV. For gRNA block design following sequence scheme was used:

U6 promoter + target sequence (without PAM sequence) + guide RNAscaffold + termination signal

TGTACAAAAAAGCAGGCTTTAAAGGAACCAATTCAGTCGACTGGATCCGGTACCAAG
GTCGGGCAGGAAGAGGGCCTATTTCCCATGATTCCTTCATATTTGCATATACGATACA
AGGCTGTTAGAGAGATAATTAGAATTAATTTGACTGTAAACACAAAGATATTAGTAC
AAAATACGTGACGTAGAAAGTAATAATTTCTTGGGTAGTTTGCAGTTTTAAAATTATG
TTTTAAAATGGACTATCATATGCTTACCGTAACTTGAAAGTATTTCGATTTCTTGGCTT
TATATATCTTGTGGAAAGGACGAAACACCGXXXXXXXXXXXXXXXXXXXGTTTTAGA
GCTAGAAATAGCAAGTTAAAATAAGGCTAGTCCGTTATCAACTTGAAAAAGTGGCAC
CGAGTCGGTGCTTTTTTTCTAGACCCAGCTTTCTTGTACAAAGTTGGCATTA

Luciferase reporter array

For analysis of transcription factor activity a Cignal Finder Reporter Array (Qiagen, #336821) was used as recommended by the manufacturer. Human pericytes were transfected with LNA GapmeRs as already described. After transfection, $4x10^4$ pericytes/well were seeded into 96 well plates from Qiagen. Cells were seeded in 50 µl Opti-MEM containing 10% FCS while each well contained 100 µl Opti-MEM supplemented with Lipofectamine RNAiMAX. Cell culture plates were incubated for 4 hours (humidified atmosphere, 5% CO_2, 20% O_2, 37°C). Subsequently, medium was changed to pericyte culture medium and culture plates were incubated for another 24 hours following transfection in the culture plates. Luciferase signals were measured with a GloMax-Multi Detection System from Promega.

Preparation of poly-$A^{+/-}$ RNA

Preparation was performed as already described[8]. In brief, oligo-$d(T)^{25}$-magnetic beads (NEB, #S14195) were used to separate poly-A tail positive from poly-A tail negative RNA. Washed beads and RNA were incubated with binding buffer while rotating for 10 min. Separation of poly-A^- RNA was done by collecting the supernatant after binding of the beads with a magnet. Afterwards, beads were washed and incubated in elution buffer for 2 min at 50°C to obtain poly-A^+ RNA. RNA levels were measured with RT-qPCR as described above.

Matrigel co-culture assays

Human pericytes were transduced with a lentivirus for expression of a green fluorescent protein (GFP). Transduction followed standard procedures and precise protocol is available on demand. Transduced pericytes were transfected with LNA GapmeRs as described above. As endothelial cells are known for acetylated LDL uptake[9], we labeled HCMEC with 10 µg/ml Dil-Acetylated LDL (CellSystems, #CS-D0120) for 16 hours. Matrigel (Corning, #354230) beforehand thawed on ice was transferred in 150 µl doses to pre-cooled 24 or 48 well plates from Corning avoiding bubble formation. Plates were incubated for 30 min (humidified atmosphere, 5% CO_2, 20% O_2, 37°C). 10^5 stained HCMEC were seeded on top of the matrigel layer in a maximum volume of 500 µl and incubated for 3 hours. Afterwards, medium was removed and 10^4 GFP-expressing pericytes were added in a maximum volume of 500 µl for 3 hours. Both steps had the same incubation conditions as the matrigel layer. Cell medium was removed and another layer of 150 µl Matrigel was added avoiding bubbles and incubated at described conditions for another 30 min. Pericyte culture medium and ECM (1:1) were added to reach a final volume of 500 µl and the plate was incubated for another 16 hours. Next, cells were fixed for 10 min using 4% Paraformaldehyd (PFA; Roti-Histofix, Carl Roth). 3 randomly chosen fields per view per well were generated using confocal z-stack imaging. GFP-positive pericytes were defined as recruited when attached to HCMEC. Recruited pericytes were counted using Fiji is just ImageJ cell counter tool. The average of recruited pericytes per field per view is presented.

Barrier function assay

The assay was performed as described previously with modifications[10]. In brief, human pericytes were transfected with LNA GapmeRs as described above. ThinCerts (Greiner Bio-One, #662610) with 1 µm pores were coated on the outer pore section with 70 µl of 0.001% Poly-L-Lysin (PLL; Sigma-Aldrich,

#P4832-50ML) in sterile water for 45 min at room temperature. Afterwards, the inner pore section part was coated with 150 µl of 5 µg/cm^2 fibronection (FN; Sigma-Aldrich, #F0895-5MG) in PBS (Thermo Fisher Scientific, #14190-094) for 45 min at room temperature. 24 hours after transfection, 3x10^4 pericytes in 70 µl pericyte culture medium were transferred to the PLL coated outer section for 45 min at room temperature. Subsequently, 3x10^4 HCMEC in 250 µl ECM were transferred to the FN coated inner section. Cells were incubated for 48 hours (humidified atmosphere, 5% CO_2, 20% O_2, 37°C). 0.25 mg/ml fluorescin Isothiocyanat-dextran (average molecular weight 70,000; Sigma-Aldrich, #FD70S-100MG) in ECM were given in the inner compartment. After 30 min 80 µl out of the outer compartment were transferred to a 96 well plate and fluorescence was measured after excitation with 485 nm using a Synergy HT microplate reader (BioTek).

Intercellular dye transfer assay and live cell imaging

HUVEC were seeded on 6 cm dishes. At 60-80% confluency, HUVEC were stained with CellTrace calcein red-orange AM (Life Technologies, #C34851) according to the manufacturer's instructions. Pericytes were grown to confluency in a culture dish and labeled with CellTrace calcein green AM (5 µmol/l, 30 min; Life Technologies, #C34852). Subsequently, pericytes were washed, trypsinized and transferred into the HUVEC grown culture 6 cm dish at a pericyte/HUVEC ratio of 1:4. After 4 hours of co-culture, live cell imaging was performed using a Zeiss epifluorescent microscope.

MTT assay

Human Pericytes were cultured in 24 well plates and transfected with LNA GapmeRs for 48 hours. After removal of culture medium 3-(4,5-Dimethylthiazol-2-yl)-2,5-diphenyltetrazolium bromid (MTT; 5 mg/ml in PBS; Life Technologies, #M-6494) diluted 1:10 in DMEM (Gibco, #41965-039) was applied. Culture plates were incubated for 1 hour (humidified atmosphere, 5% CO_2, 20% O_2, 37°C). DMEM with MTT was removed and pericytes were resuspended in DMSO. 100 µl of each well were transferred to a 96 well plate and absorption was measured at 565 nm in a Synergy HT microplate reader (BioTek). Blank wells treated with DMEM with MTT and DMSO were used for background subtraction.

Caspase-3/7 Assay

Human pericytes (2x10^4 per well) were seeded in a black 96 well plate (Corning, #353219). Pericytes were transfected as described above. Positive control was treated with 200 nM Staurosporine for 4 hours. All pericytes were stained with 5 µM CellTrace calcein red-orange AM (Life Technologies, #C34851) in pericyte culture medium for 30 min. After washing, cells were incubated with Caspase-3/7 reagent (Apo-One Homogeneous Caspase-3/7 Assay, Promega, #G7790) composited as recommended for 2 hours with light exclusion at room temperature. Fluorescence (calcein red-orange excitation: 577 nm, Caspase-3/7 reagent excitation: 499 nm) was measured with a Synergy HT microplate reader (BioTek).

Immunofluorescence (IF)

Standard immunofluorescent staining procedures were done as already described[3,4,11]. In brief, human pericytes were washed with PBS (4°C) and fixed in ice cold acetone (-20°C) for 10 min. Cells were incubated with 7% donkey serum (Dianova) and Triton X-100 in PBS (4°C) for 2 hours at room temperature. Primary antibody incubation (anti-Ki67 and anti-PDGFRβ) was performed with 2% bovine serum albumin (BSA; Dianova), 0.05% azide and 0.1% Triton X-100 in PBS (4°C) for 16 hours at room temperature. Secondary antibodies (anti-rabbit 488 and anti-goat Cy3) and Hoechst (1:1000) were applied in 2% BSA and 0.05% azide in PBS (4°C) for 2 hours at room temperature. Pericytes were embedded in Fluoromount Aqueous Mounting (Sigma-Aldrich, #F4680-25ML) for microscopy.

Flow cytometry analysis

For quantification of early apoptotic and necrotic cells, a flow cytometry detection kit was used as recommended by the manufacturer (BD Bioscience, #556547). In brief, human pericytes were grown on 10 cm dishes at a density of 5x10^5 cells/dish. Transfection procedures were carried out as documented above. For Annexin V labeling, a V450 Annexin V antibody (BD Bioscience, #560506) was used. Cells were starved for 4 hours in Opti-MEM medium in order to induce apoptosis (positive control). For propidium iodide positive controls, cells were treated with 80% ethanol for 5 min at room temperature.

Upon silencing of HypERlnc with siRNA or LNA GapmeRs, cells were washed once with PBS (4°C), trypsinized and centrifuged for 5 min at 1000 g. Washing with PBS and centrifugation was repeated for 2 times. Next, cells were resuspended in binding buffer (4°C). 100 µl of cell suspension ($4x10^6$ cells/ml) were stained using 5 µl of V450 Annexin V and 5 µl of propidium iodide solution for 15 min at room temperature in the dark. Subsequently, 200 µl binding buffer was added to the vial and measurements were carried out. Analysis was done using a BD FACSCantoTM II flow cytometer and BD FACSDiva Software (from BD Biosciences).

RNA-fluorescent in situ hybridization (RNA-FISH)

RNA-FISH probes were designed using the Stellaris probe design tool. Incubation of RNA-FISH oligos directed against HypERlnc labelled with Quasar dye 570 were applied for in situ hybridization as recommended by the manufacturer (Stellaris). MALAT1 RNA-FISH oligos (Quasar dye 570) were used as a positive control. In brief, human pericytes were grown on coverslips. After reaching confluency, cells were exposed towards 24 hours of hypoxia as described above. Following hypoxia, cells were washed with PBS and fixed in 3.7% formaldehyde in RNAse free 1x PBS for 10 min at room temperature. Subsequently, probes were washed twice with PBS and permeabilized using 70% ethanol for at least 1 hour at 4°C. Next, cells were washed as recommended. Finally, probes were hybridized with oligos against HypERlnc or MALAT1 respectively for 4 hours at 37°C. Cells were then washed and counterstained with Hoechst (Invitrogen, 1:2000) for 30 min. After a final washing step cells were embedded in fluoromount and imaging was performed with a Zeiss epifluorescent microscope using an oil objective with 100x magnification.

Protein isolation, SDS-PAGE, immunoblotting

Human pericytes were washed with PBS (4°C) and snap frozen in liquid nitrogen. Next, RIPA buffer (4°C; Thermo Fisher Scientific) containing protease inhibitor (Roche Diagnostics) was applied and cells were scraped off with a pre-cooled rubber policeman (-20°C). Pericyte lysate was incubated on ice for 45 min. Next, protein lysate was centrifuged for 10 min with 2350 g at 4°C. Supernatant was carefully removed and transferred to ice-cooled vials. Concentration was measured with a spectrophotometer and Bradford protein assay with Roti-Quant (Carl Roth) following manufacturer's instructions. Equal volumes of lysate containing 40 µg of protein were mixed with an equal volume of 2x Laemmli buffer (Sigma-Aldrich). Mini-PROTEAN TGX Precast Gels (Bio-Rad) were used for SDS-PAGE at 150 V for 50 min in TBST (Bio-Rad). Gels were blotted using a Pierce G2 Fast Blotter (Thermo Fisher Scientific) as recommended. Western blots (WBs) were blocked with 5% milk/BSA in TBST. Primary antibodies were incubated for 16 hours in 5% milk/BSA in TBST at 4°C. Secondary antibodies were incubated for 1 hour in 5% milk/BSA in TBST at room temperature.

Induction of autophagy

In order to block fusion of autophagosome and lysosome cells were treated with 50 µmol/l chloroquine (CQ; Novus Biologicals) for 24 hours or with 100 µmol/l rapamycin (Invivogen) for 4 hours to induce autophagy.

Confocal microscopy and image analysis

Fluorescent images were acquired with a Leica SP5 confocal setup (Leica Microsystems). Z-stacks with z-stack step size smaller than 1.8 µm were acquired. Three excitation wavelengths were used (405 nm, 488 nm and 552 nm). Image analysis was done with Fiji is just ImageJ for windows. To analyze Ki67 positive cells, images were randomized. Cells with a positive Ki67 signal were counted. Hoechst stained nuclei were counted after creation of binary images with Fiji automated particle analysis. Ki67 positive cells were set in relation to Hoechst positive cells to determine the relative number of proliferating cells. PDGFRβ was used as a control marker for pericytes.

Patient cohort analyses

Human heart samples

Isolation of left ventricular total RNA was performed with an All-Prep Kit (Qiagen) as recommended including DNA digestion. Left ventricle samples from patients without diagnosis of heart failure (n=5) were compared to samples from patients with diagnosed heart failure (n=19) in RT-qPCR. Participants gave written informed consent to the current study and it was authorized by the ethics committee of the medical faculty of Heidelberg (appl. no. S-390/2011). Symptomatic heart failure patients were consecutively, prospectively enrolled in this study. Control samples were used correctly according to the protected health information (45 C.F.R. 164.514 e2) (Bioserve) and the BCI informed consent F-641-5 (Biochain).

Human lung samples

Human explanted lung tissues from subjects with IPAH (n=7), or control donors (n=7) were obtained during lung transplantation. Samples of donor lung tissue were taken from the lung that was not transplanted. The study protocol for tissue donation was approved by the ethics committee (Ethik Kommission am Fachbereich Humanmedizin der Justus Liebig Universität Giessen) of the University Hospital Giessen (Giessen, Germany) in accordance with national law and with Good Clinical Practice/International Conference on Harmonisation guidelines. Written informed consent was obtained from each individual patient or the patient's next of kin (AZ 31/93, 10/06, 58/15). All lungs were reviewed for pathology, and the IPAH lungs were classified as grade III or IV according to Heath and Yacoub.

Statistical analyses

Experiments and each experimental condition were carried out $n \geq 3$ times if not declared otherwise. Results are shown with mean ± standard error of the mean (SEM). GraphPad 7 for windows (Graphpad) was used for data analysis. Null hypothesis was rejected at $\alpha < 0.05$. The Pearson and D'Agostino omnibus or Shapiro-Wilk normality test was used for normalization control. If passed, the two sided Student's t-test was used to compare the difference between two groups, if not, analysis was done with the two sided Mann-Whitney U test. Analyses comparing more than two groups were done with One-Way ANOVA with correction for multiple comparisons (Dunnett). Correlation analyses were done using Pearson correlation if data followed Gaussian distribution, or Spearman method if data did not follow a Gaussian distribution. Grubbs' test was used for outlier detection and outliers were removed for *in vitro* experiments. Outliers in patient data sets were not removed. Venn diagram was constructed using Venny[12].

Titles and Legends to Online Figures

Online Figure I

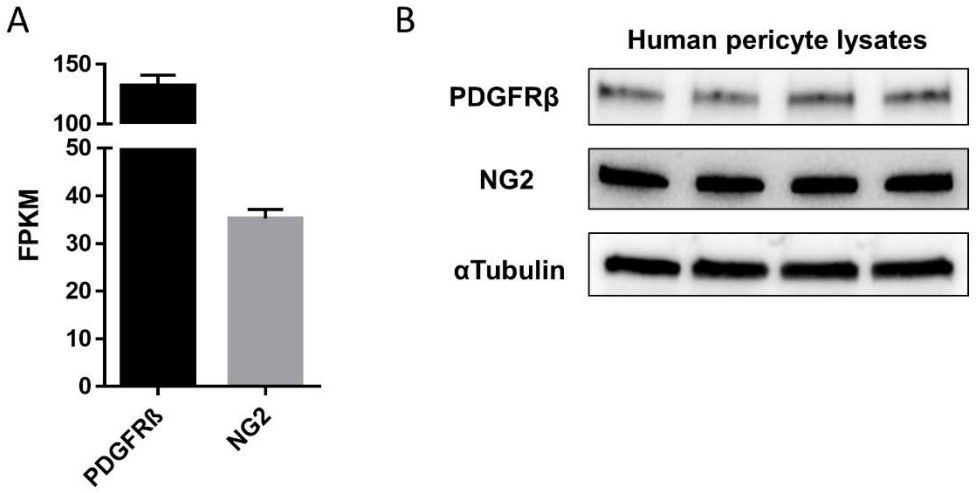

A, FPKM reads of PDGFRβ and NG2 demonstrate robust expression in human primary pericytes. **B**, Immunoblotting confirms expression of PDGFRβ and NG2 in human pericytes.

Online Figure II

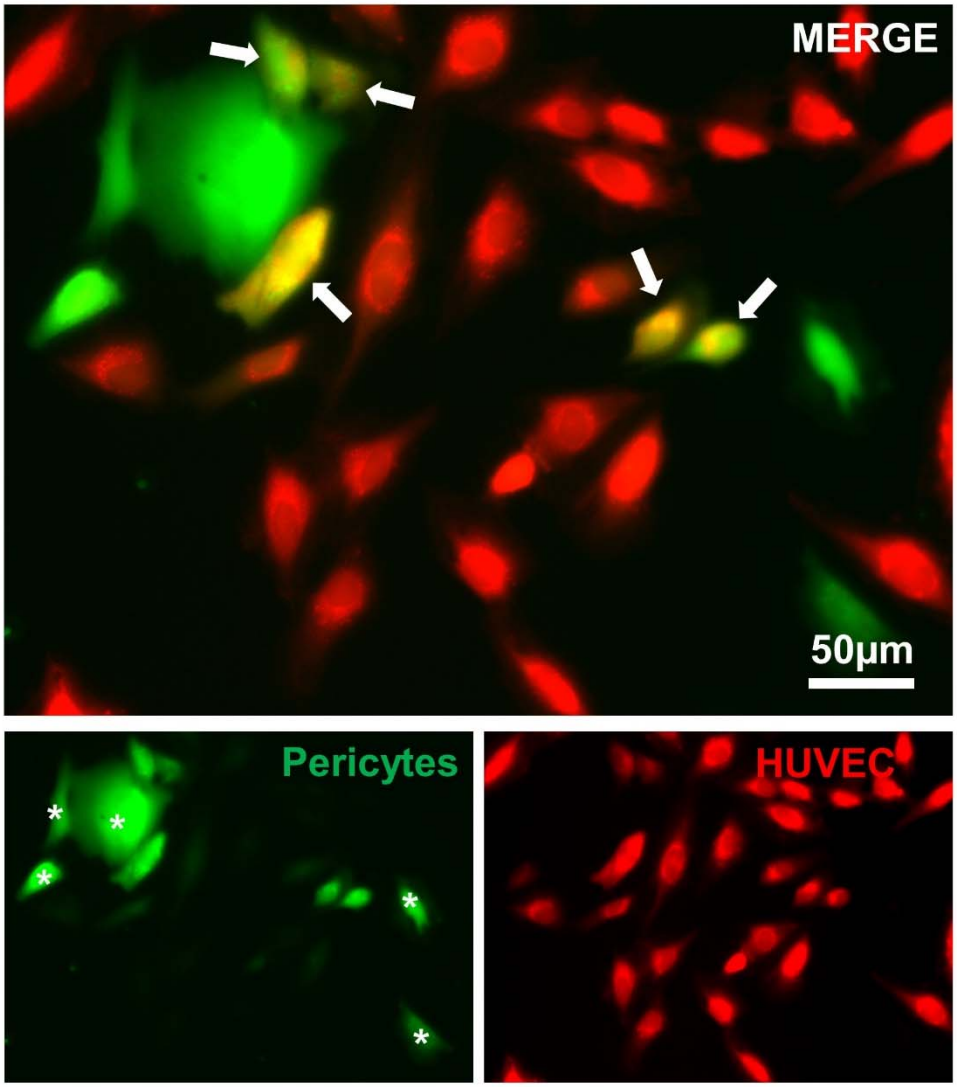

Live cell imaging in pericyte-endothelial co-cultures demonstrates formation of functional intercellular junctions between pericytes (green, indicated by asterisks) and HUVEC (red) as indicated by intercellular dye transfer (arrows).

Online Figure III

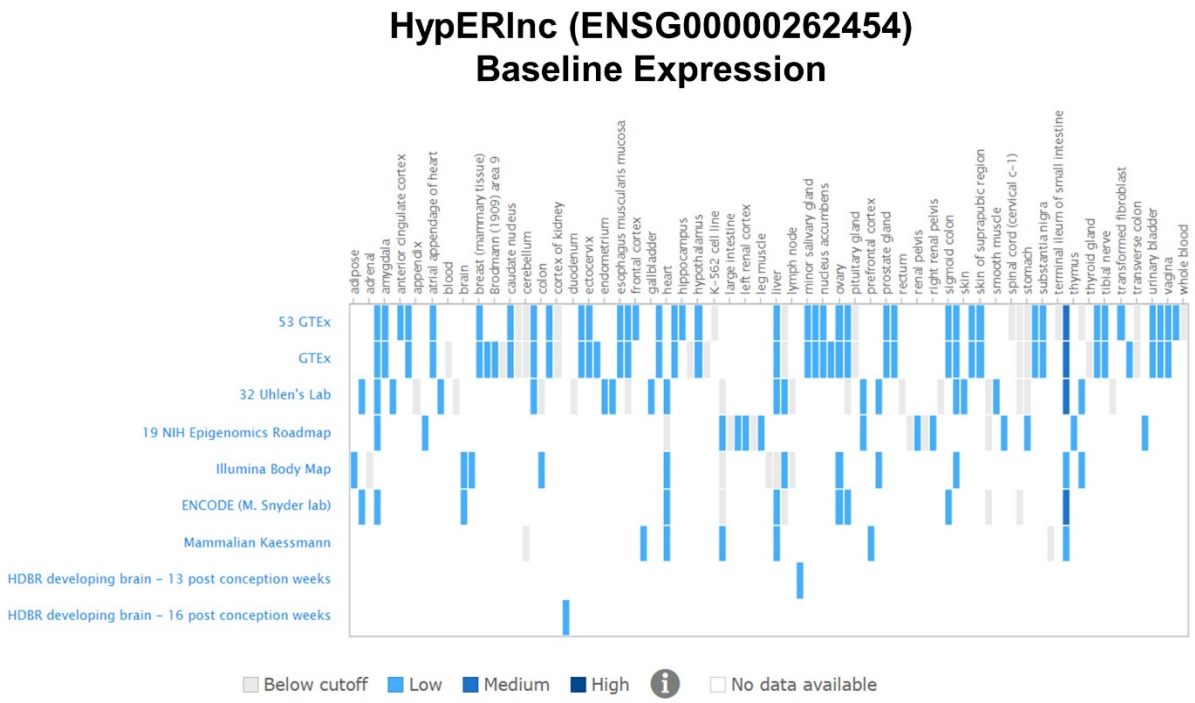

HypERlnc expression in various human organ systems and tissues are displayed. Results for the term "ENSG00000262454" and filtering for Homo sapiens "Organism part" of the EBI Gene Expression Atlas (GXA) are shown:
http://www.ebi.ac.uk/gxa/genes/ENSG00000262454?bs=%7B%22homo%20sapiens%22%3A%5B%22organism_part%22%5D%7D&ds=%7B%22kingdom%22%3A%5B%22animals%22%5D%7D#baseline

Online Figure IV

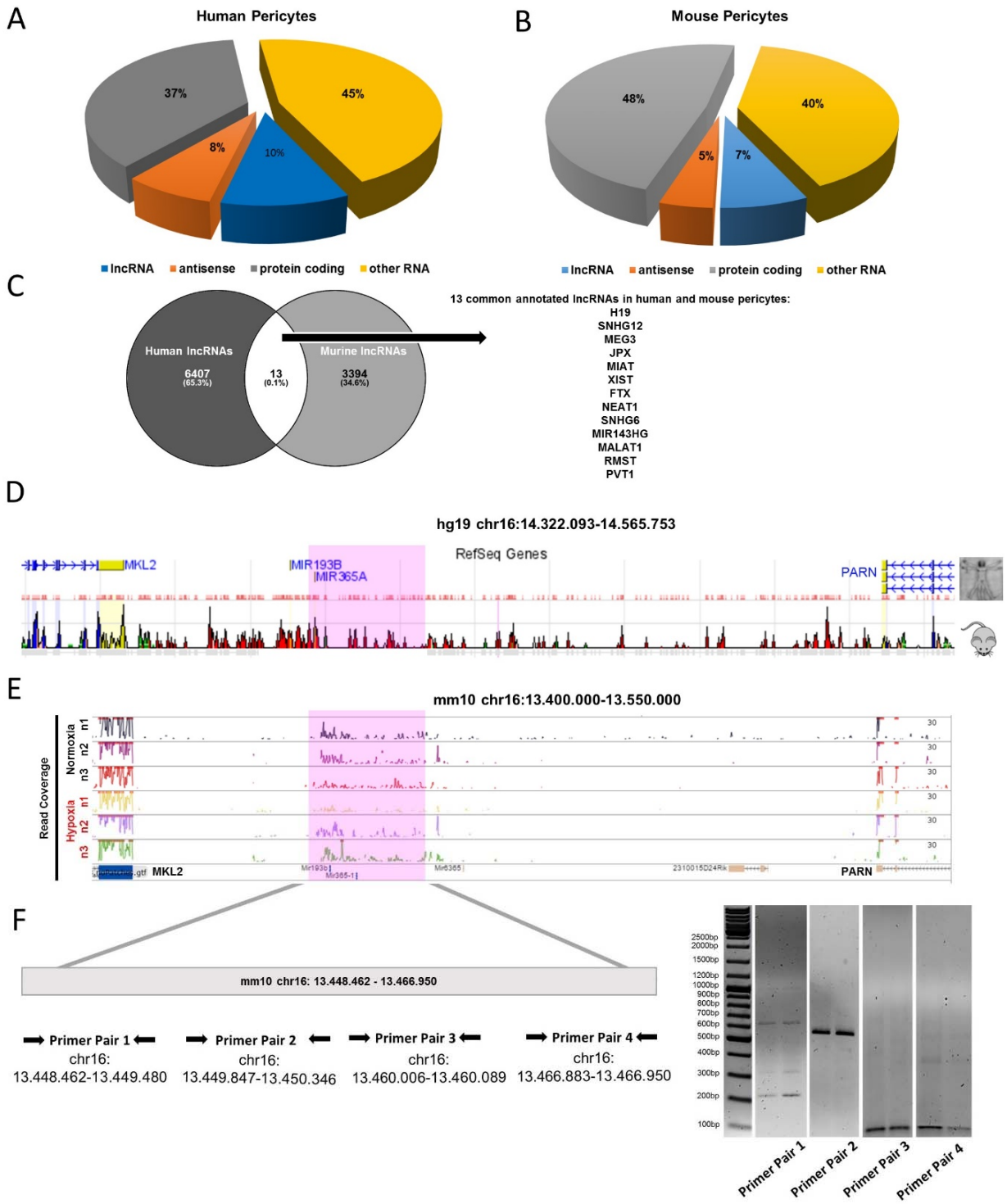

A, Chart pie diagram of non-coding RNA expression based on RNA-seq analyses in human and **B**, primary mouse pericytes. **C**, Venn diagram showing commonly annotated lncRNAs in human and mouse pericytes. **D**, ECR browser (https://ecrbrowser.dcode.org/) analysis of the human HypERlnc gene position (region highlighted in purple) indicates up to 70% sequence homology (area under the curves in red) in the mouse genome in locus conservation. HypERlnc is flanked by the neighbouring genes MKL2 and PARN. **E**, RNA-seq in primary mouse pericytes demonstrates high read coverage of the possible mHypERlnc orthologue (in purple). **F**, Primer alignment and RT-PCR validation of mHypERlnc in primary murine pericytes.

Online Figure V

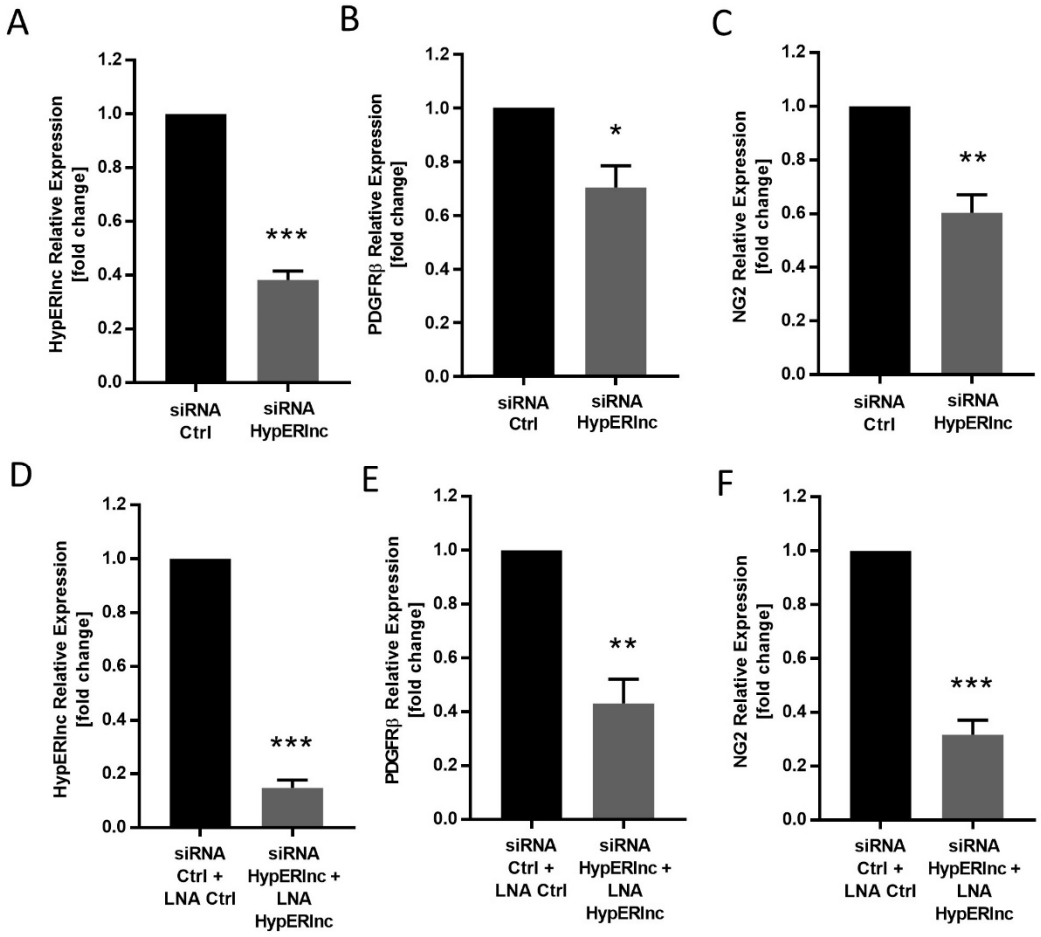

A-C, Targeting HypERlnc with small interfering RNAs results in significant HypERlnc knockdown that goes along with loss of pericyte markers PDGFRβ and NG2. **D-F,** A combined silencing strategy using both siRNAs and LNA GapmeRs enhances HypERlnc knockdown efficacy that results in de-differentiation of human pericytes. All experiments are n≥3; *P<0.05; **P<0.01; ***P<0.001

Online Figure VI

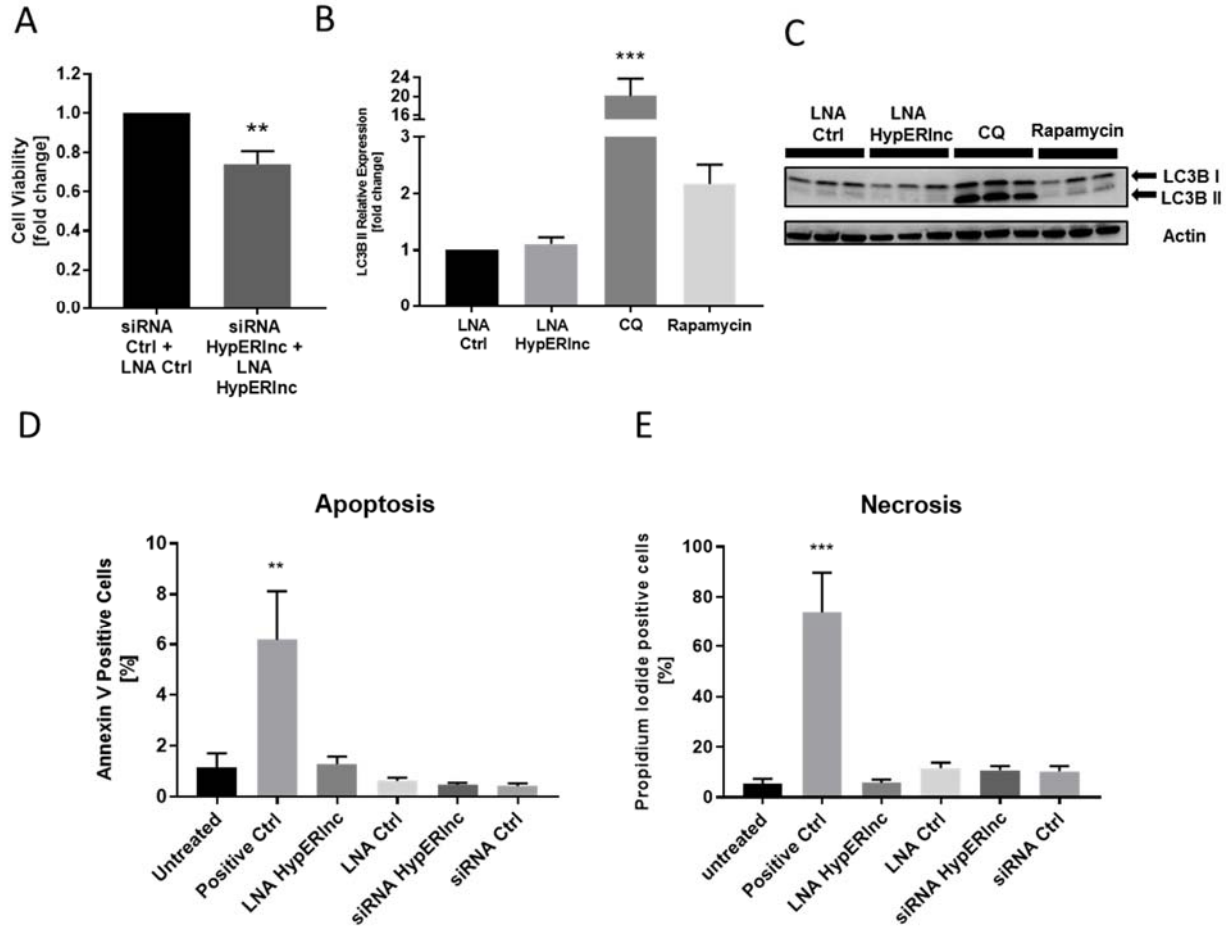

A, MTT assay demonstrates significant loss of cell viability upon HypERlnc knockdown using siRNAs and LNA GapmeRs. **B**, Quantitative analysis of the autophagy marker LC3B II demonstrates that loss of HypERlnc does not induce autophagy. **C**, Representative protein immunoblotting of LC3B. **D**, Flow cytometry analysis of annexin V positive cells suggests that loss of HypERlnc does not induce apoptosis. **E**, Analysis of propidium iodide positive cells suggests that loss of HypERlnc does not induce necrosis. CQ: Chloroquine. All experiments are n≥3; **P<0.01; ***P<0.001

Online Figure VII

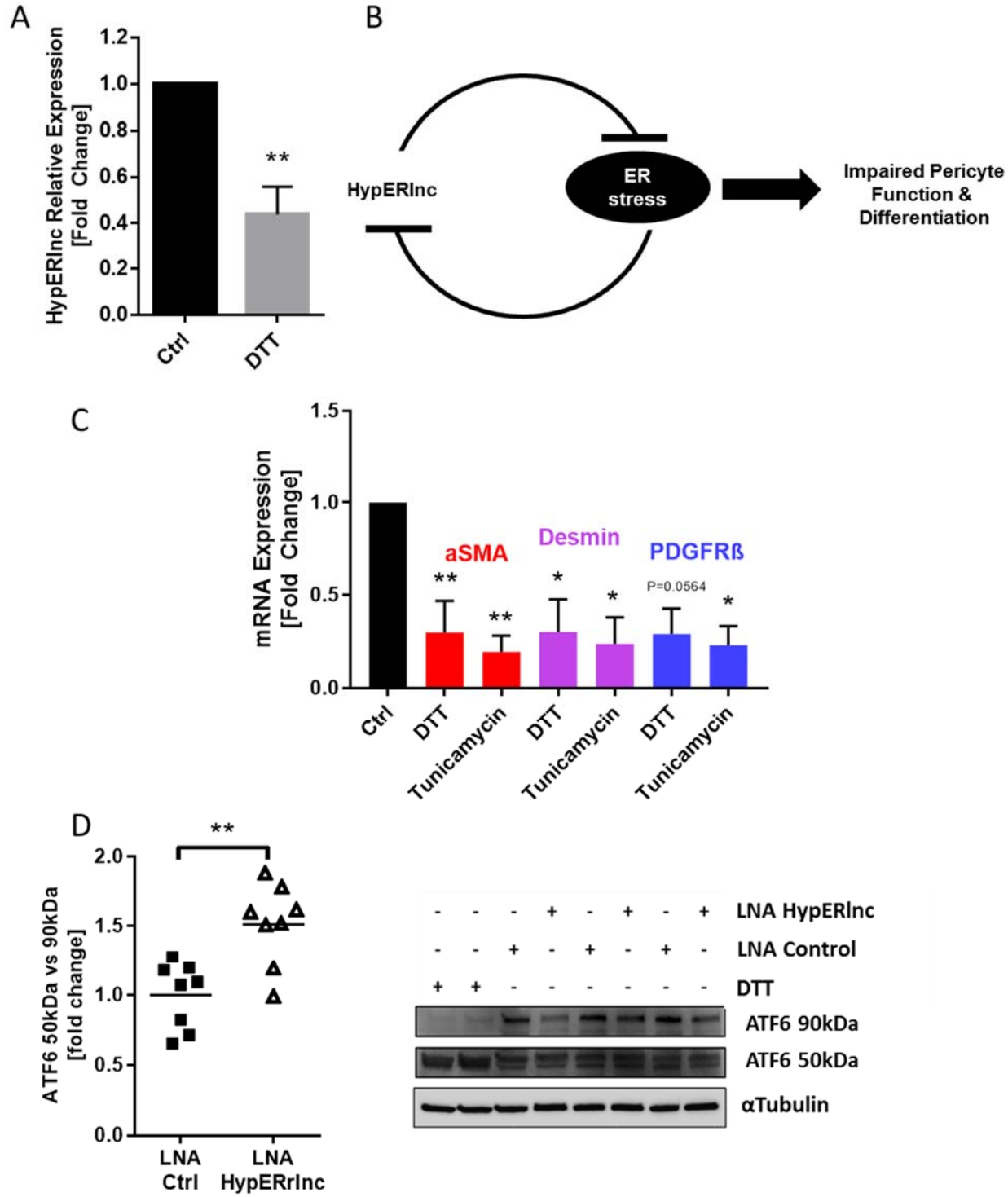

A, ER stress induction results in significant downregulation of HypERlnc. **B**, Scheme depicting regulatory feedback role between HypERlnc expression and ER stress. **C**, ER stress results in de-differentiation of pericytes. **D**, Silencing HypERlnc significantly increases proteolytic ATF6 cleavage. All experiments are n≥3; *P<0.05; **P<0.01

Online Figure VIII

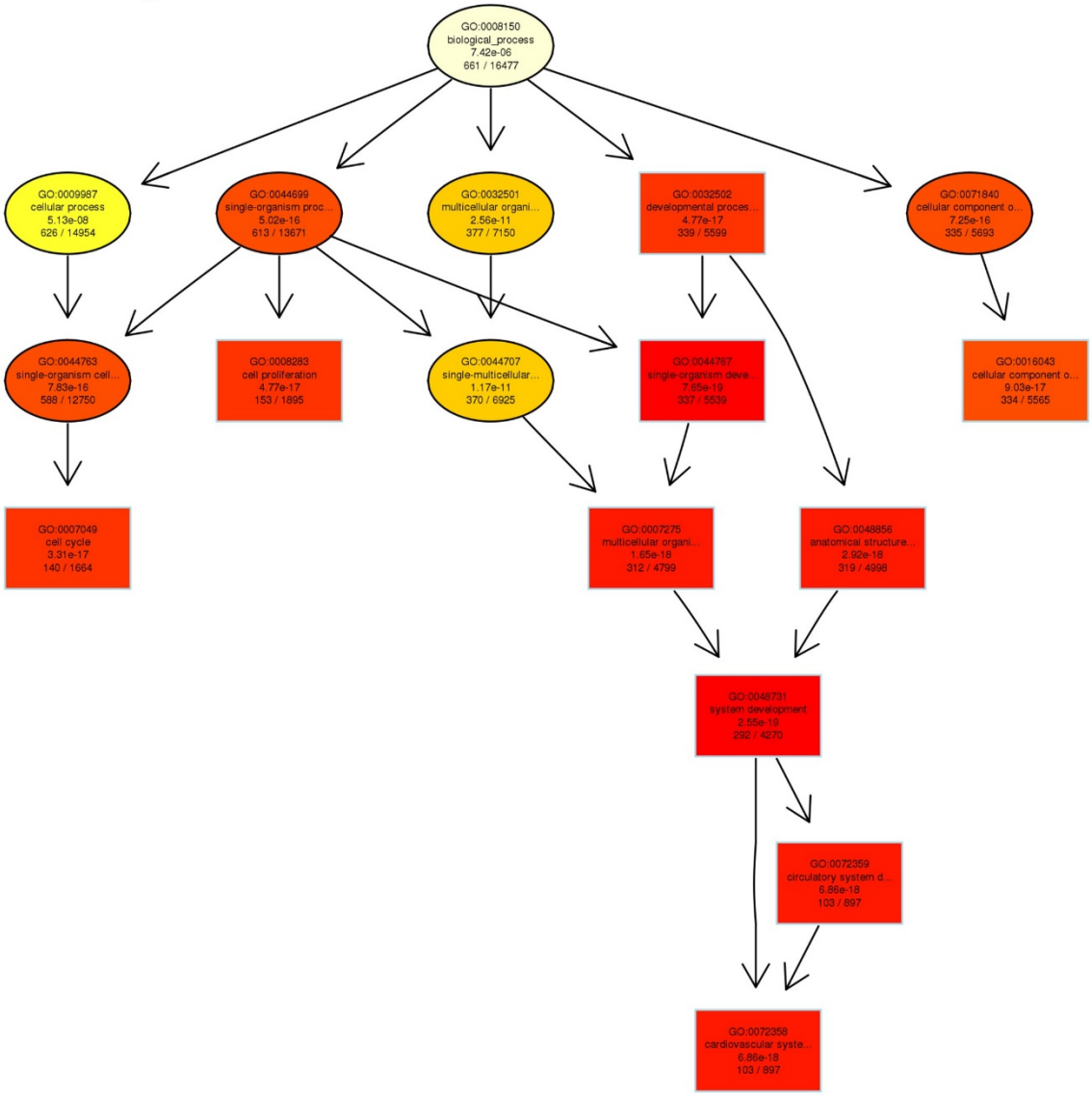

Gene Ontology analysis with regard to biological processes following HypERlnc silencing in RNA-seq demonstrates upregulation of genes affecting cardiovascular system development.

Online Figure IX

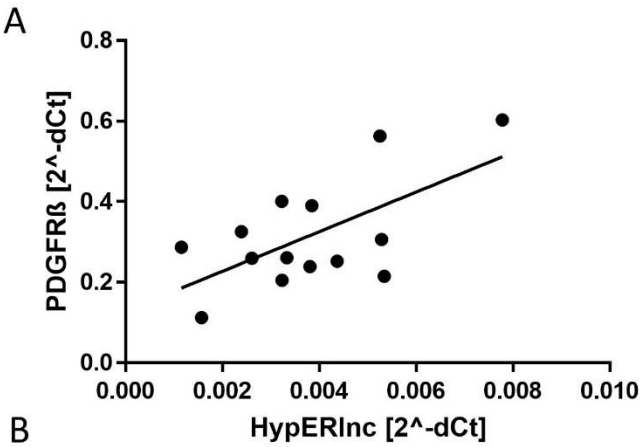

Pearson	
R	0.6311
95% confidence interval	0.1511-0.8703
R squared	0.3983
P value	
P (two-tailed)	0.0155

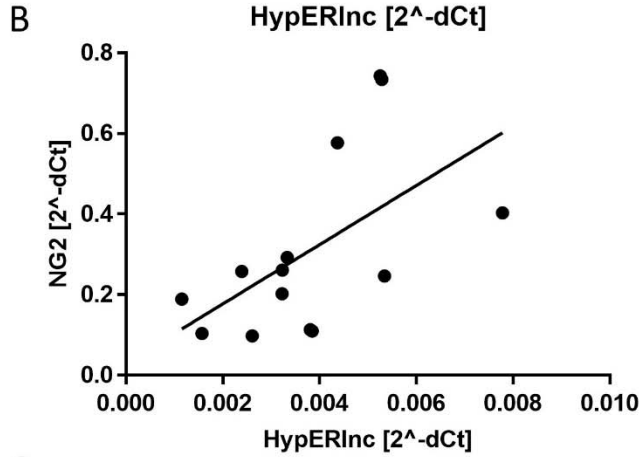

Pearson	
R	0.5704
95% confidence interval	0.05707-0.8452
R squared	0.3253
P value	
P (two-tailed)	0.0332

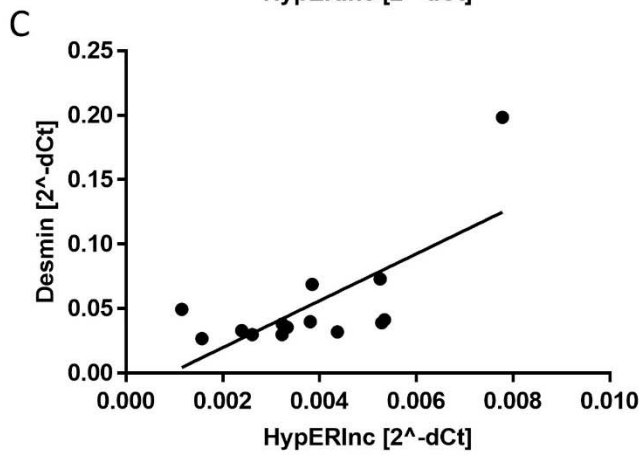

Spearman r	
R	0.578
95% confidence interval	0.05102-0.8532
P value	
P (two-tailed)	0.0333

RT-qPCR analyses of HypERlnc and pericyte markers reveal significant correlation of HypERlnc with (**A**) PDGFRβ, (**B**) NG2 and (**C**) Desmin in human lungs derived from healthy donors (n=7) and patients diagnosed with IPAH (n=7).

Online Table I Primary Antibodies

Primary Antibodies	Antibody concentration	Item number / manufacturer
anti-Ki67 (IF)	1:200	ab15580 / Abcam
anti-PDGFRβ	1:200 (IF); 1:3000 (WB)	GT15065 / Neuromics
anti-IREα (WB)	1:1000	3294 / Cell Signaling
anti-BiP (WB)	1:1000	3177 / Cell Signaling
anti-Actin (WB)	1:400	ab3280/ Abcam
anti-αTubulin (WB)	1:5000	ab6160 / Abcam
anti-HA (WB)	1:1000	2367S / Cell signaling
anti-CAS9 (WB)	1:1000	14697S / Cell signaling
anti-NG2 (WB)	1:1000	AB5320 / Millipore
anti-ATF6 (WB)	1:1000	ab122897 / Abcam
anti-LC3B (WB)	1:1000	NB100-2220 / NovusBiologicals

Online Table II Secondary Antibodies

Secondary Antibodies	Antibody concentration	Item number / manufacturer
anti-rabbit 488 (IF)	1:200	ab150073 / Abcam
anti-goat Cy3 (IF)	1:200	705-165-147 / Dianova
anti-rabbit HRP (WB)	1:2000	7074 / Cell Signaling
anti-rat HRP (WB)	1:5000	ab102265 / Abcam
anti-mouse HRP (WB)	1:3000	ab97030 / Abcam

Online Table III Primer Sequences

Species	Target	Forward	Reverse
Homo Sapiens	RPLP0 (P0)	TCGACAATGGCAGCATCTAC	ATCCGTCTCCACAGACAAGG
Homo Sapiens	NG2	TGAGATCAGAAGGGACCAGC	GAATACGATGTCTGCAGGTGG
Homo Sapiens	αSMA	GCACCCCTGAACCCCAAG	AGGCATAGAGAGACAGCACC
Homo Sapiens	VEGFA	AATGTGAATGCAGACCAAAG	GACTTATACCGGGATTTCTTG
Homo Sapiens	PDGFRβ	ACAATGACTCCCGTGGACTG	CTCGGCATCATTAGGGAGGA
Homo Sapiens	HypERlnc	AGGCCAGAGGATGGAAAAGG	TTTGCATCTCCCAACCAGCA
Homo Sapiens	Desmin	CTCTACGAGGAGGAGCTGC	ACTGAATCTCCTCCTGCAGC
Homo Sapiens	MALAT1	TGAGTGTATGAGACCTTGCAGT	GCAGCGGGATCAGAACAGTA
Mus musculus	mHypERlnc (Primer_1)	TGGGACAGGGACAAGGCG	GTTCGCAGTTCCCAGCTC
Mus musculus	mHypERlnc (Primer_2)	GGCAGCTCAGGTTCTACACA	ACCTGTGTGTCCATGTGC
Mus musculus	mHypERlnc (Primer_3)	ACAACCAGGGCTACATAGAGA	TGTTGGGCTGTTTTGTTTTGT
Mus musculus	mHypERlnc (Primer_4)	ACCAACATTGCTGCTCCATC	GCAGAAAAGAGGACAAACAACC

Online Table IV gRNA target sequences

Label	Target Sequence **PAM**
Guide#1_250bp_up	CAAATATAGTCAGCGGATAG **GGG**
Guide#2_250bp_up	GCCAAATATAGTCAGCGGAT **AGG**
Guide#1_1500bp_up	CAGGAGAATCGCCTACACCT **GGG**
Guide#2_1500bp_up	GCAGGAGAATCGCCTACACC **TGG**
Guide#1_2000bp_up	ATGTGCTTAGGTCTCGGGGT **GGG**
Guide#2_2000bp_up	CTAGCCTCAGTCTTTCGATC **TGG**
Guide#1_2500bp_up	TGAGCACTTCGCTGCCGTTA **TGG**
Guide#2_2500bp_up	CTTGAGGAACTAGACGTCTC **AGG**

Online Table V

Please download from http://circres.ahajournals.org

Online Table VI

Please download from http://circres.ahajournals.org

Online References

1. Tigges U, Welser-Alves JV, Boroujerdi A, Milner R. A novel and simple method for culturing pericytes from mouse brain. *Microvasc Res*. 2012;84:74–80.
2. Zehendner CM, Tsohataridis S, Luhmann HJ, Yang J-W. Developmental Switch in Neurovascular Coupling in the Immature Rodent Barrel Cortex. *PLoS ONE*. 2013;8:e80749.
3. Zehendner CM, Wedler HE, Luhmann HJ. A novel in vitro model to study pericytes in the neurovascular unit of the developing cortex. *PloS One*. 2013;8:e81637.
4. Zehendner CM, Librizzi L, Hedrich J, Bauer NM, Angamo EA, de Curtis M, Luhmann HJ. Moderate Hypoxia Followed by Reoxygenation Results in Blood-Brain Barrier Breakdown via Oxidative Stress-Dependent Tight-Junction Protein Disruption. *PLoS ONE*. 2013;8:e82823.
5. Michalik KM, You X, Manavski Y, Doddaballapur A, Zörnig M, Braun T, John D, Ponomareva Y, Chen W, Uchida S, Boon RA, Dimmeler S. Long noncoding RNA MALAT1 regulates endothelial cell function and vessel growth. *Circ Res*. 2014;114:1389–1397.
6. Elbashir SM, Harborth J, Lendeckel W, Yalcin A, Weber K, Tuschl T. Duplexes of 21-nucleotide RNAs mediate RNA interference in cultured mammalian cells. *Nature*. 2001;411:494–498.
7. Perez-Pinera P, Kocak DD, Vockley CM, Adler AF, Kabadi AM, Polstein LR, Thakore PI, Glass KA, Ousterout DG, Leong KW, Guilak F, Crawford GE, Reddy TE, Gersbach CA. RNA-guided gene activation by CRISPR-Cas9–based transcription factors. *Nat Methods*. 2013;10:973–976.
8. Boeckel J-N, Jaé N, Heumüller AW, Chen W, Boon RA, Stellos K, Zeiher AM, John D, Uchida S, Dimmeler S. Identification and Characterization of Hypoxia-Regulated Endothelial Circular RNANovelty and Significance. *Circ Res*. 2015;117:884–890.
9. Voyta JC, Via DP, Butterfield CE, Zetter BR. Identification and isolation of endothelial cells based on their increased uptake of acetylated-low density lipoprotein. *J Cell Biol*. 1984;99:2034–2040.
10. Czupalla CJ, Liebner S, Devraj K. In Vitro Models of the Blood–Brain Barrier. In: Milner R, editor. Cerebral Angiogenesis. New York, NY: Springer New York; 2014:415–437
11. Zehendner CM, Librizzi L, de Curtis M, Kuhlmann CRW, Luhmann HJ. Caspase-3 contributes to ZO-1 and Cl-5 tight-junction disruption in rapid anoxic neurovascular unit damage. *PloS One*. 2011;6:e16760.
12. Juan Carlos Oliveros. Venny. An interactive tool for comparing lists with Venn's diagrams. 2007; Available from: http://bioinfogp.cnb.csic.es/tools/venny/index.html

Online Table V

GO_access	Descriptio	Term_type	Over_repr	Corrected_	CAD_item	CAD_list	Bg_item	Bg_list	Gene_nam	Gene_description
GO:00487	system de	biological_	1,73E-11	2,50E-07	192	429	4269	18769	ENSG0000	RASGRP1|PALLD|ANK3|ADAMTS2|GAB1|ASNS|ROGDI [illegible]
GO:00447	single-org	biological_	3,17E-11	2,50E-07	195	429	4461	18769	ENSG0000	COL18A1|NRXN3|PTPRJ|NREP|ITGA11|DMD|G6PD [illegible]
GO:00072	multicellul	biological_	5,26E-12	2,50E-07	205	429	4798	18769	ENSG0000	EBF1|COL11A1|CCL2|BMPER|ITPR1|ELN|BMPR1A [illegible]
GO:00488	anatomica	biological_	5,36E-11	2,50E-07	210	429	4982	18769	ENSG0000	SLC38A10|PRKCA|ACTG2|BBS9|GCNT4|BMPER [illegible]
GO:00444	extracellul	cellular_co	1,71E-10	6,09E-07	147	429	3708	18769	ENSG0000	ANOS1|FBN2|MGP|PTGIS|SERAC1|CDH2|COL9A2 [illegible]
GO:00325	developme	biological_	1,96E-10	6,09E-07	223	429	5589	18769	ENSG0000	COL14A1|SCN9A|ASNS|GAB1|ROGDI|RBM20|SYNE1 [illegible]
GO:00055	extracellul	cellular_co	4,51E-10	1,21E-06	162	429	4387	18769	ENSG0000	MMP16|KRT17|SND1|MYOF|ACTC1|THBS2|PODN [illegible]
GO:00723	cardiovasc	biological_	9,45E-10	1,96E-06	68	429	897	18769	ENSG0000	SRF|PDLIM5|COL8A1|SFRP2|LOXL1|CX3CL1|PTPRM [illegible]
GO:00723	circulatory	biological_	9,45E-10	1,96E-06	68	429	897	18769	ENSG0000	AHR|EPAS1|CYP1B1|CCL11|STAT1|FOXC1|NRXN3 [illegible]
GO:00301	extracellul	biological_	5,71E-09	1,07E-05	40	429	377	18769	ENSG0000	CCDC80|COL9A2|ELN|COL18A1|COL11A1|MMP16 [illegible]
GO:00430	extracellul	biological_	6,46E-10	1,10E-05	40	429	378	18769	ENSG0000	CRISPLD2|COL21A1|LAMA2|ACAN|SFRP2|LOXL1 [illegible]
GO:00485	organ dev	biological_	1,64E-08	2,55E-05	140	429	3104	18769	ENSG0000	ITGB8|MYH10|LAMA2|MYH9|IGFBP3|NUPR1 [illegible]
GO:00096	anatomica	biological_	3,49E-08	5,02E-05	131	429	2560	18769	ENSG0000	PALLD|ANK3|ROGDI|PTK7|IFT172|ATP10A|ADAM12 [illegible]
GO:00310	extracellul	cellular_co	1,72E-07	2,29E-04	42	429	454	18769	ENSG0000	COL14A1|CLEC3B|LMCD1|SBSPON|TGFB2|COL16A1 [illegible]
GO:00300	cell-substr	cellular_co	2,48E-07	3,09E-04	37	429	391	18769	ENSG0000	ENAH|TES|HSPB1|CSRP1|ACTN1|FERMT2|PARVA [illegible]
GO:00015	blood vess	biological_	3,34E-07	3,90E-04	45	429	553	18769	ENSG0000	CYP1B1|HSPG2|CCL11|GATA6|STAT1|FOXC1|LAMA5 [illegible]
GO:00019	vasculatur	biological_	3,73E-07	3,93E-04	46	429	575	18769	ENSG0000	CDH2|THBS2|NRXN3|PTPRJ|COL18A1|CCL2|BMPER [illegible]
GO:00059	focal adhe	cellular_co	3,78E-07	3,93E-04	36	429	382	18769	ENSG0000	MYH9|CDH13|PDLIM7|TSPAN9|PTK7|FHL1|ENAH [illegible]
GO:00447	single-mul	biological_	4,26E-07	4,20E-04	241	429	6924	18769	ENSG0000	DKK2|ATXN10|GDF6|CRISPLD2|PRPS1|CLSTN2|UBA7 [illegible]
GO:00059	cell-substr	cellular_co	4,77E-07	4,46E-04	36	429	387	18769	ENSG0000	FHL1|PTK7|TSPAN9|PDLIM7|CDH13|MYH9|HSPB1 [illegible]
GO:00325	multicellul	biological_	7,74E-07	6,89E-04	245	429	7149	18769	ENSG0000	SIPA1L1|THBS2|MMP16|SND1|KRT17|ACTC1|MYOF [illegible]
GO:00015	angiogene	biological_	2,05E-06	1,74E-03	36	429	406	18769	ENSG0000	LAMA5|FOXC1|STAT1|GATA6|CCL11|HSPG2|CYP1B1 [illegible]
GO:00485	blood vess	biological_	3,22E-06	2,62E-03	40	429	488	18769	ENSG0000	SRF|JAG1|COL8A1|PTPRM|NPPB|MYH9|CX3CL1 [illegible]
GO:00098	tissue dev	biological_	3,58E-06	2,78E-03	91	429	1800	18769	ENSG0000	MYH9|ITGB8|MYH10|IGFBP3|POSTN|NUPR1|EXT1 [illegible]
GO:00301	cell differe	biological_	4,12E-06	3,08E-03	153	429	3621	18769	ENSG0000	MYH10|MYH9|LAMA2|IGFBP3|NUPR1|SERPINH1 [illegible]
GO:00156	actin cyto	cellular_co	6,67E-07	4,79E-03	40	429	438	18769	ENSG0000	FERMT2|ACTN1|PARVA|PALLD|CNN2|STK38L|MYLK [illegible]
GO:00610	muscle str	biological_	1,45E-05	1,01E-02	46	429	607	18769	ENSG0000	COL14A1|SPEG|SYNE1|DMPK|CACNA1H|MRAS|MSC [illegible]
GO:00488	cellular de	biological_	1,72E-05	1,15E-02	158	429	3857	18769	ENSG0000	SMARCD3|MSI2|ATXN10|GDF6|EXT1|JAG1|TTC3 [illegible]
GO:00059	adherens j	cellular_co	1,94E-05	1,25E-02	39	429	459	18769	ENSG0000	PTK7|FHL1|TSPAN9|CDH13|PDLIM7|MYH9|PTPRM [illegible]
GO:00432	extracellul	cellular_co	3,15E-05	1,84E-02	103	429	2714	18769	ENSG0000	MYOF|COL18A1|ACTC1|SND1|KRT17|PTPRJ|PSAT1 [illegible]
GO:00650	extracellul	cellular_co	3,15E-05	1,84E-02	103	429	2714	18769	ENSG0000	ALDH1L2|CLEC3B|COBLL1|COL14A1|PGM1|GLIPR2 [illegible]
GO:00700	extracellul	cellular_co	3,15E-05	1,84E-02	103	429	2714	18769	ENSG0000	LAMA5|INSR|INPP5A|HSPG2|HMCN1|WARS [illegible]
GO:00701	anchoring	cellular_co	4,83E-05	2,74E-02	39	429	477	18769	ENSG0000	SYNPO2|HSPB1|CSRP1|PARVA|FERMT2|ACTN1 [illegible]
GO:00098	organ mor	biological_	5,07E-05	2,79E-02	56	429	911	18769	ENSG0000	LAMA5|INSR|FOXC1|LRIG3|STAT1|EFEMP1|THBS3 [illegible]
GO:00486	anatomica	biological_	6,39E-05	3,41E-02	62	429	1068	18769	ENSG0000	ATXN10|ANKRD1|CDH13|FAT3|NPPB|PTPRM|MYH9 [illegible]
GO:00037	actin bindi	molecular_	8,27E-05	4,30E-02	38	429	387	18769	ENSG0000	DMD|DIXDC1|NEXN|TPM2|TNS1|CNN1|LMOD1 [illegible]
GO:00055	proteinace	cellular_co	9,95E-05	5,03E-02	35	429	390	18769	ENSG0000	ANOS1|FBN2|MGP|TNFRSF11B|SERAC1|ELN|THBS2 [illegible]
GO:20000	regulation	biological_	1,48E-04	7,26E-02	81	429	1557	18769	ENSG0000	GATA6|INSR|LAMA5|ADCY6|INHBA|DPYSL3|LIMS2 [illegible]
GO:00303	regulation	biological_	1,51E-04	7,26E-02	43	429	592	18769	ENSG0000	CAMK1D|PRKD1|IGF1R|GAB1|NRP2|MYLK|GLIPR2 [illegible]
GO:20001	regulation	biological_	2,22E-04	1,04E-01	44	429	629	18769	ENSG0000	JAG1|PADI2|SRF|ADARB1|SFRP2|CX3CL1|CEMIP [illegible]
GO:00071	cell adhesi	biological_	3,35E-04	1,53E-01	70	429	1092	18769	ENSG0000	SFRP2|CX3CL1|PTPRM|ACAN|FAT3|CDH13|ANTXR1 [illegible]
GO:00226	biological_	biological_	3,65E-04	1,62E-01	70	429	1098	18769	ENSG0000	SRF|COL8A1|PTPRM|ACAN|CX3CL1|SFRP2|ANTXR1 [illegible]
GO:00164	cell migrat	biological_	6,69E-04	2,91E-01	64	429	1140	18769	ENSG0000	ADGRG1|USP9Y|DPYSL3|DOCK1|LAMA5|INSR|CDH2 [illegible]
GO:00507	regulation	biological_	7,60E-04	3,16E-01	95	429	2048	18769	ENSG0000	CYP1B1|FIG4|CUX1|CCL11|EFEMP1|SDC2|STAT1 [illegible]
GO:00484	cell develo	biological_	7,61E-04	3,16E-01	104	429	2078	18769	ENSG0000	FIG4|GSN|CUX1|PLXNA1|STAT1|SDC2|ANKS1A [illegible]
GO:00318	membrane	cellular_co	9,37E-04	3,79E-01	121	429	3447	18769	ENSG0000	SERPINH1|THRB|PTPRS|USO1|CREB5|ARL15 [illegible]
GO:00301	collagen fi	biological_	9,52E-04	3,79E-01	10	429	40	18769	ENSG0000	SFRP2|ACAN|COL14A1|COL11A1|ADAMTS2|CYP1B1 [illegible]
GO:00512	regulation	biological_	1,28E-03	4,97E-01	46	429	692	18769	ENSG0000	SFRP2|CEMIP|CX3CL1|LAMA2|PTPRM|IGFBP3 [illegible]
GO:00444	contractile	cellular_co	1,91E-04	7,28E-01	22	429	200	18769	ENSG0000	TPM2|PDLIM5|JPH2|LMOD1|NEXN|OBSL1|DMD [illegible]
GO:00400	regulation	biological_	2,31E-03	8,62E-01	45	429	692	18769	ENSG0000	COL18A1|CCL2|BMPER|MINK1|PTPRJ|PODN|ITGAV [illegible]
GO:00432	contractile	cellular_co	2,71E-03	9,94E-01	23	429	218	18769	ENSG0000	SYNE1|ACTA2|PDLIM3|CALD1|SYNPO2|ANK3|DES [illegible]
GO:00069	cellular co	biological_	4,49E-03	0.0001613	87	429	1763	18769	ENSG0000	BMPER|CCL2|COL9A2|MINK1|CDH2|PRKCA|TNS1 [illegible]
GO:00015	skeletal sy	biological_	4,84E-04	0.0001706	32	429	467	18769	ENSG0000	SRF|EXT1|POSTN|RASSF2|SERPINH1|ARID5B|IFT172 [illegible]
GO:00300	myofibril	cellular_co	5,27E-03	0.0001823	22	429	206	18769	ENSG0000	FERMT2|MYL9|ACTN1|PALLD|HSPB1|CALD1|SYNPO2 [illegible]
GO:00319	vesicle	cellular_co	5,42E-03	0.0001841	121	429	3559	18769	ENSG0000	STX12|VCAM1|MAN2A1|SNX29|SLC20A2|INADL [illegible]
GO:00512	regulation	biological_	5,78E-03	0.0001929	108	429	2566	18769	ENSG0000	NREP|SEMA5A|DIXDC1|TNFRSF11B|PLCB1|DMD [illegible]
GO:00300	sarcomere	cellular_co	5,88E-03	0.000193	20	429	182	18769	ENSG0000	PDLIM5|LMOD1|JPH2|TPM2|CFL2|CAPZB|DMD [illegible]
GO:00056	extracellul	cellular_co	6,93E-03	0.0002233	51	429	1290	18769	ENSG0000	LMCD1|HSPB1|TGFB2|ACTN1|COL14A1|SIL1|IGFBP2 [illegible]
GO:00488	cell motilit	biological_	8,48E-03	0.0002642	65	429	1239	18769	ENSG0000	MINK1|CDH2|CCL2|BMPER|TNS1|GNA12|PRKCA [illegible]
GO:00516	localizatio	biological_	8,48E-03	0.0002642	65	429	1239	18769	ENSG0000	SEMA5A|ITGA11|PLCB1|ITGAV|NEXN|DIXDC1 [illegible]
GO:00319	insulin-like	molecular_	1,11E-02	0.0003400	5	429	9	18769	ENSG0000	INSR|IGFBP3|IGFBP2|ITGAV|IGF1R|
GO:00457	regulation	biological_	1,28E-03	0.0003871	18	429	193	18769	ENSG0000	SFRP2|CX3CL1|THBS2|PTPRM|NPPB|CCL2|PTGIS [illegible]
GO:00300	actin filam	biological_	1,43E-02	0.0004241	43	429	613	18769	ENSG0000	MICAL1|RHOJ|MYLK|MRAS|ACTN1|PARVA|CNN2 [illegible]
GO:00302	lamellipod	cellular_co	1,51E-02	0.0004418	20	429	164	18769	ENSG0000	ACTC1|ANTXR1|PKD2|MYH10|PTPRM|CDH2|MYO9B [illegible]
GO:00316	I band	cellular_co	1,76E-02	0.0005052	17	429	124	18769	ENSG0000	PDLIM3|DES|SYNPO2|HSPB1|PALLD|MYL9|FERMT2 [illegible]
GO:00300	actin cyto	biological_	1,81E-02	0.0005138	39	429	541	18769	ENSG0000	PLEKHH2|ASAP3|DPYSL3|CCL11|GSN|MICAL2 [illegible]
GO:00426	muscle cel	biological_	1,85E-02	0.0005155	32	429	431	18769	ENSG0000	PDLIM5|JAG1|SRF|NUPR1|CFL2|TMTC3|ADAM12 [illegible]
GO:00400	locomotio	biological_	2,04E-02	0.0005612	80	429	1624	18769	ENSG0000	GLIPR2|RPS6KA2|ANK3|MYLK|CDK6|CNN2|TGFBR1 [illegible]
GO:00300	actin filam	cellular_co	2,12E-02	0.0005748	10	429	52	18769	ENSG0000	DSTN|GSN|MICAL3|LMOD1|MICAL2|MICAL1 [illegible]
GO:19013	regulation	biological_	3,84E-02	0.0010258	18	429	210	18769	ENSG0000	STAT1|HSPB1|ADGRA2|FOXC1|CYP1B1|CCL11 [illegible]
GO:00015	ossificatio	biological_	4,21E-03	0.0011077	25	429	363	18769	ENSG0000	MMP16|SND1|PDLIM7|COL11A1|ID4|IGFBP3 [illegible]
GO:00075	heart deve	biological_	4,45E-02	0.0011555	33	429	465	18769	ENSG0000	COL11A1|ACTC1|BMPR1A|PTPRJ|OXTR|NEXN|JPH2 [illegible]
GO:00071	enzyme lir	biological_	5,92E-02	0.0015157	59	429	1113	18769	ENSG0000	ROR1|FSTL3|PTPRG|PDE1C|USP9Y|INHBA|ADCY6 [illegible]
GO:00220	neurogene	biological_	7,73E-03	0.0019535	80	429	1490	18769	ENSG0000	MAN2A1|ITGAV|DIXDC1|DMD|MICALL1|EPHA5 [illegible]
GO:00055	insulin-like	molecular_	9,14E-02	0.002276	6	429	25	18769	ENSG0000	INSR|ITGAV|IGFBP3|IGFBP2|HTRA1|IGF1R|
GO:00901	tissue mig	biological_	9,25E-02	0.002276	20	429	214	18769	ENSG0000	SEMA5A|PRKCA|ACTG2|SRF|CDH13|ACTC1 [illegible]
GO:00511	striated m	biological_	1,08E-01	0.0026206	26	429	356	18769	ENSG0000	CACNA1H|DMPK|SPEG|COL14A1|GATA6|SORT1 [illegible]
GO:00030	muscle sys	biological_	1,15E-01	0.002756	26	429	365	18769	ENSG0000	MYOF|ACTC1|OXTR|PRKCA|PPP1R12B|DMD|LMOD1 [illegible]
GO:00602	regulation	biological_	1,35E-02	0.0031898	48	429	807	18769	ENSG0000	ADGRG1|STAT1|DPYSL3|SDC2|ADCY6|FOXC1|FIG4 [illegible]
GO:00446	single-org	biological_	1,49E-01	0.0034901	342	429	12562	18769	ENSG0000	ACTN1|ARSB|TMX1|RHOJ|NEGR1|TSPAN2|SLC7A11 [illegible]
GO:00160	cellular co	biological_	1,56E-01	0.0035904	184	429	5464	18769	ENSG0000	HLCS|MICAL2|GBP1|HSPG2|PRICKLE2|INHBA|ADCY6 [illegible]
GO:00082	cell prolife	biological_	1,69E-01	0.0038539	73	429	1895	18769	ENSG0000	PTPRJ|PODN|OSMR|COL18A1|MMP16|VCAM1 [illegible]
GO:00901	mesenchy	biological_	1,74E-02	0.0039256	3	429	5	18769	ENSG0000	ACTC1|ACTG2|ACTA2|
GO:00426	actomyosi	cellular_co	1,78E-01	0.0039568	10	429	62	18769	ENSG0000	FERMT2|ACTN1|MYL9|CNN2|MYLK|ACTC1|PDLIM7 [illegible]
GO:00421	regulation	biological_	1,81E-01	0.0039568	60	429	1468	18769	ENSG0000	VCAM1|PRKCA|SEMA5A|ITGAV|BMPR1A|CDH2 [illegible]
GO:00017	stress fibe	cellular_co	1,82E-01	0.0039568	9	429	52	18769	ENSG0000	PDLIM7|ENAH|MYH9|MYH10|CNN2|MYL9|FERMT2 [illegible]
GO:00485	positive re	biological_	2,07E-02	0.0044435	156	429	4686	18769	ENSG0000	CACNA1H|ACTA2|MCU|PRKD1|TGFB2|ADGRA2 [illegible]
GO:00075	muscle org	biological_	2,13E-01	0.004523	30	429	456	18769	ENSG0000	COL14A1|SPEG|DMPK|ASS1|CACNA1H|TAGLN|MSC [illegible]
GO:00030	heart mor	biological_	2,20E-01	0.0046214	18	429	220	18769	ENSG0000	TEAD1|MICAL2|GATA6|FOXC1|INSR|PARVA|TGFBR1 [illegible]
GO:00080	cytoskelet	molecular_	2,66E-01	0.0055286	48	429	796	18769	ENSG0000	PDLIM3|TAGLN|MYO1D|PLEKHH2|MYL9|GSN|CALD1 [illegible]
GO:00300	cell junctic	cellular_co	3,28E-02	0.0066896	62	429	1121	18769	ENSG0000	LPP|PDCD6IP|OXTR|MINK1|PTPRJ|CDH2|AFAP1 [illegible]
GO:00447	single-org	biological_	3,29E-01	0.0066896	322	429	11641	18769	ENSG0000	INSR|DOCK1|HAPLN1|DPYSL3|CALD1|ASS1|SPON2 [illegible]
GO:00486	generatior	biological_	3,36E-01	0.0067215	75	429	1410	18769	ENSG0000	CDK6|TGFBR1|RPS6KA2|ANK3|ENAH|IFT172|PTK7 [illegible]
[illegible]										
GO:00106	positive re	biological_	0.0034653	0.24631	49	429	1331	18769	ENSG0000	IFT172|JAG1|RASSF2|FBXO18|IGFBP3|CLSTN2 [illegible]
GO:00012	RNA polyn	molecular_	0.0034838	0.24669	3	429	9	18769	ENSG0000	HIVEP1|BACH1|MSC|
GO:00430	camera-ty	biological_	0.0035567	0.25064	17	429	297	18769	ENSG0000	SLC7A11|TGFBR1|FOXC1|EFEMP1|INHBA|CYP1B1 [illegible]
GO:00082	positive re	biological_	0.0035663	0.25064	31	429	806	18769	ENSG0000	CCL11|GATA6|CDK6|TGFBR1|TGFB2|TRAF5|INSR [illegible]
GO:00336	cell adhesi	biological_	0.0035954	0.25173	6	429	64	18769	ENSG0000	ITGA11|TGFB2|SFRP2|CDH2|CYP1B1|COL16A1|
GO:00447	single orga	biological_	0.0036637	0.25556	182	429	6155	18769	ENSG0000	RGS5|THBS2|SIPA1L1|MYOF|DGKI|KRT17|DIXDC1 [illegible]
GO:00308	positive re	biological_	0.0036934	0.25608	3	429	11	18769	ENSG0000	SEMA5A|CFL2|DSTN|
GO:00713	cellular re	biological_	0.0036987	0.25608	69	429	2018	18769	ENSG0000	FOXC1|STAT1|CCL11|CYP1B1|STC2|DAPK1|PDE1C [illegible]
GO:00071	signal tran	biological_	0.0037209	0.25667	164	429	5571	18769	ENSG0000	DIXDC1|RASL10B|PLCB1|EPHA5|SEMA5A|RGS5 [illegible]
GO:00703	ERK1 and I	biological_	0.0037493	0.25768	13	429	232	18769	ENSG0000	STYX|CCL2|BMPER|OXTR|CX3CL1|ITGAV|DMD [illegible]
GO:00071	cell comm	biological_	0.003768	0.25802	184	429	6250	18769	ENSG0000	NXN|DOCK1|INSR|FSTL3|PTPN13|PRKCA|BMPR1A [illegible]
GO:00230	signaling	biological_	0.0037825	0.25806	182	429	6158	18769	ENSG0000	GPC4|GUCY1A2|CCL2|BMPER|ITPR1|BMPR1A|NPR3 [illegible]
GO:00444	cell cortex	cellular_co	0.003897	0.26491	10	429	115	18769	ENSG0000	CDH2|MYH9|DSTN|PKD2|EXOC6B|EXOC4|CALD1 [illegible]
GO:00106	regulation	biological_	0.0039403	0.26689	12	429	151	18769	ENSG0000	GLIPR2|PRKCA|SEMA5A|HSPB1|ADGRA2|ARSB [illegible]
GO:00007	syncytium	biological_	0.0039778	0.26845	6	429	51	18769	ENSG0000	SH3PXD2A|CACNA1H|MYH9|MYOF|ADAM12|STAT1|
GO:00550	cardiac my	biological_	0.0040945	0.27533	4	429	17	18769	ENSG0000	SRF|MYH10|OBSL1|ACTC1|
GO:00506	chondroiti	biological_	0.0041318	0.27684	7	429	60	18769	ENSG0000	CHSY3|HSPG2|GPC6|GPC4|SDC2|UST|ARSB|
GO:00082	heparin bi	molecular_	0.004193	0.27994	10	429	147	18769	ENSG0000	THBS3|POSTN|CFH|ANOS1|CCL2|CRISPLD2|NRP2 [illegible]
GO:00001	MAPK casc	biological_	0.004211	0.28014	31	429	710	18769	ENSG0000	PRKCA|DIXDC1|ITGAV|DMD|PLCB1|DACT1|RASSF2 [illegible]
GO:00708	response t	biological_	0.0043212	0.28595	33	429	707	18769	ENSG0000	ANKRD1|ZEB1|HTRA1|NRP2|GAB1|AKAP13|PRKD1 [illegible]
GO:00072	intracellula	biological_	0.0043289	0.28595	42	429	1102	18769	ENSG0000	PKD2|GDF6|IGFBP3|SFRP2|CX3CL1|TPD52L1|CAPZB [illegible]
GO:00016	osteoblast	biological_	0.004376	0.28762	12	429	200	18769	ENSG0000	BMPR1A|PRKD1|SFRP2|PDLIM7|SND1|ID4|IGFBP3 [illegible]
GO:00125	programm	biological_	0.004416	0.28762	60	429	1837	18769	ENSG0000	SFRP2|TXNIP|CX3CL1|MGMT|TPD52L1|NRBP2 [illegible]
GO:00164	myosin coi	cellular_co	0.0044162	0.28762	7	429	66	18769	ENSG0000	MYH10|MYH9|ACTG2|MYL9|MYO9B|MYO1D|CGNL1 [illegible]
GO:00073	gastrulatic	biological_	0.0044277	0.28762	11	429	186	18769	ENSG0000	COL8A1|INHBA|FOXC1|ITGAV|DACT1|GATA6|SRF [illegible]
GO:00053	inorganic	molecular_	0.0044311	0.28762	2	429	4	18769	ENSG0000	ANKH|SLC20A2|
GO:20010	positive re	biological_	0.0044984	0.29034	3	429	9	18769	ENSG0000	PRKD1|SEMA5A|HSPB1|
GO:00316	response t	biological_	0.004504	0.29034	18	429	431	18769	ENSG0000	NRBP2|CCL2|SFRP2|MGMT|PIP4K2A|TNFRSF11B [illegible]
GO:00518	positive re	biological_	0.0045513	0.29071	2	429	5	18769	ENSG0000	GATA6|TGFB2|
GO:00300	myeloid ce	biological_	0.0045549	0.29071	16	429	339	18769	ENSG0000	G6PD|PRKCA|PIP4K2A|SRF|JAG1|SH3PXD2A|RASSF2 [illegible]
GO:00430	regulation	biological_	0.0045565	0.29071	48	429	1413	18769	ENSG0000	RPS6KA2|MICAL1|AVEN|TGFBR1|TGFB2|ACTN1 [illegible]
GO:00713	cellular re	biological_	0.0046071	0.29294	6	429	83	18769	ENSG0000	ANKRD1|PTGIS|PLCB1|CCL2|CX3CL1|CCL11|
GO:00069	syncytium	biological_	0.0046706	0.29589	6	429	54	18769	ENSG0000	MYH9|SH3PXD2A|CACNA1H|STAT1|ADAM12|MYOF|
GO:00151	L-alanine t	molecular_	0.0047168	0.29589	2	429	7	18769	ENSG0000	SLC36A1|SLC1A4|
GO:00158	L-alanine t	biological_	0.0047168	0.29589	2	429	7	18769	ENSG0000	SLC1A4|SLC36A1|
GO:00228	alanine tra	molecular_	0.0047168	0.29589	2	429	7	18769	ENSG0000	SLC1A4|SLC36A1|
GO:00487	skeletal sy	biological_	0.0048093	0.30069	13	429	218	18769	ENSG0000	THBS3|MGP|FBN2|ARID5B|SERPINH1|TGFBR1 [illegible]
GO:00609	cardiac va	biological_	0.0049058	0.30479	2	429	7	18769	ENSG0000	SRF|GATA6|
GO:00509	positive re	biological_	0.0049075	0.30479	8	429	115	18769	ENSG0000	CDH13|CCL2|PRKD1|CAMK1D|CX3CL1|SEMA5A [illegible]
GO:00343	cell junctic	biological_	0.0049512	0.30555	16	429	218	18769	ENSG0000	CDH11|COL16A1|RAPGEF1|FERMT2|ACTN1|LAMA5 [illegible]
GO:00434	regulation	biological_	0.0049524	0.30555	28	429	644	18769	ENSG0000	STYX|GAB1|IGF1R|GBP1|GLIPR2|RAPGEF1|CCL11 [illegible]
GO:00902	regulation	biological_	0.0050011	0.30754	13	429	191	18769	ENSG0000	SRF|CNN1|MYL9|DMD|PPP1R12B|LMCD1|PRKCA [illegible]
GO:00517	muscle alp	molecular_	0.0050496	0.30892	3	429	9	18769	ENSG0000	PALLD|PKD2|SYNPO2|
GO:00602	hematopo	biological_	0.0050567	0.30892	3	429	16	18769	ENSG0000	FOXC1|CDK6|SRF|
GO:00603	cell chemc	biological_	0.0050999	0.31054	12	429	228	18769	ENSG0000	PRKD1|CX3CL1|CAMK1D|CCL2|CCL11|PADI2|SEMA5A [illegible]
GO:00325	response t	biological_	0.0051594	0.31315	4	429	38	18769	ENSG0000	CCL2|TGFB2|OXTR|TXNIP|
GO:00444	endoplasm	cellular_co	0.0052428	0.31699	38	429	1067	18769	ENSG0000	COL21A1|VTI1A|ARSJ|FADS3|PKD2|CLSTN2 [illegible]
GO:00106	regulation	biological_	0.005267	0.31699	37	429	955	18769	ENSG0000	DACT1|PLCB1|DMD|DIXDC1|PRKCA|SEMA5A|PTPRJ [illegible]
GO:00017	endoderm	biological_	0.0052736	0.31699	5	429	54	18769	ENSG0000	GATA6|COL8A1|INHBA|ITGAV|COL11A1|
GO:00107	positive re	biological_	0.005331	0.31942	2	429	10	18769	ENSG0000	CX3CL1|CCL2|
GO:00343	cell junctic	biological_	0.005488	0.32777	17	429	244	18769	ENSG0000	LIMS2|RSU1|LAMA5|TGFB2|ACTN1|FERMT2|COL16A1 [illegible]
GO:00302	platelet fo	biological_	0.005535	0.32953	3	429	19	18769	ENSG0000	ACTN1|SRF|MYH9|
GO:00081	biological_	biological_	0.0055999	0.33233	398	429	16477	18769	ENSG0000	ZER1|PRKD1|COMMD7|PRSS35|CDKN2B|HSPB1 [illegible]
GO:00550	cardiac mu	biological_	0.0056228	0.33264	9	429	99	18769	ENSG0000	PDLIM5|GATA6|SRF|NEXN|OBSL1|MYH10|SPEG [illegible]
GO:00108	positive re	biological_	0.0056982	0.33603	9	429	99	18769	ENSG0000	CDH13|CCDC80|PTPRJ|RSU1|CDK6|DMD|COL8A1 [illegible]
GO:00400	positive re	biological_	0.0057196	0.33623	19	429	371	18769	ENSG0000	PRKD1|CAMK1D|NRP2|IGF1R|GLIPR2|CCL11|MYLK [illegible]
GO:00509	glucurono	molecular_	0.0057498	0.33628	2	429	3	18769	ENSG0000	EXT1|EXTL1|
GO:00480	CCR chem	molecular_	0.0057755	0.33628	3	429	34	18769	ENSG0000	CCL2|CX3CL1|CCL11|
GO:00097	response t	biological_	0.0057802	0.33628	54	429	1487	18769	ENSG0000	SRF|JAG1|FBXO18|THRB|TXNIP|ABAT|MGMT|HTRA1 [illegible]
GO:00429	regulation	biological_	0.0057924	0.33628	47	429	1400	18769	ENSG0000	MINK1|COL18A1|CCL2|ACTC1|DEPTOR|G6PD|ITGAV [illegible]
GO:00340	response t	biological_	0.0058575	0.33841	24	429	701	18769	ENSG0000	PLCB1|PTGIS|PRKCA|PADI2|SRF|VCAM1|CCL2 [illegible]
GO:00107	positive re	biological_	0.0058835	0.33841	2	429	4	18769	ENSG0000	MICAL2|SRF|
GO:19018	regulation	biological_	0.0058923	0.33841	7	429	76	18769	ENSG0000	CAPZB|PLEKHH2|CFL2|SEMA5A|DSTN|GSN|LMOD1|
GO:00058	cytoskelet	cellular_co	0.005902	0.33841	78	429	2075	18769	ENSG0000	DAPK1|IGF2BP2|MYO1D|TRAF5|GSN|DES|DGKI [illegible]
GO:00364	platelet m	biological_	0.0059195	0.33841	3	429	20	18769	ENSG0000	SRF|MYH9|ACTN1|
GO:00151	L-proline t	molecular_	0.0059951	0.34065	2	429	7	18769	ENSG0000	SLC1A4|SLC36A1|
GO:00352	proline tra	biological_	0.0059951	0.34065	2	429	7	18769	ENSG0000	SLC36A1|SLC1A4|
GO:00071	cell-matrix	biological_	0.0060319	0.3417	14	429	192	18769	ENSG0000	CDH13|PTPRJ|MINK1|THBS3|ITGA11|CDK6|LAMA5 [illegible]
GO:00301	platelet ac	biological_	0.0061371	0.34638	14	429	248	18769	ENSG0000	MYH9|ITPR1|CX3CL1|SLC7A11|DGKI|GNA12|SRF [illegible]
GO:00435	muscle adi	biological_	0.0061517	0.34638	7	429	78	18769	ENSG0000	AKAP13|COL14A1|LMCD1|PRKCA|TEAD1|GATA6 [illegible]
GO:00060	glycosami	biological_	0.0062271	0.34859	6	429	60	18769	ENSG0000	CEMIP|GPC6|HSPG2|ARSB|GPC4|SDC2|
GO:00192	transmem	molecular_	0.0062282	0.34859	9	429	81	18769	ENSG0000	BMPR1A|ROR1|NPTN|NRP2|IGF1R|EPHA5|EFEMP1 [illegible]
GO:00506	positive re	biological_	0.0062641	0.34891	10	429	155	18769	ENSG0000	SEMA5A|PRKCA|TGFBR1|CCL11|CDH13|NRP2|HTRA1 [illegible]
GO:00510	actin filam	biological_	0.0062712	0.34891	2	429	6	18769	ENSG0000	GSN|DSTN|
GO:00480	insulin-like	biological_	0.0063775	0.35377	5	429	38	18769	ENSG0000	IGFBP2|IGFBP3|IGF1R|PLCB1|ATXN1|
GO:00055	collagen bi	molecular_	0.0064373	0.35501	6	429	63	18769	ENSG0000	PODN|ADGRG1|ANTXR1|COL14A1|SERPINH1|ITGA11 [illegible]
GO:00055	phosphati	molecular_	0.0064377	0.35501	6	429	46	18769	ENSG0000	JPH2|SNX18|COMMD1|PLCB1|SYTL2|ASAP1|
GO:00432	lysosomal	cellular_co	0.0064711	0.3558	6	429	75	18769	ENSG0000	ARSB|GPC4|SDC2|GPC6|HSPG2|LGMN|
GO:00480	vascular e	biological_	0.0065198	0.35742	10	429	128	18769	ENSG0000	ITPR1|PRKD1|NRP2|MYOF|CCL2|DOCK1|HSPB1 [illegible]
GO:00071	cell surfac	biological_	0.0065804	0.35969	104	429	3508	18769	ENSG0000	RAMP1|VCAM1|ITGA11|PLCB1|ITGAV|DIXDC1|NREP [illegible]
GO:00067	sulfur com	biological_	0.006616	0.36007	15	429	279	18769	ENSG0000	GPC4|EXTL1|SULT1E1|UST|SDC2|ARSB|G6PD|GCLC [illegible]
GO:00086	diuretic hc	molecular_	0.0066259	0.36007	1	429	1	18769	ENSG0000	NPPB|
GO:00359	skeletal m	biological_	0.0066932	0.36267	9	429	131	18769	ENSG0000	MYH9|DMPK|CACNA1H|ANKRD1|MYOF|NUPR1|DMD [illegible]
GO:00426	regulation	biological_	0.0067165	0.36288	2	429	7	18769	ENSG0000	BMPR1A|SFRP2|
GO:00517	positive re	biological_	0.0068078	0.36491	2	429	10	18769	ENSG0000	KRT17|TGFB2|
GO:00022	endothelia	biological_	0.0068278	0.36491	1	429	1	18769	ENSG0000	C8orf4|
GO:00165	negative n	biological_	0.0068333	0.36491	6	429	67	18769	ENSG0000	STAT1|FOXC1|CCL2|NPPB|PTPRM|THBS2|
GO:00016	eye develc	biological_	0.0068395	0.36491	18	429	341	18769	ENSG0000	SLC7A11|RHOJ|CYP1B1|FOXC1|TGFBR1|TGFB2|INHBA [illegible]
GO:00509	regulation	biological_	0.0068515	0.36491	10	429	153	18769	ENSG0000	CDH13|CCL2|PRKD1|CX3CL1|CAMK1D|HSPB1|PRKCA [illegible]

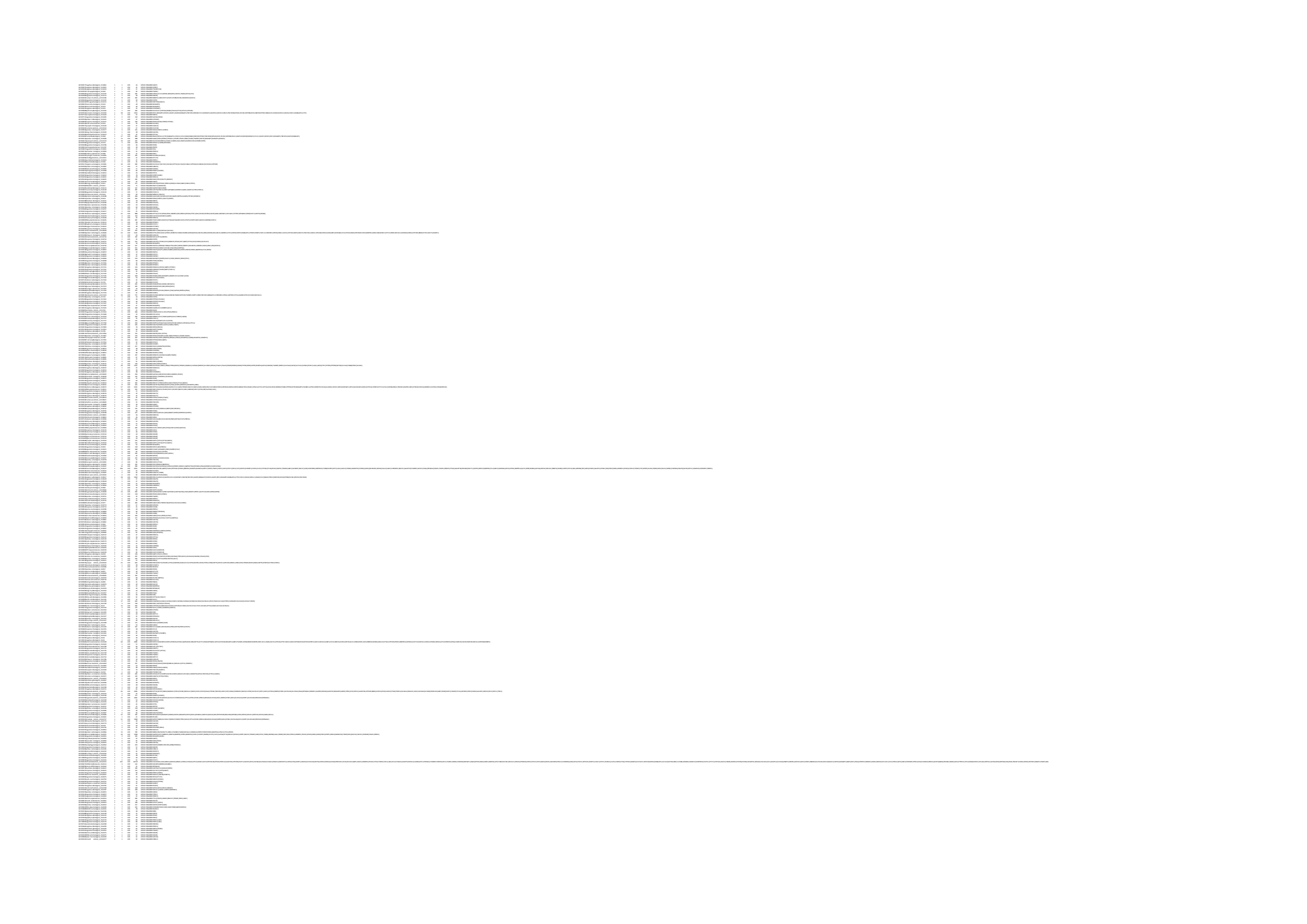

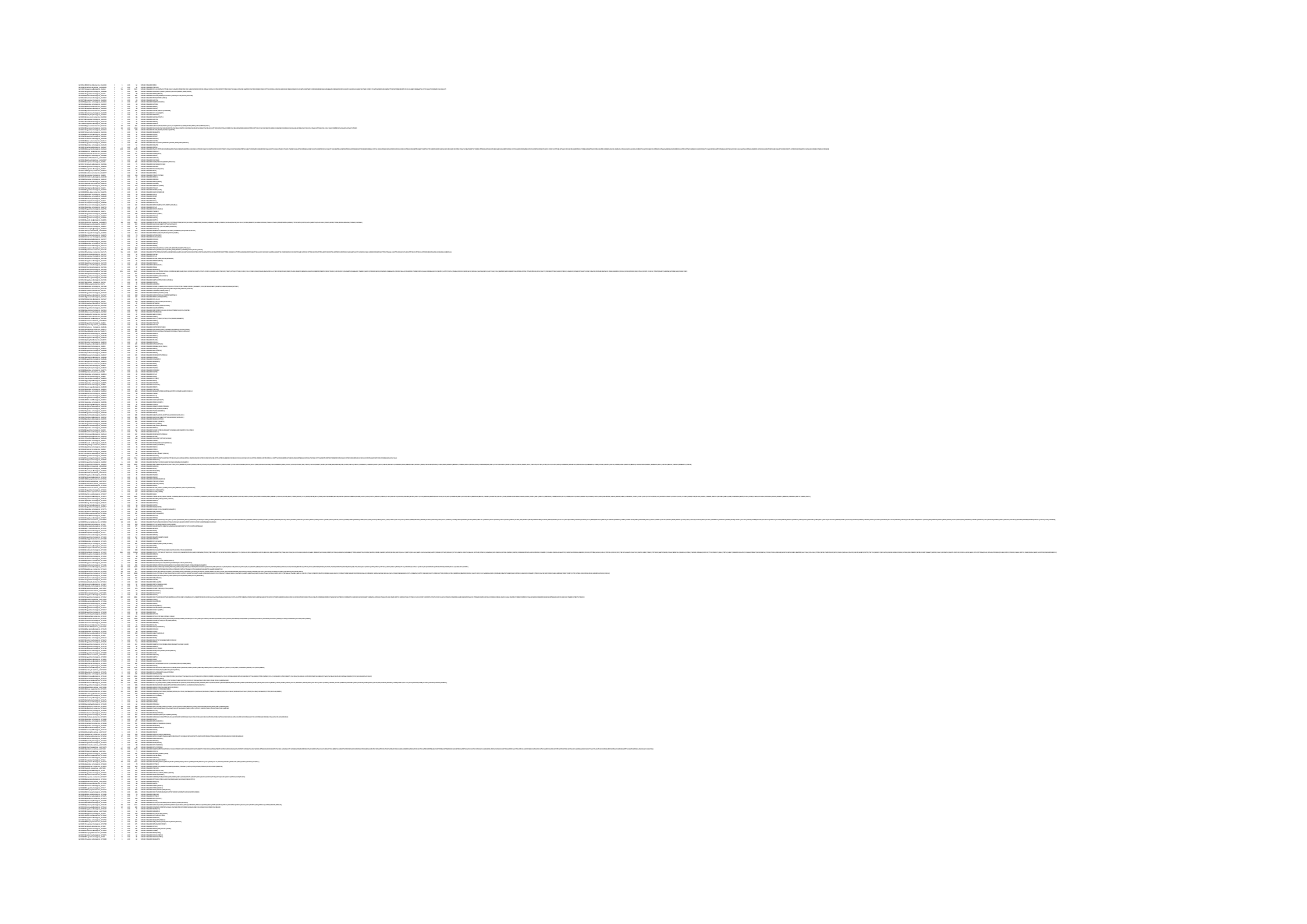

Online Table VI

Statistic method: hypergeometric test

FDR correction method: Benjamini and Hochberg

Term	Sample number	Background number	P-value	Corrected P-value	UniGenes	KO	Entrez ID	Ensembl ID
Dilated cardiomyopathy	12	90	6,12E+06	0.00611546192107	ENSG00000105855 ENSG00000159251 ENSG00000175084 ENSG00000198947 ENSG00000174233 ENSG00000092969 ENSG00000153956 ENSG00000198467 ENSG00000137809 ENSG00000196569 ENSG00000138448 ENSG00000075461	hsa:3696 hsa:70 hsa:1674 hsa:1756 hsa:112 hsa:7042 hsa:781 hsa:7169 hsa:22801 hsa:3908 hsa:3685 hsa:27092	3696 70 1674 1756 112 7042 781 7169 22801 3908 3685 27092	ITGB8 ACTC1, ACTC, ASD5, CMD1R, CMH11, LVNC4 DES, CSM1, CSM2, LGMD2R DMD, BMD, CMD3B, DXS142, DXS164, DXS206, DXS230, DXS239, DXS268, DXS269, DXS270, DXS272, MRX85 ADCY6, AC6 TGFB2, LDS4, TGF-beta CACNA2, CACNL2A, CCHL2A, LINC01112, lncRNA-N3, MHS3 TPM2, AMCD1, DA1, DA2B, HEL-S-273, NEM4, TMSB ITGA11, HsT18964 LAMA2, LAMM ITGAV, CD51, MSK8, VNRA, VTNR CACNG4
Vascular smooth muscle contraction	14	121	6,30E+06	0.00611546192107	ENSG00000101335 ENSG00000065534 ENSG00000132329 ENSG00000174233 ENSG00000146535 ENSG00000107796 ENSG00000122786 ENSG00000163017 ENSG00000150995 ENSG00000077157 ENSG00000182621 ENSG00000072952 ENSG00000152402 ENSG00000154229	hsa:10398 hsa:4638 hsa:10267 hsa:112 hsa:10672 hsa:59 hsa:800 hsa:59 hsa:3708 hsa:4659 hsa:23236 hsa:10335 hsa:2977 hsa:5578	10398 4638 10267 112 10672 59 800 59 3708 4659 23236 10335 2977 5578	MYL9, LC20, MLC-2C, MLC2, MRLC1, MYRL2 MYLK, AAT7, KRP, MLCK, MLCK1, MLCK108, MLCK210, MSTP083, MYLK1, smMLCK RAMP1 ADCY6, AC6 GNA13, G13 ACTA2, AAT6, ACTSA, MYMY5 CALD1, CDM, H-CAD, HCAD, L-CA NAG22 ACTA2, AAT6, ACTSA, MYMY5 ITPR1, ACV, CLA4, INSP3R1, IP3R, IP3R1, PPP1R94, SCA15, SCA16, SCA29 PPP1R12A, M130, MBS, MYPT1 PLCB1, EIEE12, PI-PLC, PLC-154, PLC-I, PLC154, PLCB1A, PLCB1B MRVI1, IRAG, JAW GC-SA2, GUC1A2 PRKCA, AAG6, PKC-alpha, PKCA, PRKACA
Hypertrophic cardiomyopathy (HCM)	11	83	0.000128991468902	0.00834144832231	ENSG00000105855 ENSG00000159251 ENSG00000175084 ENSG00000198947 ENSG00000092969 ENSG00000153956 ENSG00000198467 ENSG00000137809 ENSG00000196569 ENSG00000138448 ENSG00000075461	hsa:3696 hsa:70 hsa:1674 hsa:1756 hsa:7042 hsa:781 hsa:7169 hsa:22801 hsa:3908 hsa:3685 hsa:27092	3696 70 1674 1756 7042 781 7169 22801 3908 3685 27092	ITGB8 ACTC1, ACTC, ASD5, CMD1R, CMH11, LVNC4 DES, CSM1, CSM2, LGMD2R DMD, BMD, CMD3B, DXS142, DXS164, DXS206, DXS230, DXS239, DXS268, DXS269, DXS270, DXS272, MRX85 TGFB2, LDS4, TGF-beta2 CACNA2D1 CACNL2A, CCHL2A, LINC01112, lncRNA-N3, MHS3 TPM2, AMCD1, DA1, DA2B, HEL-S-273, NEM4, TMSB ITGA11, HsT18964 LAMA2, LAMM ITGAV, CD51, MSK8, VNRA, VTNR CACNG4
Focal adhesion	18	207	0.000185472949355	0.00871065206167	ENSG00000060718 ENSG00000101335 ENSG00000065534 ENSG00000186340 ENSG00000081052 ENSG00000169231 ENSG00000130702 ENSG00000105855 ENSG00000150760 ENSG00000140443 ENSG00000072110 ENSG00000197702 ENSG00000077157 ENSG00000137809 ENSG00000107263 ENSG00000196569 ENSG00000154229 ENSG00000138448	hsa:1301 hsa:10398 hsa:4638 hsa:7058 hsa:1286 hsa:7059 hsa:3911 hsa:3696 hsa:1793 hsa:3480 hsa:87 hsa:55742 hsa:4659 hsa:22801 hsa:2889 hsa:3908 hsa:5578 hsa:3685	1301 10398 4638 7058 1286 7059 3911 3696 1793 3480 87 55742 4659 22801 2889 3908 5578 3685	COL11A1, CO11A1, COLL6, STL2 MYL9, LC20, MLC-2C, MLC2, MRLC1, MYRL2 MYLK, AAT7, KRP, MLCK, MLCK1, MLCK108, MLCK210, MSTP083, MYLK1, smMLCK THBS2, TSP2 COL4A4, CA44 THBS3, TSP3 LAMA5 ITGB8 DOCK1, D IGF1R, CD221, IGFIR, IGFR, JTK13 ACTN1, BDPLT15 PARVA, CH-ILKBP, MXRA2 PPP1R12A, M130, MBS, MYPT1 ITGA11, HsT18964 RAPGEF1, C3G, GRF2 LAMA2, LAMM PRKCA, AAG6, PKC-alpha, PKCA, PRKACA ITGAV, CD51, MSK VTNR
Arrhythmogenic right ventricular cardiomyopathy (ARVC)	10	74	0.000224501341796	0.00871065206167	ENSG00000105855 ENSG00000175084 ENSG00000198947 ENSG00000153956 ENSG00000072110 ENSG00000170558 ENSG00000137809 ENSG00000196569 ENSG00000138448 ENSG00000075461	hsa:3696 hsa:1674 hsa:1756 hsa:781 hsa:87 hsa:1000 hsa:22801 hsa:3908 hsa:3685 hsa:27092	3696 1674 1756 781 87 1000 22801 3908 3685 27092	ITGB8 DES, CSM1, CSM2, LGMD2R DMD, BMD, CMD3B, DXS142, DXS164, DXS206, DXS230, DXS239, DXS268, DXS269, DXS270, DXS272, MRX85 CACNA2D1, CACNA2, CACNL2A, CCHL2A, LINC01112, lncRNA-N3, MHS3 ACTN1, CD325, CDHN, CDw325, NCAD ITGA11, HsT18964 LAMA2, LAMM ITGAV, CD51, MSK8, VNRA, VTNR CACNG4
ECM-receptor interaction	10	87	0.000719609304565	0.0232673675143	ENSG00000060718 ENSG00000105855 ENSG00000186340 ENSG00000081052 ENSG00000169231 ENSG00000130702 ENSG00000137809 ENSG00000142798 ENSG00000196569 ENSG00000138448	hsa:1301 hsa:3696 hsa:7058 hsa:1286 hsa:7059 hsa:3911 hsa:22801 hsa:3339 hsa:3908 hsa:3685	1301 3696 7058 1286 7059 3911 22801 3339 3908 3685	COL11A1, CO11A1, COLL6, STL2 ITGB8 THBS2, TSP2 COL4A4, CA44 THBS3, TSP3 LAMA5 ITGA11, HsT18964 HSPG2, HSPG, PLC, PRCAN, SJA, SJS, SJS1 LAMA2, LAMM ITGAV, CD51, MSK8, VNRA, VTNR
cGMP-PKG signaling pathway	14	167	0.00128645539576	0.0356531923969	ENSG00000171105 ENSG00000065534 ENSG00000101335 ENSG00000120937 ENSG00000174233 ENSG00000151729 ENSG00000150995 ENSG00000146592 ENSG00000077157 ENSG00000182621 ENSG00000072952 ENSG00000152402 ENSG00000146535 ENSG00000112658	hsa:3643 hsa:4638 hsa:10398 hsa:4879 hsa:112 hsa:291 hsa:3708 hsa:9586 hsa:4659 hsa:23236 hsa:10335 hsa:2977 hsa:10672 hsa:6722	3643 4638 10398 4879 112 291 3708 9586 4659 23236 10335 2977 10672 6722	INSR, CD220, HHF5 MYLK, AAT7, KRP, MLCK, MLCK1, MLCK108, MLCK210, MSTP083, MYLK1, smMLCK MYL9, LC20, MLC-2C, MLC2, MRLC1, MYRL2 NPPB, BNP ADCY6, AC6 SLC25A4, 1, AAC1, ANT, ANT_1, ANT1, MTDPS12, PEO ITPR1, ACV, CLA4, INSP3R1, IP3R, IP3R1, PPP1R94, SCA15, SCA16, SCA29 CREB5, CRE-BPA PPP1R12A, M130, MBS, MYPT1 PLCB1, EIEE12, PI-PLC, PLC-154, PLC-I, PLC154, PLCB1A, PLCB1B MRVI1, IRAG, JAW1L GUCY1A2, GC-SA GNA13, G13 SRF, MCM1
Regulation of actin cytoskeleton	16	215	0.00191363395271	0.0464056233533	ENSG00000105855 ENSG00000101335 ENSG00000065534 ENSG00000100345 ENSG00000150867 ENSG00000146535 ENSG00000133026 ENSG00000158186 ENSG00000165410 ENSG00000072110 ENSG00000148180 ENSG00000077157 ENSG00000137809 ENSG00000154380 ENSG00000150760 ENSG00000138448	hsa:3696 hsa:10398 hsa:4638 hsa:4627 hsa:5305 hsa:10672 hsa:4628 hsa:22808 hsa:1073 hsa:87 hsa:2934 hsa:4659 hsa:22801 hsa:55740 hsa:1793 hsa:3685	3696 10398 4638 4627 5305 10672 4628 22808 1073 87 2934 4659 22801 55740 1793 3685	ITGB8 MYL9, LC20, MLC-2C, MLC2, MRLC1, MYRL2 MYLK, AAT7, KRP, MLCK, MLCK1, MLCK108, MLCK210, MSTP083, MYLK1, smMLCK MYH9, BDPLT6, DFNA17, EPSTS, FTNS, MHA, NMHC-II-A, NMMHC-IIA, NMMHCA PIP4K2A, PIP5K2A, PIP5KII-alpha, PIP5KIIA, PIPK GNA13, G13 MYH10, NMMHC-IIB, NMMHCB MRAS, M-RAs, R-RAS3, RRAS3 CFL2, NEM7 ACTN1, BDPLT15 GSN, ADF, AGEL PPP1R12A, M130, MBS, MYPT1 ITGA11, HsT18964 ENAH, ENA, DOCK1, DOCK180, ced5 ITGAV, CD51, MSK8, VNRA, VTNR
Malaria	6	49	0.00622769826901	0.134241496021	ENSG00000108691 ENSG00000186340 ENSG00000169231 ENSG00000092969 ENSG00000162692 ENSG00000169439	hsa:6347 hsa:7058 hsa:7059 hsa:7042 hsa:7412 hsa:6383	6347 7058 7059 7042 7412 6383	CCL2, GDCF-2, HC11, HSMCR30, MCAF, MCP-1, MCP1, SCYA2, SMC-CF THBS2, TSP2 THBS3, TSP3 TGFB2, LDS4, TGF-beta2 VCAM1, CD106, INCAM-100 SDC2, CD362, HSPG, HSPG1, SYND2
Protein digestion and absorption	8	89	0.00928698285471	0.172813232725	ENSG00000060718 ENSG00000124749 ENSG00000123643 ENSG00000182871 ENSG00000049540 ENSG00000049089 ENSG00000187955 ENSG00000081052	hsa:1301 hsa:81578 hsa:206358 hsa:80781 hsa:2006 hsa:1298 hsa:7373 hsa:1286	1301 81578 206358 80781 2006 1298 7373 1286	COL11A1, CO11A1, COLL6, STL2 COL21A1, COLA1L, dJ682J15.1, dJ708F5.1 SLC36A1, Dct1, LYAAT1, PAT1, TRAMD3 COL18A1, KNO, KNO1, KS ELN, SVAS, WBS, WS COL9A2, DJ39G22.4, EDM2, MED, STL5 COL14A1, UND COL4A4
Amoebiasis	9	109	0.00979868845346	0.172813232725	ENSG00000060718 ENSG00000092969 ENSG00000081052 ENSG00000130702 ENSG00000106211 ENSG00000072110 ENSG00000182621 ENSG00000196569 ENSG00000154229	hsa:1301 hsa:7042 hsa:1286 hsa:3911 hsa:3315 hsa:87 hsa:23236 hsa:3908 hsa:5578	1301 7042 1286 3911 3315 87 23236 3908 5578	COL11A1, CO11A1, COLL6, STL2 TGFB2, LDS4, TGF-beta2 COL4A4, CA44 LAMA5 HSPB1, CMT2F, HEL-S-102, HMN2B, HS.76067, HSP27, HSP28, Hsp25, SRP27 ACTN1, BDPLT15 PLCB1, EIEE12, PI-PLC, PLC-154, PLC-I, PLC154, PLC LAMA2, LAMM PRKCA, AAG6, PKC-alpha, PKCA, PRKACA
Oxytocin signaling pathway	11	159	0.0147830593552	0.220628678466	ENSG00000101335 ENSG00000065534 ENSG00000075461 ENSG00000174233 ENSG00000153956 ENSG00000183049 ENSG00000150995 ENSG00000077157 ENSG00000182621 ENSG00000152402 ENSG00000154229	hsa:10398 hsa:4638 hsa:27092 hsa:112 hsa:781 hsa:57118 hsa:3708 hsa:4659 hsa:23236 hsa:2977 hsa:5578	10398 4638 27092 112 781 57118 3708 4659 23236 2977 5578	MYL9, LC20, MLC-2C, MLC2, MRLC1, MYRL2 MYLK, AAT7, KRP, MLCK, MLCK1, MLCK108, MLCK210, MSTP083, MYLK1, smMLCK CACNG4 ADCY6, AC6 CACNA2D1, CACNA2, CACNL2A, CCHL2A, LINC01112, lncRNA-N3, MHS3 CAM CaM-K1, CaMKID ITPR1, ACV, CLA4, INSP3R1, IP3R, IP3R1, PPP1R94, SCA15, SCA16, SCA29 PPP1R12A, M130, MBS, MYPT1 PLCB1, EIEE12, PI-PLC, PLC-154, PLC-I, PLC154, PLCB1A, PLCB1B GUCY1A2, GC-SA2, GUC1A2 PRKCA, A alpha, PKCA, PRKACA
Long-term depression	6	60	0.0147843959797	0.220628678466	ENSG00000150995 ENSG00000146535 ENSG00000140443 ENSG00000182621 ENSG00000152402 ENSG00000154229	hsa:3708 hsa:10672 hsa:3480 hsa:23236 hsa:2977 hsa:5578	3708 10672 3480 23236 2977 5578	ITPR1, ACV, CLA4, INSP3R1, IP3R, IP3R1, PPP1R94, SCA15, SCA16, SCA29 GNA13, G13 IGF1R, CD221, IGFIR, IGFR, JTK13 PLCB1, EIEE12, PI-PLC, PLC-154, PLC-I, PLC154, PLCB1A, PLCB1B GUCY1A2, GC-SA2, GUC1A2 PRKCA, AAG6 PKCA, PRKACA
TGF-beta signaling pathway	7	80	0.0164623798728	0.228121549666	ENSG00000147883 ENSG00000106799 ENSG00000092969 ENSG00000107779 ENSG00000156466 ENSG00000122641 ENSG00000172201	hsa:1030 hsa:7046 hsa:7042 hsa:657 hsa:392255 hsa:3624 hsa:3400	1030 7046 7042 657 392255 3624 3400	CDKN2B, CDK4I, INK4B, MTS2, P15, TP15, p15INK4b TGFBR1, AAT5, ACVRLK4, ALK-5, ALK5, ESS1, LDS1, LDS1A, LDS2A, MSSE, SKR4, TGFR-1 TGFB2, LDS4, TGF-beta2 BMPR1A, 10q23del, ACVRLK3, ALK3, CD292, SKR5 GDF6, BM CDMP2, KFM, KFS, KFS1, KFSL, LCA17, MCOP4, MCOPCB6, SCDO4, SGM1 INHBA, EDF, FRP ID4, IDB4, bHLHb27
Mucin type O-Glycan biosynthesis	4	31	0.0207928138275	0.268920392168	ENSG00000176928 ENSG00000110328 ENSG00000164574 ENSG00000143641	hsa:51301 hsa:374378 hsa:55568 hsa:2590	51301 374378 55568 2590	GCNT4, C2GNT3 GALNT18, GALNACT18, GALNT15, GALNTL4, GalNAc-T15, GalNAc-T18 GALNT10, GALNACT10, PPGALNACT10, PPGANTASE10 GALNT2, GalNAc-T2
Small cell lung cancer	7	86	0.0228983579113	0.277642589674	ENSG00000147883 ENSG00000081052 ENSG00000130702 ENSG00000105810 ENSG00000082512 ENSG00000196569 ENSG00000138448	hsa:1030 hsa:1286 hsa:3911 hsa:1021 hsa:7188 hsa:3908 hsa:3685	1030 1286 3911 1021 7188 3908 3685	CDKN2B, CDK4I, INK4B, MTS2, P15, TP15, p15INK4b COL4A4, CA44 LAMA5 CDK6, PLSTIRE TRAF5, MGC:39780, RNF84 LAMA2, LAMM ITGAV, CD51, MSK8, VNRA, VTNR
Platelet activation	9	131	0.0269503098923	0.307550595241	ENSG00000060718 ENSG00000172575 ENSG00000065534 ENSG00000174233 ENSG00000150995 ENSG00000077157 ENSG00000182621 ENSG00000152402 ENSG00000146535	hsa:1301 hsa:10125 hsa:4638 hsa:112 hsa:3708 hsa:4659 hsa:23236 hsa:2977 hsa:10672	1301 10125 4638 112 3708 4659 23236 2977 10672	COL11A1, CO11A1, COLL6, STL2 RASGRP1, CALDAG-GEFI, CALDAG-GEFII, RASGRP, V, hRasGRP1 MYLK, AAT7, KRP, MLCK, MLCK1, MLCK108, MLCK210, MSTP083, MYLK1, smMLCK ADCY6, AC6 ITPR1, ACV, CLA4, INSP3R1, IP3R, PPP1R94, SCA15, SCA16, SCA29 PPP1R12A, M130, MBS, MYPT1 PLCB1, EIEE12, PI-PLC, PLC-154, PLC-I, PLC154, PLCB1A, PLCB1B GUCY1A2, GC-SA2, GUC1A2 GNA13, G13
Proteoglycans in cancer	12	204	0.0324266057398	0.333543037298	ENSG00000150995 ENSG00000124749 ENSG00000092969 ENSG00000158186 ENSG00000151150 ENSG00000140443 ENSG00000109458 ENSG00000169439 ENSG00000077157 ENSG00000142798 ENSG00000154229 ENSG00000138448	hsa:3708 hsa:81578 hsa:7042 hsa:22808 hsa:288 hsa:3480 hsa:2549 hsa:6383 hsa:4659 hsa:3339 hsa:5578 hsa:3685	3708 81578 7042 22808 288 3480 2549 6383 4659 3339 5578 3685	ITPR1, ACV, CLA4, INSP3R1, IP3R, IP3R1, PPP1R94, SCA15, SCA16, SCA29 COL21A1, COLA1L, dJ682J15.1, dJ708F5.1 TGFB2, LDS4, TGF-beta2 MRAS, M-RAs, R-RAS3, RRAS3 ANK3, ANKYRIN-G, MRT37 IGF1R, CD221, IGFIR, IGFR, SDC2, CD362, HSPG, HSPG1, SYND2 PPP1R12A, M130, MBS, MYPT1 HSPG2, HSPG, PLC, PRCAN, SJA, SJS, SJS1 PRKCA, AAG6, PKC-alpha, PKCA, PRKACA ITGAV, CD51, MSK8, VNRA, VTNR
Adherens junction	6	73	0.0326665861271	0.333543037298	ENSG00000171105 ENSG00000106799 ENSG00000140443 ENSG00000149177 ENSG00000173482 ENSG00000072110	hsa:3643 hsa:7046 hsa:3480 hsa:5795 hsa:5797 hsa:87	3643 7046 3480 5795 5797 87	INSR, CD220, HHF5 TGFBR1, AAT5, ACVRLK4, ALK-5, ALK5, ESS1, LDS1, LDS1A, LDS2A, MSSE, SKR4, TGFR-1 IGF1R, CD221, IGFIR, IGFR, JTK13 PTPRJ, CD148, DEP1, HPTPeta, R-PTP-ETA, SCC1 PTPRM, PTPRL1, R-PTP-MU, RPTPM, PTPu ACTN1, BDPLT15
Phosphatidylinositol signaling system	6	81	0.0486569188068	0.471972112426	ENSG00000150995 ENSG00000150867 ENSG00000068383 ENSG00000157680 ENSG00000182621 ENSG00000154229	hsa:3708 hsa:5305 hsa:3632 hsa:9162 hsa:23236 hsa:5578	3708 5305 3632 9162 23236 5578	ITPR1, ACV, CLA4, INSP3R1, IP3R, IP3R1, PPP1R94, SCA15, SCA16, SCA29 PIP4K2A, PI5P4KA, PIP5K2A, PIP5KII-alpha, PIP5KIIA, PIPK INPP5A, 5PTASE DGKI, DGK-IOTA PLCB1, EIEE12, PI-PLC, PLC-154, PLC-I, PLC154, PLCB1A, PLCB AAG6, PKC-alpha, PKCA, PRKACA
Pentose phosphate pathway	3	28	0.066509951845	0.596110739196	ENSG00000079739 ENSG00000147224 ENSG00000160211	hsa:5236 hsa:5634 hsa:2539	5236 5634 2539	PGM1, CDG1T, GSD14 PRPS2, PRSII G6PD, G6PD1
Tight junction	8	134	0.0676001869191	0.596110739196	ENSG00000101335 ENSG00000100345 ENSG00000131558 ENSG00000132849 ENSG00000158186 ENSG00000072110 ENSG00000133026 ENSG00000154229	hsa:10398 hsa:4627 hsa:60412 hsa:10207 hsa:22808 hsa:87 hsa:4628 hsa:5578	10398 4627 60412 10207 22808 87 4628 5578	MYL9, LC20, MLC-2C, MLC2, MRLC1, MYRL2 MYH9, BDPLT6, DFNA17, EPSTS, FTNS, MHA, NMHC-II-A, NMMHC-IIA, NMMHCA EXOC4, SEC8, SEC8L1, Sec8p INADL, Cipp, PATJ, hINADL MRAS, M-RAs, R-RAS3, RRAS3 ACTN1, BDPL NMMHC-IIB, NMMHCB PRKCA, AAG6, PKC-alpha, PKCA, PRKACA
Thyroid hormone synthesis	5	72	0.0842500703335	0.685793004186	ENSG00000150995 ENSG00000182621 ENSG00000146592 ENSG00000174233 ENSG00000154229	hsa:3708 hsa:23236 hsa:9586 hsa:112 hsa:5578	3708 23236 9586 112 5578	ITPR1, ACV, CLA4, INSP3R1, IP3R, IP3R1, PPP1R94, SCA15, SCA16, SCA29 PLCB1, EIEE12, PI-PLC, PLC-154, PLC-I, PLC154, PLCB1A, PLCB1B CREB5, CRE-BPA ADCY6, AC6 PRKCA, AAG6, PKC-alpha, PKCA, PRKACA
Ovarian steroidogenesis	4	51	0.0849953562404	0.685793004186	ENSG00000171105 ENSG00000140443 ENSG00000174233 ENSG00000138061	hsa:3643 hsa:3480 hsa:112 hsa:1545	3643 3480 112 1545	INSR, CD220, HHF5 IGF1R, CD221, IGFIR, IGFR, JTK13 ADCY6, AC6 CYP1B1, CP1B, CYPIB1, GLC3A, P4501B1
Circadian entrainment	6	97	0.0929830035448	0.685793004186	ENSG00000150995 ENSG00000174233 ENSG00000182621 ENSG00000152402 ENSG00000154229 ENSG00000196557	hsa:3708 hsa:112 hsa:23236 hsa:2977 hsa:5578 hsa:8912	3708 112 23236 2977 5578 8912	ITPR1, ACV, CLA4, INSP3R1, IP3R, IP3R1, PPP1R94, SCA15, SCA16, SCA29 ADCY6, AC6 PLCB1, EIEE12, PI-PLC, PLC-154, PLC-I, PLC154, PLCB1A, PLCB1B GUCY1A2, GC-SA2, GUC1A2 PRKCA, AAG6, PKC-alpha, PKCA, PRKACA CACN CACNA1HB, Cav3.2, ECA6, EIG6
Cell adhesion molecules (CAMs)	8	145	0.0942951040262	0.685793004186	ENSG00000105855 ENSG00000172260 ENSG00000021645 ENSG00000170558 ENSG00000162692 ENSG00000169439 ENSG00000173482 ENSG00000138448	hsa:3696 hsa:257194 hsa:9369 hsa:1000 hsa:7412 hsa:6383 hsa:5797 hsa:3685	3696 257194 9369 1000 7412 6383 5797 3685	ITGB8 NEGR1, DMML2433, IGLON4, KILON, Ntra NRXN3, C14orf60 CDH2, CD325, CDHN, CDw325, NCAD VCAM1, CD106, INCAM-100 SDC2, CD362, HSPG, HSPG1, SYND2 PTPRM, PTPRL1, R-PTP-MU, RPTPM, RPTPU, hR-PTPu IT MSK8, VNRA, VTNR
Gastric acid secretion	5	75	0.0954454181083	0.685793004186	ENSG00000150995 ENSG00000182621 ENSG00000065534 ENSG00000174233 ENSG00000154229	hsa:3708 hsa:23236 hsa:4638 hsa:112 hsa:5578	3708 23236 4638 112 5578	ITPR1, ACV, CLA4, INSP3R1, IP3R, IP3R1, PPP1R94, SCA15, SCA16, SCA29 PLCB1, EIEE12, PI-PLC, PLC-154, PLC-I, PLC154, PLCB1A, PLCB1B MYLK, AAT7, KRP, MLCK, MLCK1, MLCK108, MLCK210, MSTP083, MYLK1, smMLCK ADCY AAG6, PKC-alpha, PKCA, PRKACA
African trypanosomiasis	3	34	0.100906379112	0.693319507522	ENSG00000162692 ENSG00000182621 ENSG00000154229	hsa:7412 hsa:23236 hsa:5578	7412 23236 5578	VCAM1, CD106, INCAM-100 PLCB1, EIEE12, PI-PLC, PLC-154, PLC-I, PLC154, PLCB1A, PLCB1B PRKCA, AAG6, PKC-alpha, PKCA, PRKACA
Adrenergic signaling in cardiomyocytes	8	149	0.105304012743	0.693319507522	ENSG00000159251 ENSG00000075461 ENSG00000174233 ENSG00000153956 ENSG00000198467 ENSG00000146592 ENSG00000182621 ENSG00000154229	hsa:70 hsa:27092 hsa:112 hsa:781 hsa:7169 hsa:9586 hsa:23236 hsa:5578	70 27092 112 781 7169 9586 23236 5578	ACTC1, ACTC, ASD5, CMD1R, CMH11, LVNC4 CACNG4 ADCY6, AC6 CACNA2D1, CACNA2, CACNL2A, CCHL2A, LINC01112, lncRNA-N3, MHS3 TPM2, AMCD1, DA1, DA2B, HEL-S-273, NEM4, TMSB CREB5, CRE-BPA PLCB1, EIEE12, I 154, PLC-I, PLC154, PLCB1A, PLCB1B PRKCA, AAG6, PKC-alpha, PKCA, PRKACA
Alanine, aspartate and glutamate metabolism	3	35	0.107214356833	0.693319507522	ENSG00000070669 ENSG00000183044 ENSG00000130707	hsa:440 hsa:18 hsa:445	440 18 445	ASNS, ASNSD, TS11 ABAT, GABA-AT, GABAT, NPD009 ASS1, ASS, CTLN1
TNF signaling pathway	6	110	0.140780020255	0.799838376139	ENSG00000108691 ENSG00000006210 ENSG00000162692 ENSG00000146592 ENSG00000082512 ENSG00000101384	hsa:6347 hsa:6376 hsa:7412 hsa:9586 hsa:7188 hsa:182	6347 6376 7412 9586 7188 182	CCL2, GDCF-2, HC11, HSMCR30, MCAF, MCP-1, MCP1, SCYA2, SMC-CF CX3CL1, ABCD-3, C3Xkine, CXC3, CXC3C, NTN, NTT, SCYD1, fractalkine, neurotactin VCAM1, CD106, INCAM-100 CREB5, CRE-BPA TRAF5, MGC:39780, RNF8 AHD, AWS, CD339, HJ1, JAGL1
Glycosaminoglycan biosynthesis - chondroitin sulfate / dermatan sulfate	2	20	0.142402247219	0.799838376139	ENSG00000111962 ENSG00000198108	hsa:10090 hsa:337876	10090 337876	UST, 2OST CHSY3, CHSY2, CSS3
Biosynthesis of unsaturated fatty acids	2	21	0.152987893093	0.799838376139	ENSG00000099194 ENSG00000206527	hsa:6319 hsa:201562	6319 201562	SCD, FADS5, MSTP008, SCD1, SCDOS PTPLB, HACD2
Pathways in cancer	14	327	0.15609572185	0.799838376139	ENSG00000115415 ENSG00000092969 ENSG00000105810 ENSG00000081052 ENSG00000106799 ENSG00000130702 ENSG00000082512 ENSG00000140443 ENSG00000116016 ENSG00000147883 ENSG00000196730 ENSG00000196569 ENSG00000154229 ENSG00000138448	hsa:6772 hsa:7042 hsa:1021 hsa:1286 hsa:7046 hsa:3911 hsa:7188 hsa:3480 hsa:2034 hsa:1030 hsa:1612 hsa:3908 hsa:5578 hsa:3685	6772 7042 1021 1286 7046 3911 7188 3480 2034 1030 1612 3908 5578 3685	STAT1, CANDF7, ISGF-3, STAT91 TGFB2, LDS4, TGF-beta2 CDK6, PLSTIRE COL4A4, CA44 TGFBR1, AAT5, ACVRLK4, ALK-5, ALK5, ESS1, LDS1, LDS1A, LDS2A, MSSE, SKR4, TGFR-1 LAMA5 TRAF5, MGC:39780, RNF84 IGF1R, CD221, JTK13 EPAS1, ECYT4, HIF2A, HLF, MOP2, PASD2, bHLHe73 CDKN2B, CDK4I, INK4B, MTS2, P15, TP15, p15INK4b DAPK1, DAPK LAMA2, LAMM PRKCA, AAG6, PKC-alpha, PKCA, PRKACA ITGAV, CD51, MSK8, VNRA, VTNR
Gap junction	5	89	0.156672577732	0.799838376139	ENSG00000152402 ENSG00000182621 ENSG00000150995 ENSG00000174233 ENSG00000154229	hsa:2977 hsa:23236 hsa:3708 hsa:112 hsa:5578	2977 23236 3708 112 5578	GUCY1A2, GC-SA2, GUC1A2 PLCB1, EIEE12, PI-PLC, PLC-154, PLC-I, PLC154, PLCB1A, PLCB1B ITPR1, ACV, CLA4, INSP3R1, IP3R, IP3R1, PPP1R94, SCA15, SCA16, SCA29 ADCY6, AC6 PRKCA, AAG6, PKC-alpha, PKCA, PRKACA
Salivary secretion	5	90	0.161557204034	0.799838376139	ENSG00000152402 ENSG00000182621 ENSG00000150995 ENSG00000174233 ENSG00000154229	hsa:2977 hsa:23236 hsa:3708 hsa:112 hsa:5578	2977 23236 3708 112 5578	GUCY1A2, GC-SA2, GUC1A2 PLCB1, EIEE12, PI-PLC, PLC-154, PLC-I, PLC154, PLCB1A, PLCB1B ITPR1, ACV, CLA4, INSP3R1, IP3R, IP3R1, PPP1R94, SCA15, SCA16, SCA29 ADCY6, AC6 PRKCA, AAG6, PKC-alpha, PKCA, PRKACA
Pancreatic cancer	4	66	0.162456745328	0.799838376139	ENSG00000105810 ENSG00000106799 ENSG00000092969 ENSG00000115415	hsa:1021 hsa:7046 hsa:7042 hsa:6772	1021 7046 7042 6772	CDK6, PLSTIRE TGFBR1, AAT5, ACVRLK4, ALK-5, ALK5, ESS1, LDS1, LDS1A, LDS2A, MSSE, SKR4, TGFR-1 TGFB2, LDS4, TGF-beta2 STAT1, CANDF7, ISGF-3, STAT91
Renal cell carcinoma	4	66	0.162456745328	0.799838376139	ENSG00000116016 ENSG00000107263 ENSG00000109458 ENSG00000092969	hsa:2034 hsa:2889 hsa:2549 hsa:7042	2034 2889 2549 7042	EPAS1, ECYT4, HIF2A, HLF, MOP2, PASD2, bHLHe73 RAPGEF1, C3G, GRF2 GAB1 TGFB2, LDS4, TGF-beta2
Fc gamma R-mediated phagocytosis	5	91	0.166502478218	0.799838376139	ENSG00000148180 ENSG00000088280 ENSG00000165410 ENSG00000154229 ENSG00000153317	hsa:2934 hsa:55616 hsa:1073 hsa:5578 hsa:50807	2934 55616 1073 5578 50807	GSN, ADF, AGEL ASAP3, ACAP4, CENTB6, DDEFL1, UPLC1 CFL2, NEM7 PRKCA, AAG6, PKC-alpha, PKCA, PRKACA ASAP1, AMAP1, CENTB4, DDEF1, PAG2, PAP, ZG14P
Long-term potentiation	4	67	0.168329605159	0.799838376139	ENSG00000182621 ENSG00000150995 ENSG00000154229 ENSG00000071242	hsa:23236 hsa:3708 hsa:5578 hsa:6196	23236 3708 5578 6196	PLCB1, EIEE12, PI-PLC, PLC-154, PLC-I, PLC154, PLCB1A, PLCB1B ITPR1, ACV, CLA4, INSP3R1, IP3R, IP3R1, PPP1R94, SCA15, SCA16, SCA29 PRKCA, AAG6, PKC-alpha, PKCA, PRKACA RPS6KA2, HU-2, MAPKAPK1C, RSK, RSK3, S6K-a alpha2, p90-RSK3, pp90RSK3
Thyroid hormone signaling pathway	6	119	0.179325235115	0.799838376139	ENSG00000151090 ENSG00000115415 ENSG00000108510 ENSG00000182621 ENSG00000154229 ENSG00000138448	hsa:7068 hsa:6772 hsa:9969 hsa:23236 hsa:5578 hsa:3685	7068 6772 9969 23236 5578 3685	THRB, C-ERBA-2, C-ERBA-BETA, ERBA2, GRTH, NR1A2, PRTH, THR1, THRB1, THRB2 STAT1, CANDF7, ISGF-3, STAT91 MED13, ARC250, DRIP250, HSPC221, THRAP1, TRAP240 PLCB1, EIEE12, PI-PLC, PLC-154, PLC-I, PLC154, PLCB1 PRKCA, AAG6, PKC-alpha, PKCA, PRKACA ITGAV, CD51, MSK8, VNRA, VTNR
Hepatitis B	7	146	0.183289808034	0.799838376139	ENSG00000115415 ENSG00000106799 ENSG00000092969 ENSG00000105810 ENSG00000146592 ENSG00000142798 ENSG00000154229	hsa:6772 hsa:7046 hsa:7042 hsa:1021 hsa:9586 hsa:3339 hsa:5578	6772 7046 7042 1021 9586 3339 5578	STAT1, CANDF7, ISGF-3, STAT91 TGFBR1, AAT5, ACVRLK4, ALK-5, ALK5, ESS1, LDS1, LDS1A, LDS2A, MSSE, SKR4, TGFR-1 TGFB2, LDS4, TGF-beta2 CDK6, PLSTIRE CREB5, CRE-BPA HSPG2, HSPG, PLC, PRCAN, SJA, SJS, SJS1 PRKCA, alpha, PKCA, PRKACA
Glycosaminoglycan biosynthesis - heparan sulfate / heparin	2	24	0.185550270232	0.799838376139	ENSG00000158008 ENSG00000182197	hsa:2134 hsa:2131	2134 2131	EXTL1, EXTL EXT1, EXT, LGCR, LGS, TRPS2, TTV
Pancreatic secretion	5	96	0.192083696278	0.799838376139	ENSG00000080493 ENSG00000182621 ENSG00000150995 ENSG00000174233 ENSG00000154229	hsa:8671 hsa:23236 hsa:3708 hsa:112 hsa:5578	8671 23236 3708 112 5578	SLC4A4, HNBC1, KNBC, NBC1, NBC2, NBCe1-A, SLC4A5, hhNMC, pNBC PLCB1, EIEE12, PI-PLC, PLC-154, PLC-I, PLC154, PLCB1A, PLCB1B ITPR1, ACV, CLA4, INSP3R1, IP3R, IP3R1, PPP1R94, SCA15, SCA16, SCA29 ADCY6, AC6 PRKC alpha, PKCA, PRKACA
MAPK signaling pathway	11	257	0.192139784667	0.799838376139	ENSG00000172575 ENSG00000075461 ENSG00000071242 ENSG00000106799 ENSG00000092969 ENSG00000153956 ENSG00000158186 ENSG00000106211 ENSG00000196557 ENSG00000154229 ENSG00000112658	hsa:10125 hsa:27092 hsa:6196 hsa:7046 hsa:7042 hsa:781 hsa:22808 hsa:3315 hsa:8912 hsa:5578 hsa:6722	10125 27092 6196 7046 7042 781 22808 3315 8912 5578 6722	RASGRP1, CALDAG-GEFI, CALDAG-GEFII, RASGRP, V, hRasGRP1 CACNG4 RPS6KA2, HU-2, MAPKAPK1C, RSK, RSK3, S6K-alpha, S6K-alpha2, p90-RSK3, pp90RSK3 TGFBR1, AAT5, ACVRLK4, ALK-5, ALK5, ESS1, LDS1, LDS1A, LDS2A, TGFR-1 TGFB2, LDS4, TGF-beta2 CACNA2D1, CACNA2, CACNL2A, CCHL2A, LINC01112, lncRNA-N3, MHS3 MRAS, M-RAs, R-RAS3, RRAS3 HSPB1, CMT2F, HEL-S-102, HMN2B, HS.76067, HSP27, HSP28, Hsp25, SRP27 CACNA1H, C. Cav3.2, ECA6, EIG6 PRKCA, AAG6, PKC-alpha, PKCA, PRKACA SRF, MCM1
Fatty acid metabolism	3	47	0.192848817313	0.799838376139	ENSG00000099194 ENSG00000206527 ENSG00000110090	hsa:6319 hsa:201562 hsa:1374	6319 201562 1374	SCD, FADS5, MSTP008, SCD1, SCDOS PTPLB, HACD2 CPT1A, CPT1, CPT1-L, L-CPT1
Vitamin B6 metabolism	1	6	0.193775276693	0.799838376139	ENSG00000135069	hsa:29968	29968	PSAT1, EPIP, PSA, PSAT
Endocrine and other factor-regulated calcium reabsorption	3	48	0.200633525187	0.810893830964	ENSG00000182621 ENSG00000174233 ENSG00000154229	hsa:23236 hsa:112 hsa:5578	23236 112 5578	PLCB1, EIEE12, PI-PLC, PLC-154, PLC-I, PLC154, PLCB1A, PLCB1B ADCY6, AC6 PRKCA, AAG6, PKC-alpha, PKCA, PRKACA
PI3K-Akt signaling pathway	14	347	0.208615613648	0.825947531584	ENSG00000060718 ENSG00000171105 ENSG00000186340 ENSG00000081052 ENSG00000169231 ENSG00000130702 ENSG00000105855 ENSG00000105810 ENSG00000140443 ENSG00000146592 ENSG00000137809 ENSG00000196569 ENSG00000154229 ENSG00000138448	hsa:1301 hsa:3643 hsa:7058 hsa:1286 hsa:7059 hsa:3911 hsa:3696 hsa:1021 hsa:3480 hsa:9586 hsa:22801 hsa:3908 hsa:5578 hsa:3685	1301 3643 7058 1286 7059 3911 3696 1021 3480 9586 22801 3908 5578 3685	COL11A1, CO11A1, COLL6, STL2 INSR, CD220, HHF5 THBS2, TSP2 COL4A4, CA44 THBS3, TSP3 LAMA5 ITGB8 CDK6, PLSTIRE IGF1R, CD221, IGFIR, IGFR, JTK13 CREB5, CRE-BPA ITGA11, HsT18964 LAMA2, LAMM PRKCA, AAG6, PK PKCA, PRKACA ITGAV, CD51, MSK8, VNRA, VTNR
Rap1 signaling pathway	9	211	0.225150677963	0.873584630498	ENSG00000171105 ENSG00000184304 ENSG00000174233 ENSG00000197555 ENSG00000158186 ENSG00000140443 ENSG00000182621 ENSG00000107263 ENSG00000154229	hsa:3643 hsa:5587 hsa:112 hsa:26037 hsa:22808 hsa:3480 hsa:23236 hsa:2889 hsa:5578	3643 5587 112 26037 22808 3480 23236 2889 5578	INSR, CD220, HHF5 PRKD1, PKC-MU, PKCM, PKD, PRKCM ADCY6, AC6 SIPA1L1, E6TP1 MRAS, M-RAs, R-RAS3, RRAS3 IGF1R, CD221, IGFIR, IGFR, JTK13 PLCB1, EIEE12, PI-PLC, PLC-154, PLC-I, PLC154, PLCB1A, PLCB1B RAPGEF1, PRKCA, AAG6, PKC-alpha, PKCA, PRKACA
Cardiac muscle contraction	4	78	0.237185815571	0.902236239623	ENSG00000198467 ENSG00000159251 ENSG00000075461 ENSG00000153956	hsa:7169 hsa:70 hsa:27092 hsa:781	7169 70 27092 781	TPM2, AMCD1, DA1, DA2B, HEL-S-273, NEM4, TMSB ACTC1, ACTC, ASD5, CMD1R, CMH11, LVNC4 CACNG4 CACNA2D1, CACNA2, CACNL2A, CCHL2A, LINC01112, lncRNA-N3, MHS3
beta-Alanine metabolism	2	30	0.252818983208	0.943209283507	ENSG00000183044 ENSG00000137124	hsa:18 hsa:219	18 219	ABAT, GABA-AT, GABAT, NPD009 ALDH1B1, ALDH5, ALDHX
Wnt signaling pathway	6	140	0.282228159523	0.999932625528	ENSG00000163637 ENSG00000145423 ENSG00000076716 ENSG00000155011 ENSG00000182621 ENSG00000154229	hsa:166336 hsa:6423 hsa:2239 hsa:27123 hsa:23236 hsa:5578	166336 6423 2239 27123 23236 5578	PRICKLE2, EPM5 SFRP2, FRP-2, SARP1, SDF-5 GPC4, K-glypican DKK2, DKK-2 PLCB1, EIEE12, PI-PLC, PLC-154, PLC-I, PLC154, PLCB1A, PLCB1B PRKCA, AAG6, PKC-alpha, PKCA, PRKACA
Cholinergic synapse	5	113	0.287338529128	0.999932625528	ENSG00000150995 ENSG00000182621 ENSG00000146592 ENSG00000174233 ENSG00000154229	hsa:3708 hsa:23236 hsa:9586 hsa:112 hsa:5578	3708 23236 9586 112 5578	ITPR1, ACV, CLA4, INSP3R1, IP3R, IP3R1, PPP1R94, SCA15, SCA16, SCA29 PLCB1, EIEE12, PI-PLC, PLC-154, PLC-I, PLC154, PLCB1A, PLCB1B CREB5, CRE-BPA ADCY6, AC6 PRKCA, AAG6, PKC-alpha, PKCA, PRKACA
Insulin secretion	4	86	0.290751930534	0.999932625528	ENSG00000182621 ENSG00000146592 ENSG00000174233 ENSG00000154229	hsa:23236 hsa:9586 hsa:112 hsa:5578	23236 9586 112 5578	PLCB1, EIEE12, PI-PLC, PLC-154, PLC-I, PLC154, PLCB1A, PLCB1B CREB5, CRE-BPA ADCY6, AC6 PRKCA, AAG6, PKC-alpha, PKCA, PRKACA
Signaling pathways regulating pluripotency of stem cells	6	142	0.292697113241	0.999932625528	ENSG00000145623 ENSG00000140836 ENSG00000107779 ENSG00000140443 ENSG00000122641 ENSG00000172201	hsa:3977 hsa:463 hsa:657 hsa:3480 hsa:3624 hsa:3400	3977 463 657 3480 3624 3400	LIFR, CD118, LIF-R, SJS2, STWS, SWS ZFHX3, ATBF1, ATBT, ZNF927 BMPR1A, 10q23del, ACVRLK3, ALK3, CD292, SKR5 IGF1R, CD221, IGFIR, IGFR, JTK13 INHBA, EDF, FRP ID4, IDB4, bHLHb27
Inositol phosphate metabolism	3	61	0.306529522489	0.999932625528	ENSG00000150867 ENSG00000182621 ENSG00000068383	hsa:5305 hsa:23236 hsa:3632	5305 23236 3632	PIP4K2A, PI5P4KA, PIP5K2A, PIP5KII-alpha, PIP5KIIA, PIPK PLCB1, EIEE12, PI-PLC, PLC-154, PLC-I, PLC154, PLCB1A, PLCB1B INPP5A, 5PTASE
Arginine and proline metabolism	3	61	0.306529522489	0.999932625528	ENSG00000137124 ENSG00000126790 ENSG00000130707	hsa:219 hsa:112849 hsa:445	219 112849 445	ALDH1B1, ALDH5, ALDHX L3HYPDH, C14orf149 ASS1, ASS, CTLN1
Viral carcinogenesis	8	206	0.323340195633	0.999932625528	ENSG00000147883 ENSG00000197157 ENSG00000105810 ENSG00000148180 ENSG00000146592 ENSG00000072110 ENSG00000082512 ENSG00000112658	hsa:1030 hsa:27044 hsa:1021 hsa:2934 hsa:9586 hsa:87 hsa:7188 hsa:6722	1030 27044 1021 2934 9586 87 7188 6722	CDKN2B, CDK4I, INK4B, MTS2, P15, TP15, p15INK4b SND1, TDRD11, p100 CDK6, PLSTIRE GSN, ADF, AGEL CREB5, CRE-BPA ACTN1, BDPLT15 TRAF5, MGC:39780, RNF84 SRF, MCM1
GnRH signaling pathway	4	92	0.331915622487	0.999932625528	ENSG00000182621 ENSG00000150995 ENSG00000174233 ENSG00000154229	hsa:23236 hsa:3708 hsa:112 hsa:5578	23236 3708 112 5578	PLCB1, EIEE12, PI-PLC, PLC-154, PLC-I, PLC154, PLCB1A, PLCB1B ITPR1, ACV, CLA4, INSP3R1, IP3R, IP3R1, PPP1R94, SCA15, SCA16, SCA29 ADCY6, AC6 PRKCA, AAG6, PKC-alpha, PKCA, PRKACA

Calcium signaling pathway	7	180	0.3391177494	0.999932	ENSG00000150995 ENSG00000151729 ENSG00000065534 ENSG00000154678 ENSG00000182621 ENSG00000154229	hsa:3708 hsa:291 hsa:4638 hsa:5137 hsa:23236 hsa:5578 hsa:8912	3708 291 4638 5137 23236 5578 8912	ITPR1, ACV, CLA4, INSP3R1, IP3R, IP3R1, PPP1R9A, SCA1S, SCA16, SCA29 SLC25A4, 1, AAC1, ANT, ANT_1, ANT1, MTDPS12, PEO2, PEO3, T1 MYLK, AAT7, KRP, MLCK, MLCK1, MLCK108, MLCK210, MSTP083, MYLK1, smMLCK PD
Glioma	3	65	0.3398758983	0.999932	ENSG00000196557 ENSG00000105810 ENSG00000140443 ENSG00000154229	hsa:1021 hsa:3480 hsa:5578	1021 3480 5578	cam-PDE_1C, hCam-3 PLCB1, EIEE12, PI-PLC, PLC-154, PLC-I, PLC154, PLCB1A, PLCB1B PRKCA, AAG6, PKC-alpha, PKCA, PRKACA CACNA1H, CACNA1HB, Cav3.2, EC46, EIG6 CDK6, PLSTIRE IGF1R, CD221, IGFIR, IGFR, ITK13 PRKCA, AAG6, PKC-alpha, PKCA, PRKACA
AMPK signaling pathway	5	124	0.3529288026	0.999932	ENSG00000171105 ENSG00000140443 ENSG00000146592 ENSG00000099194 ENSG00000110090	hsa:3643 hsa:3480 hsa:9586 hsa:6319 hsa:1374	3643 3480 9586 6319 1374	INSR, CD220, HHF5 IGF1R, CD221, IGFIR, IGFR, ITK13 CREB5, CRE-BPA SCD, FADS5, MSTP008, SCD1, SCDO5 CPT1A, CPT1, CPT1-L, L-CPT1
Aldosterone-regulated sodium reabsorption	2	39	0.3539649565	0.999932	ENSG00000171105 ENSG00000154229	hsa:3643 hsa:5578	3643 5578	INSR, CD220, HHF5 PRKCA, AAG6, PKC-alpha, PKCA, PRKACA
Hippo signaling pathway	6	154	0.3568039029	0.999932	ENSG00000132849 ENSG00000106799 ENSG00000092969 ENSG00000187079 ENSG00000107779 ENSG00000156466	hsa:10207 hsa:7046 hsa:7042 hsa:7003 hsa:657 hsa:392255	10207 7046 7042 7003 657 392255	INADL, Cpp, PATJ, hINADL TGFBR1, AAT5, ACVRLK4, ALK-5, ALK5, ESS1, LDS1, LDS1A, LDS2A, MSSE, SKR4, TGFR-1 TGFB2, LDS4, TGF-beta2 TEAD1, AA, NTEF-1, REF1, TCF-13, TCF13, TEAD-1, TEF-1 BMPR1A, 10q23del, ACVRLK3
p53 signaling pathway	3	68	0.3648234687	0.999932	ENSG00000146674 ENSG00000105810 ENSG00000149212	hsa:3486 hsa:1021 hsa:143686	3486 1021 143686	SKR5 GDF6, BMP-13, BMP13, CDMP2, KFM, KF5, KFS1, LCA17, MCOPI4, MCOPCB6, SCDO4, SGM1 IGFBP3, BP-53, IBP3 CDK6, PLSTIRE SESN3, SEST3
Pyruvate metabolism	2	40	0.3649683766	0.999932	ENSG00000065833 ENSG00000137124	hsa:4199 hsa:219	4199 219	ME1, HUMNDME, MES ALDH1B1, ALDH5, ALDHX
Tryptophan metabolism	2	40	0.3649683766	0.999932	ENSG00000138061 ENSG00000137124	hsa:1545 hsa:219	1545 219	CYP1B1, CP1B, CYPIB1, GLC3A, P450181 ALDH1B1, ALDH5, ALDHX
Axon guidance	5	127	0.3710023434	0.999932	ENSG00000114554 ENSG00000165410 ENSG00000153993 ENSG00000112902 ENSG00000145242	hsa:5361 hsa:1073 hsa:223117 hsa:9037 hsa:2044	5361 1073 223117 9037 2044	PLXNA1, NOV, NOVP, PLEXIN-A1, PLXN1 CFL2, NEM7 SEMA3D, Sema-22, coll-2 SEMA5A, SEMAF, semF EPHA5, CEK7, EHK-1, EHK1, EK7, HEK7, TYRO4
PPAR signaling pathway	3	69	0.3731081109	0.999932	ENSG00000065833 ENSG00000099194 ENSG00000110090	hsa:4199 hsa:6319 hsa:1374	4199 6319 1374	ME1, HUMNDME, MES SCD, FADS5, MSTP008, SCD1, SCDO5 CPT1A, CPT1, CPT1-L, L-CPT1
Inflammatory mediator regulation of TRP channels	4	99	0.3802339553	0.999932	ENSG00000182621 ENSG00000150995 ENSG00000174233 ENSG00000154229	hsa:23236 hsa:3708 hsa:112 hsa:5578	23236 3708 112 5578	PLCB1, EIEE12, PI-PLC, PLC-154, PLC-I, PLC154, PLCB1A, PLCB1B ITPR1, ACV, CLA4, INSP3R1, IP3R, IP3R1, PPP1R9A, SCA1S, SCA16, SCA29 ADCY6, AC6 PRKCA, AAG6, PKC-alpha, PKCA, PRKACA
Estrogen signaling pathway	4	100	0.3871209919	0.999932	ENSG00000150995 ENSG00000182621 ENSG00000146592 ENSG00000174233	hsa:3708 hsa:23236 hsa:9586 hsa:112	3708 23236 9586 112	ITPR1, ACV, CLA4, INSP3R1, IP3R, IP3R1, PPP1R9A, SCA1S, SCA16, SCA29 PLCB1, EIEE12, PI-PLC, PLC-154, PLC-I, PLC154, PLCB1A, PLCB1B CREB5, CRE-BPA ADCY6, AC6
Chronic myeloid leukemia	3	73	0.4060036143	0.999932	ENSG00000105810 ENSG00000106799 ENSG00000092969	hsa:1021 hsa:7046 hsa:7042	1021 7046 7042	CDK6, PLSTIRE TGFBR1, AAT5, ACVRLK4, ALK-5, ALK5, ESS1, LDS1, LDS1A, LDS2A, MSSE, SKR4, TGFR-1 TGFB2, LDS4, TGF-beta2
Retrograde endocannabinoid signaling	4	103	0.4077140915	0.999932	ENSG00000182621 ENSG00000150995 ENSG00000174233 ENSG00000154229	hsa:23236 hsa:3708 hsa:112 hsa:5578	23236 3708 112 5578	PLCB1, EIEE12, PI-PLC, PLC-154, PLC-I, PLC154, PLCB1A, PLCB1B ITPR1, ACV, CLA4, INSP3R1, IP3R, IP3R1, PPP1R9A, SCA1S, SCA16, SCA29 ADCY6, AC6 PRKCA, AAG6, PKC-alpha, PKCA, PRKACA
Fatty acid degradation	2	44	0.4082023457	0.999932	ENSG00000137124 ENSG00000110090	hsa:219 hsa:1374	219 1374	ALDH1B1, ALDH5, ALDHX CPT1A, CPT1, CPT1-L, L-CPT1
Valine, leucine and isoleucine degradation	2	44	0.4082023457	0.999932	ENSG00000183044 ENSG00000137124	hsa:18 hsa:219	18 219	ABAT, GABA-AT, GABAT, NPD009 ALDH1B1, ALDH5, ALDHX
FoxO signaling pathway	5	134	0.4131925038	0.999932	ENSG00000171105 ENSG00000140443 ENSG00000092969 ENSG00000147883 ENSG00000106799	hsa:3643 hsa:3480 hsa:7042 hsa:1030 hsa:7046	3643 3480 7042 1030 7046	INSR, CD220, HHF5 IGF1R, CD221, IGFIR, IGFR, ITK13 TGFB2, LDS4, TGF-beta2 CDKN2B, CDK4I, INK4B, MTS2, P15, TP15, p15INK4b TGFBR1, AAT5, ACVRLK4, ALK-5, ALK5, ESS1, LDS1, LDS1A, LDS2A, MSSE, SKR4, TGFR-1
Biosynthesis of amino acids	3	74	0.4141516573	0.999932	ENSG00000147224 ENSG00000130707 ENSG00000135069	hsa:5634 hsa:445 hsa:29968	5634 445 29968	PRPS2, PRSI ASS1, ASS, CTLN1 PSAT1, EPIP, PSA, PSAT G6PD, G6PD1
Chagas disease (American trypanosomiasis)	4	104	0.4145494935	0.999932	ENSG00000108691 ENSG00000106799 ENSG00000092969 ENSG00000182621	hsa:6347 hsa:7046 hsa:7042 hsa:23236	6347 7046 7042 23236	CCL2, GDCF-2, HC11, HSMCR30, MCAF, MCP-1, MCP1, SCYA2, SMC-CF TGFBR1, AAT5, ACVRLK4, ALK-5, ALK5, ESS1, LDS1, LDS1A, LDS2A, MSSE, SKR4, TGFR-1 TGFB2, LDS4, TGF-beta2 PLCB1, EIEE12, PI-PLC, PLC-154, PLC-I, PLC PLCB1B
Vasopressin-regulated water reabsorption	2	45	0.4187865983	0.999932	ENSG00000174233 ENSG00000146592	hsa:112 hsa:9586	112 9586	ADCY6, AC6 CREB5, CRE-BPA
Carbon metabolism	4	106	0.4281660123	0.999932	ENSG00000065833 ENSG00000147224 ENSG00000135069 ENSG00000160211	hsa:4199 hsa:5634 hsa:29968 hsa:2539	4199 5634 29968 2539	ME1, HUMNDME, MES PRPS2, PRSII PSAT1, EPIP, PSA, PSAT G6PD, G6PD1
Cytokine-cytokine receptor interaction	9	265	0.4503369134	0.999932	ENSG00000108691 ENSG00000172156 ENSG00000145623 ENSG00000006210 ENSG00000106799 ENSG00000092969 ENSG00000107779 ENSG00000164761 ENSG00000122641	hsa:6347 hsa:6356 hsa:3977 hsa:6376 hsa:7046 hsa:7042 hsa:657 hsa:4982 hsa:3624	6347 6356 3977 6376 7046 7042 657 4982 3624	CCL2, GDCF-2, HC11, HSMCR30, MCAF, MCP-1, MCP1, SCYA2, SMC-CF CCL11, SCYA11 LIFR, CD118, LIF-R, SIS2, STWS, SWS CX3CL1, ABCD-3, C3Xkine, CXC3, CXC3C, NTN, NTT, SCYD1, fractalkine, neurotactin TGFBR1, AAT5, ACV ALK5, ESS1, LDS1, LDS1A, LDS2A, MSSE, SKR4, TGFR-1 TGFB2, LDS4, TGF-beta2 BMPR1A, 10q23del, ACVRLK3, ALK3, CD292, SKR5 TNFRSF11B, OCIF, OPG, TR1 INHBA, EDF, FRP
Oocyte meiosis	3	110	0.4551347150	0.999932	ENSG00000140443 ENSG00000150995 ENSG00000174233 ENSG00000071242	hsa:3480 hsa:3708 hsa:112 hsa:6196	3480 3708 112 6196	IGF1R, CD221, IGFIR, IGFR, ITK13 ITPR1, ACV, CLA4, INSP3R1, IP3R, IP3R1, PPP1R9A, SCA1S, SCA16, SCA29 ADCY6, AC6 RPS6KA2, HU-2, MAPKAPK1C, RSK, RSK3, S6K-alpha, S6K-alpha2, p90-RSK3, pp90RSK3
Glutathione metabolism	2	49	0.4601288919	0.999932	ENSG00000001084 ENSG00000160211	hsa:2729 hsa:2539	2729 2539	GCLC, GCL, GCS, GLCL, GLCLC G6PD, G6PD1
Steroid biosynthesis	1	20	0.4760527221	0.999932	ENSG00000052802	hsa:6307	6307 MSMO1, DESP4, ERG25, SC4MOL	
One carbon pool by folate	1	20	0.4760527221	0.999932	ENSG00000136010	hsa:160428	160428 ALDH12, mtFDH	
Glutamatergic synapse	4	116	0.4947431424	0.999932	ENSG00000182621 ENSG00000150995 ENSG00000174233 ENSG00000154229	hsa:23236 hsa:3708 hsa:112 hsa:5578	23236 3708 112 5578	PLCB1, EIEE12, PI-PLC, PLC-154, PLC-I, PLC154, PLCB1A, PLCB1B ITPR1, ACV, CLA4, INSP3R1, IP3R, IP3R1, PPP1R9A, SCA1S, SCA16, SCA29 ADCY6, AC6 PRKCA, AAG6, PKC-alpha, PKCA, PRKACA
Leukocyte transendothelial migration	4	118	0.5076769746	0.999932	ENSG00000101335 ENSG00000162692 ENSG00000154229 ENSG00000072110	hsa:10398 hsa:7412 hsa:5578 hsa:87	10398 7412 5578 87	MYL9, LC20, MLC-2C, MLC2, MRLC1, MYRL2 VCAM1, CD106, INCAM-100 PRKCA, AAG6, PKC-alpha, PKCA, PRKACA ACTN1, BDPLT15
Progesterone-mediated oocyte maturation	3	86	0.5084531494	0.999932	ENSG00000140443 ENSG00000174233 ENSG00000071242	hsa:3480 hsa:112 hsa:6196	3480 112 6196	IGF1R, CD221, IGFIR, IGFR, ITK13 ADCY6, AC6 RPS6KA2, HU-2, MAPKAPK1C, RSK, RSK3, S6K-alpha, S6K-alpha2, p90-RSK3, pp90RSK3
Glycerolipid metabolism	2	55	0.5187770502	0.999932	ENSG00000137124 ENSG00000157680	hsa:219 hsa:9162	219 9162	ALDH1B1, ALDH5, ALDHX DGKI, DGK-IOTA
Neurotrophin signaling pathway	4	120	0.5204602279	0.999932	ENSG00000107263 ENSG00000109458 ENSG00000071242 ENSG00000134243	hsa:2889 hsa:2549 hsa:6196 hsa:6272	2889 2549 6196 6272	RAPGEF1, C3G, GRF2 GAB1 RPS6KA2, HU-2, MAPKAPK1C, RSK, RSK3, S6K-alpha, S6K-alpha2, p90-RSK3, pp90RSK3 SORT1, Gp95, LDLCQ8, NT3
Toxoplasmosis	4	120	0.5204602279	0.999932	ENSG00000115415 ENSG00000130702 ENSG00000196569 ENSG00000092969	hsa:6772 hsa:3911 hsa:3908 hsa:7042	6772 3911 3908 7042	STAT1, CANDF7, ISGF-3, STAT91 LAMA5 LAMA2, LAMM TGFB2, LDS4, TGF-beta2
Fatty acid elongation	1	23	0.5222881316	0.999932	ENSG00000206527	hsa:201562	201562 PTPLB, HACD2	
Histidine metabolism	1	23	0.5222881316	0.999932	ENSG00000137124	hsa:219	219 ALDH1B1, ALDH5, ALDHX	
Proximal tubule bicarbonate reclamation	1	23	0.5222881316	0.999932	ENSG00000080493	hsa:8671	8671 SLC4A4, HNBC1, KNBC, NBC1, NBC2, NBCe1-A, SLC4A5, hNNMC, pNBC	
Starch and sucrose metabolism	2	56	0.5281329171	0.999932	ENSG00000079739 ENSG00000114480	hsa:5236 hsa:2632	5236 2632	PGM1, CDG1T, GSD14 GBE1, APBD, GBE, GSD4
Non-small cell lung cancer	2	56	0.5281329171	0.999932	ENSG00000105810 ENSG00000154229	hsa:1021 hsa:5578	1021 5578	CDK6, PLSTIRE PRKCA, AAG6, PKC-alpha, PKCA, PRKACA
Dorso-ventral axis formation	1	24	0.5367597184	0.999932	ENSG00000139083	hsa:2120	2120 ETV6, TEL, TEL/ABL	
Steroid hormone biosynthesis	2	57	0.5373613948	0.999932	ENSG00000138061 ENSG00000109193	hsa:1545 hsa:6783	1545 6783	CYP1B1, CP1B, CYPIB1, GLC3A, P450181 SULT1E1, EST, EST-1, ST1E1, STE
GABAergic synapse	3	90	0.5381041242	0.999932	ENSG00000183044 ENSG00000174233 ENSG00000154229	hsa:18 hsa:112 hsa:5578	18 112 5578	ABAT, GABA-AT, GABAT, NPD009 ADCY6, AC6 PRKCA, AAG6, PKC-alpha, PKCA, PRKACA
Chemokine signaling pathway	6	189	0.5423108296	0.999932	ENSG00000115415 ENSG00000172156 ENSG00000108691 ENSG00000006210 ENSG00000174233 ENSG00000182621	hsa:6772 hsa:6356 hsa:6347 hsa:6376 hsa:112 hsa:23236	6772 6356 6347 6376 112 23236	STAT1, CANDF7, ISGF-3, STAT91 CCL11, SCYA11 CCL2, GDCF-2, HC11, HSMCR30, MCAF, MCP-1, MCP1, SCYA2, SMC-CF CX3CL1, ABCD-3, C3Xkine, CXC3, CXC3C, NTN, NTT, SCYD1, fractalkine, neurotactin ADCY6, AC6 PLCB1, EIE PLC-154, PLC-I, PLC154, PLCB1A, PLCB1B
Glycosylphosphatidylinositol(GPI)-anchor biosynthesis	1	25	0.5508249991	0.999932	ENSG00000174227	hsa:54872	54872 PIGG, GPI7, LAS21, PRO4405, RLGS1930	
Morphine addiction	3	93	0.5596573207	0.999932	ENSG00000174233 ENSG00000154229 ENSG00000154678	hsa:112 hsa:5578 hsa:5137	112 5578 5137	ADCY6, AC6 PRKCA, AAG6, PKC-alpha, PKCA, PRKACA PDE1C, Hcam3, cam-PDE_1C, hCam-3
mTOR signaling pathway	2	60	0.5642965388	0.999932	ENSG00000154229 ENSG00000071242	hsa:5578 hsa:6196	5578 6196	PRKCA, AAG6, PKC-alpha, PKCA, PRKACA RPS6KA2, HU-2, MAPKAPK1C, RSK, RSK3, S6K-alpha, S6K-alpha2, p90-RSK3, pp90RSK3
Viral myocarditis	2	60	0.5642965388	0.999932	ENSG00000196569 ENSG00000198947	hsa:3908 hsa:1756	3908 1756	LAMA2, LAMM DMD, BMD, CMD3B, DXS142, DXS164, DXS206, DXS230, DXS239, DXS26B, DXS269, DXS270, DXS272, MRX85
Butanoate metabolism	1	26	0.5644484948	0.999932	ENSG00000183044	hsa:18	18 ABAT, GABA-AT, GABAT, NPD009	
HTLV-I infection	8	261	0.5710786698	0.999932	ENSG00000147883 ENSG00000115729 ENSG00000106799 ENSG00000092969 ENSG00000158186 ENSG00000162692 ENSG00000174233 ENSG00000112658	hsa:1030 hsa:291 hsa:7046 hsa:7042 hsa:22808 hsa:7412 hsa:112 hsa:6722	1030 291 7046 7042 22808 7412 112 6722	CDKN2B, CDK4I, INK4B, MTS2, P15, TP15, p15INK4b SLC25A4, 1, AAC1, ANT, ANT_1, ANT1, MTDPS12, PEO2, PEO3, T1 TGFBR1, AAT5, ACVRLK4, ALK-5, ALK5, ESS1, LDS1, LDS1A, LDS2A, MSSE, SKR4, TGFR-1 TGFB2, LDS4, TGF-b RAs, R-RAS3, RRAS3 VCAM1, CD106, INCAM-100 ADCY6, AC6 SRF, MCM1
VEGF signaling pathway	2	61	0.5730289647	0.999932	ENSG00000106211 ENSG00000154229	hsa:3315 hsa:5578	3315 5578	HSPB1, CMT2F, HEL-S-102, HMN28, HS.76067, HSP27, HSP28, Hsp25, SRP27 PRKCA, AAG6, PKC-alpha, PKCA, PRKACA
Ascorbate and aldarate metabolism	1	27	0.5776593122	0.999932	ENSG00000137124	hsa:219	219 ALDH1B1, ALDH5, ALDHX	
Colorectal cancer	2	62	0.5816173924	0.999932	ENSG00000106799 ENSG00000092969	hsa:7046 hsa:7042	7046 7042	TGFBR1, AAT5, ACVRLK4, ALK-5, ALK5, ESS1, LDS1, LDS1A, LDS2A, MSSE, SKR4, TGFR-1 TGFB2, LDS4, TGF-beta2
Osteoclast differentiation	4	131	0.5877272175	0.999932	ENSG00000115415 ENSG00000106799 ENSG00000092969 ENSG00000164761	hsa:6772 hsa:7046 hsa:7042 hsa:4982	6772 7046 7042 4982	STAT1, CANDF7, ISGF-3, STAT91 TGFBR1, AAT5, ACVRLK4, ALK-5, ALK5, ESS1, LDS1, LDS1A, LDS2A, MSSE, SKR4, TGFR-1 TGFB2, LDS4, TGF-beta2 TNFRSF11B, OCIF, OPG, TR1
Dopaminergic synapse	4	131	0.5877272175	0.999932	ENSG00000150995 ENSG00000182621 ENSG00000146592 ENSG00000154229	hsa:3708 hsa:23236 hsa:9586 hsa:5578	3708 23236 9586 5578	ITPR1, ACV, CLA4, INSP3R1, IP3R, IP3R1, PPP1R9A, SCA1S, SCA16, SCA29 PLCB1, EIEE12, PI-PLC, PLC-154, PLC-I, PLC154, PLCB1A, PLCB1B CREB5, CRE-BPA PRKCA, AAG6, PKC-alpha, PKCA, PRKACA
Nicotinate and nicotinamide metabolism	1	28	0.5904699548	0.999932	ENSG00000166741	hsa:4837	4837 NNMT	
Propanoate metabolism	1	28	0.5904699548	0.999932	ENSG00000183044	hsa:18	18 ABAT, GABA-AT, GABAT, NPD009	
Melanogenesis	3	101	0.6140525957	0.999932	ENSG00000182621 ENSG00000174233 ENSG00000154229	hsa:23236 hsa:112 hsa:5578	23236 112 5578	PLCB1, EIEE12, PI-PLC, PLC-154, PLC-I, PLC154, PLCB1A, PLCB1B ADCY6, AC6 PRKCA, AAG6, PKC-alpha, PKCA, PRKACA
Glycolysis / Gluconeogenesis	2	66	0.6147234858	0.999932	ENSG00000079739 ENSG00000137124	hsa:5236 hsa:219	5236 219	PGM1, CDG1T, GSD14 ALDH1B1, ALDH5, ALDHX
Inflammatory bowel disease (IBD)	2	67	0.6226718673	0.999932	ENSG00000115415 ENSG00000092969	hsa:6772 hsa:7042	6772 7042	STAT1, CANDF7, ISGF-3, STAT91 TGFB2, LDS4, TGF-beta2
Galactose metabolism	1	31	0.6266203542	0.999932	ENSG00000079739	hsa:5236	5236 PGM1, CDG1T, GSD14	
Amphetamine addiction	2	68	0.6305053148	0.999932	ENSG00000146592 ENSG00000154229	hsa:9586 hsa:5578	9586 5578	CREB5, CRE-BPA PRKCA, AAG6, PKC-alpha, PKCA, PRKACA
Asthma	1	32	0.6379474117	0.999932	ENSG00000172156	hsa:6356	6356 CCL11, SCYA11	
Purine metabolism	5	176	0.6444023854	0.999932	ENSG00000079739 ENSG00000174233 ENSG00000147224 ENSG00000152402 ENSG00000154678	hsa:5236 hsa:112 hsa:5634 hsa:2977 hsa:5137	5236 112 5634 2977 5137	PGM1, CDG1T, GSD14 ADCY6, AC6 PRPS2, PRSII GUCY1A2, GC-SA2, GUC1A2 PDE1C, Hcam3, cam-PDE_1C, hCam-3
HIF-1 signaling pathway	3	106	0.6456675713	0.999932	ENSG00000171105 ENSG00000140443 ENSG00000154229	hsa:3643 hsa:3480 hsa:5578	3643 3480 5578	INSR, CD220, HHF5 IGF1R, CD221, IGFIR, IGFR, ITK13 PRKCA, AAG6, PKC-alpha, PKCA, PRKACA
Melanoma	2	71	0.6532286415	0.999932	ENSG00000105810 ENSG00000140443	hsa:1021 hsa:3480	1021 3480	CDK6, PLSTIRE IGF1R, CD221, IGFIR, IGFR, ITK13
Endocytosis	6	213	0.6548805405	0.999932	ENSG00000170248 ENSG00000153317 ENSG00000088280 ENSG00000106799 ENSG00000092969 ENSG00000140443	hsa:10015 hsa:50807 hsa:55616 hsa:7046 hsa:7042 hsa:3480	10015 50807 55616 7046 7042 3480	PDCD6IP, AIP1, ALIX, DRIP4, HP95 ASAP1, AMAP1, CENTB4, DDEF1, PAG2, PAP, ZG14P ASAP3, ACAP4, CENTB6, DDEFL1, UPLC1 TGFBR1, AAT5, ACVRLK4, ALK-5, ALK5, ESS1, LDS1, LDS1A, LDS2A, MSSE, SKR4, TGFR-1 TGFB2, LDS
Transcriptional misregulation in cancer	5	179	0.6586201401	0.999932	ENSG00000146674 ENSG00000148516 ENSG00000139083 ENSG00000140443 ENSG00000176046	hsa:3486 hsa:6935 hsa:2120 hsa:3480 hsa:26471	3486 6935 2120 3480 26471	IGF1R, CD221, IGFIR, IGFR, ITK13 IGFBP3, BP-53, IBP3 ZEB1, AREB6, BZP, DELTAEF1, FECD6, NIL2A, PPCD3, TCF8, ZFHEP, ZFHX1A ETV6, TEL, TEL/ABL IGF1R, CD221, IGFIR, IGFR, ITK13 NUPR1, COM1, P8
SNARE interactions in vesicular transport	1	34	0.6595829544	0.999932	ENSG00000151532	hsa:143187	143187 VTI1A, MMDS3, Mvb1, VTI1RP2, Vti-rp2	
Bile secretion	2	72	0.6605513239	0.999932	ENSG00000080493 ENSG00000174233	hsa:8671 hsa:112	8671 112	SLC4A4, HNBC1, KNBC, NBC1, NBC2, NBCe1-A, SLC4A5, hNNMC, pNBC ADCY6, AC6
Leishmaniasis	2	74	0.6748235787	0.999932	ENSG00000115415 ENSG00000092969	hsa:6772 hsa:7042	6772 7042	STAT1, CANDF7, ISGF-3, STAT91 TGFB2, LDS4, TGF-beta2
Pentose and glucuronate interconversions	1	36	0.6799272294	0.999932	ENSG00000137124	hsa:219	219 ALDH1B1, ALDH5, ALDHX	

Bacterial invasion of epithelial cells	2	76	0.68860407843 1	0.999932 625528	ENSG00000109458 ENSG00000150760	hsa:2549 hsa:1793	2549 1793	GAB1 DOCK1, DOCK180, ced5
Serotonergic synapse	3	114	0.69234250605 1	0.999932 625528	ENSG00000182621 ENSG00000150995 ENSG00000154229	hsa:23236 hsa:3708 hsa:5578	23236 3708 5578	PLCB1, EIEE12, PI-PLC, PLC-154, PLC-I, PLC154, PLCB1A, PLCB1B ITPR1, ACV, CLA4, INSP3R1, IP3R, IP3R1, PPP1R94, SCA15, SCA16, SCA29 PRKCA, AAG6, PKC-alpha, PKCA, PRKACA
Bladder cancer	1	38	0.69905718744 4	0.999932 625528	ENSG00000196730	hsa:1612	1612 DAPK1, DAPK	
Phagosome	4	155	0.71349114957 7	0.999932 625528	ENSG00000186340 ENSG00000117758 ENSG00000169231 ENSG00000138448	hsa:7058 hsa:23673 hsa:7059 hsa:3685	7058 23673 7059 3685	THBS2, TSP2 STX12, STX13, STX14 THBS3, TSP3 ITGAV, CD51, MSK8, VNRA, VTNR
Ras signaling pathway	6	228	0.71584197188 7	0.999932 625528	ENSG00000172575 ENSG00000171105 ENSG00000158186 ENSG00000140443 ENSG00000109458 ENSG00000154229	hsa:10125 hsa:3643 hsa:22808 hsa:3480 hsa:2549 hsa:5578	10125 3643 22808 3480 2549 5578	RASGRP1, CALDAG-GEFI, CALDAG-GEFII, RASGRP, V, hRasGRP1 INSR, CD220, HHF5 MRAS, M-RAs, R-RAS3, RRAS3 IGF1R, CD221, IGFIR, IGFR, JTK13 GAB1 PRKCA, AAG6, PKC-alpha, PKCA, PRKACA
Glycine, serine and threonine metabolism	1	40	0.71704523594 3	0.999932 625528	ENSG00000135069	hsa:29968	29968 PSAT1, EPIP, PSA, PSAT	
Cell cycle	3	124	0.74397135557 4	0.999932 625528	ENSG00000105810 ENSG00000092969 ENSG00000147883	hsa:1021 hsa:7042 hsa:1030	1021 7042 1030	CDK6, PLSTIRE TGFB2, LDS4, TGF-beta2 CDKN2B, CDK4I, INK4B, MTS2, P15, TP15, p15INK4b
Salmonella infection	2	86	0.75042851697 6	0.999932 625528	ENSG00000133026 ENSG00000100345	hsa:4628 hsa:4627	4628 4627	MYH10, NMMHC-IIB, NMMHCB MYH9, BDPLT6, DFNA17, EPST5, FTNS, MHA, NMHC-II-A, NMMHC-IIA, NMMHCA
ErbB signaling pathway	2	87	0.75599116925 2	0.999932 625528	ENSG00000109458 ENSG00000154229	hsa:2549 hsa:5578	2549 5578	GAB1 PRKCA, AAG6, PKC-alpha, PKCA, PRKACA
Prostate cancer	2	89	0.76679566438 9	0.999932 625528	ENSG00000140443 ENSG00000146592	hsa:3480 hsa:9586	3480 9586	IGF1R, CD221, IGFIR, IGFR, JTK13 CREBS, CRE-BPA
Amino sugar and nucleotide sugar metabolism	1	47	0.77195776837 1	0.999932 625528	ENSG00000079739	hsa:5236	5236 PGM1, CDG1T, GSD14	
Rheumatoid arthritis	2	91	0.77718175943 8	0.999932 625528	ENSG00000108691 ENSG00000092969	hsa:6347 hsa:7042	6347 7042	CCL2, GDCF-2, HC11, HSMCR30, MCAF, MCP-1, MCP1, SCYA2, SMC-CF TGFB2, LDS4, TGF-beta2
NF-kappa B signaling pathway	2	91	0.77718175943 8	0.999932 625528	ENSG00000082512 ENSG00000162692	hsa:7188 hsa:7412	7188 7412	TRAF5, MGC:39780, RNF84 VCAM1, CD106, INCAM-100
Notch signaling pathway	1	48	0.77888046246 9	0.999932 625528	ENSG00000101384	hsa:182	182 JAG1, AGS, AHD, AWS, CD339, HJ1, JAGL1	
Type II diabetes mellitus	1	48	0.77888046246 9	0.999932 625528	ENSG00000171105	hsa:3643	3643 INSR, CD220, HHF5	
N-Glycan biosynthesis	1	49	0.78559327592 6	0.999932 625528	ENSG00000112893	hsa:4124	4124 MAN2A1, AMan_II, GOLIM7, MANA2, MANII	
Cocaine addiction	1	50	0.79210256360 5	0.999932 625528	ENSG00000146592	hsa:9586	9586 CREBS, CRE-BPA	
Lysine degradation	1	51	0.79841448820 4	0.999932 625528	ENSG00000137124	hsa:219	219 ALDH1B1, ALDH5, ALDHX	
Influenza A	4	177	0.80185743033 4	0.999932 625528	ENSG00000115415 ENSG00000154229 ENSG00000102580 ENSG00000108691	hsa:6772 hsa:5578 hsa:5611 hsa:6347	6772 5578 5611 6347	STAT1, CANDF7, ISGF-3, STAT91 PRKCA, AAG6, PKC-alpha, PKCA, PRKACA DNAIC3, ERdj6, HPS8, P58, P58IPK, PRKRI CCL2, GDCF-2, HC11, HSMCR30, MCAF, MCP-1, MCP1, SCYA2, SMC-CF
Taste transduction	1	53	0.81046097277 1	0.999932 625528	ENSG00000174233	hsa:112	112 ADCY6, AC6	
Insulin signaling pathway	3	141	0.81562388048 7	0.999932 625528	ENSG00000171105 ENSG00000107263 ENSG00000119938	hsa:3643 hsa:2889 hsa:5507	3643 2889 5507	INSR, CD220, HHF5 RAPGEF1, C3G, GRF2 PPP1R3C, PPP1R5
Vibrio cholerae infection	1	54	0.81622494866 5	0.999932 625528	ENSG00000154229	hsa:5578	5578 PRKCA, AAG6, PKC-alpha, PKCA, PRKACA	
Huntington's disease	4	183	0.82172429629 6	0.999932 625528	ENSG00000150995 ENSG00000182621 ENSG00000146592 ENSG00000151729	hsa:3708 hsa:23236 hsa:9586 hsa:291	3708 23236 9586 291	ITPR1, ACV, CLA4, INSP3R1, IP3R, IP3R1, PPP1R94, SCA15, SCA16, SCA29 PLCB1, EIEE12, PI-PLC, PLC-154, PLC-I, PLC154, PLCB1A, PLCB1B CREBS, CRE-BPA SLC25A4, 1, AAC1, ANT, ANT_1, ANT1, MTDPS12, PEO2, PEO3, T1
Pathogenic Escherichia coli infection	1	55	0.82180540408 8	0.999932 625528	ENSG00000154229	hsa:5578	5578 PRKCA, AAG6, PKC-alpha, PKCA, PRKACA	
Parkinson's disease	3	143	0.82282191176 3	0.999932 625528	ENSG00000184702 ENSG00000182179 ENSG00000151729	hsa:5413 hsa:7318 hsa:291	5413 7318 291	SEPT5, CDCREL, CDCREL-1, CDCREL1, HS, HCDCREL-1, PNUTL1 UBA7, D8, UBA1B, UBE1L, UBE2 SLC25A4, 1, AAC1, ANT, ANT_1, ANT1, MTDPS12, PEO2, PEO3, T1
Staphylococcus aureus infection	1	57	0.83246373563 7	0.999932 625528	ENSG00000000971	hsa:3075	3075 CFH, AHUS1, AMBP1, ARMD4, ARMS1, CFHL3, FH, FHL1, HF, HF1, HF2, HUS	
NOD-like receptor signaling pathway	1	57	0.83246373563 7	0.999932 625528	ENSG00000108691	hsa:6347	6347 CCL2, GDCF-2, HC11, HSMCR30, MCAF, MCP-1, MCP1, SCYA2, SMC-CF	
Shigellosis	1	61	0.85190827019 6	0.999932 625528	ENSG00000150760	hsa:1793	1793 DOCK1, DOCK180, ced5	
Arachidonic acid metabolism	1	62	0.85460645364 3	0.999932 625528	ENSG00000124212	hsa:5740	5740 PTGIS, CYP8, CYP8A1, PGIS, PTGI	
Synaptic vesicle cycle	1	63	0.86076818477 4	0.999932 625528	ENSG00000105402	hsa:8775	8775 NAPA, SNAPA	
cAMP signaling pathway	4	200	0.86923076674 2	0.999932 625528	ENSG00000077157 ENSG00000174233 ENSG00000146592 ENSG00000101335	hsa:4659 hsa:112 hsa:9586 hsa:10398	4659 112 9586 10398	PPP1R12A, M130, MBS, MYPT1 ADCY6, AC6 CREBS, CRE-BPA MYL9, LC20, MLC-2C, MLC2, MRLC1, MYRL2
Aminoacyl-tRNA biosynthesis	1	66	0.87307538178 7	0.999932 625528	ENSG00000140105	hsa:7453	7453 WARS, GAMMA-2, IFI53, IFP53	
Complement and coagulation cascades	1	69	0.88429602510 5	0.999932 625528	ENSG00000000971	hsa:3075	3075 CFH, AHUS1, AMBP1, ARMD4, ARMS1, CFHL3, FH, FHL1, HF, HF1, HF2, HUS	
Adipocytokine signaling pathway	1	70	0.88781159352 8	0.999932 625528	ENSG00000110090	hsa:1374	1374 CPT1A, CPT1, CPT1-L, L-CPT1	
Fc epsilon RI signaling pathway	1	70	0.88781159352 8	0.999932 625528	ENSG00000154229	hsa:5578	5578 PRKCA, AAG6, PKC-alpha, PKCA, PRKACA	
RIG-I-like receptor signaling pathway	1	70	0.88781159352 8	0.999932 625528	ENSG00000187608	hsa:9636	9636 ISG15, G1P2, IFI15, IP17, UCRP, hUCRP	
Lysosome	2	122	0.89318441409 4	0.999932 625528	ENSG00000100600 ENSG00000134243	hsa:5641 hsa:6272	5641 6272	LGMN, AEP, LGMN1, PRSC1 SORT1, Gp95, LDLCQ6, NT3
Prolactin signaling pathway	1	72	0.89452592539	0.999932 625528	ENSG00000115415	hsa:6772	6772 STAT1, CANDF7, ISGF-3, STAT91	
MicroRNAs in cancer	6	297	0.89981629964 8	0.999932 625528	ENSG00000105810 ENSG00000138061 ENSG00000092969 ENSG00000156103 ENSG00000148516 ENSG00000154229	hsa:1021 hsa:1545 hsa:7042 hsa:4325 hsa:6935 hsa:5578	1021 1545 7042 4325 6935 5578	CDK6, PLSTIRE CYP1B1, CP1B, CYPIB1, GLC3A, P4501B1 TGFB2, LDS4, TGF-beta2 MMP16, C8orf57, MMP-X2, MT-MMP2, MT-MMP3, MT3-MMP ZEB1, AREB6, BZP, DELTAEF1, FECD6, NIL2A, PPCD3, TCF8, ZFHEP, ZFHX1A PRKCA alpha, PKCA, PRKACA
Metabolism of xenobiotics by cytochrome P450	1	74	0.90083891744 3	0.999932 625528	ENSG00000138061	hsa:1545	1545 CYP1B1, CP1B, CYPIB1, GLC3A, P4501B1	
Pertussis	1	75	0.90385245517	0.999932 625528	ENSG00000165410	hsa:1073	1073 CFL2, NEM7	
Antigen processing and presentation	1	79	0.91501927481 5	0.999932 625528	ENSG00000100600	hsa:5641	5641 LGMN, AEP, LGMN1, PRSC1	
Chemical carcinogenesis	1	80	0.91760239088 8	0.999932 625528	ENSG00000138061	hsa:1545	1545 CYP1B1, CP1B, CYPIB1, GLC3A, P4501B1	
Peroxisome	1	81	0.92002709093 8	0.999932 625528	ENSG00000100372	hsa:10478	10478 SLC25A17, PMP34	
Measles	2	134	0.92059839051 1	0.999932 625528	ENSG00000105810 ENSG00000115415	hsa:1021 hsa:6772	1021 6772	CDK6, PLSTIRE STAT1, CANDF7, ISGF-3, STAT91
Systemic lupus erythematosus	2	136	0.92446823124 7	0.999932 625528	ENSG00000246705 ENSG00000072110	hsa:55766 hsa:87	55766 87	H2AFJ, H2AJ ACTN1, BDPLT15
Ubiquitin mediated proteolysis	2	137	0.92633581637 7	0.999932 625528	ENSG00000186591 ENSG00000182179	hsa:7328 hsa:7318	7328 7318	UBE2H, E2-20K, GID3, UBC8, UBCH, UBCH2 UBA7, D8, UBA1B, UBE1L, UBE2
Ribosome biogenesis in eukaryotes	1	84	0.92717411120 6	0.999932 625528	ENSG00000076043	hsa:25996	25996 REXO2, REX2, RFN, SFN	
Herpes simplex infection	3	186	0.92841563008	0.999932 625528	ENSG00000082512 ENSG00000115415 ENSG00000108691	hsa:7188 hsa:6772 hsa:6347	7188 6772 6347	TRAF5, MGC:39780, RNF84 STAT1, CANDF7, ISGF-3, STAT91 CCL2, GDCF-2, HC11, HSMCR30, MCAF, MCP-1, MCP1, SCYA2, SMC-CF
mRNA surveillance pathway	1	91	0.94133027094 3	0.999932 625528	ENSG00000153944	hsa:124540	124540 MSI2, MSI2H	
Glycerophospholipid metabolism	1	92	0.94311449389 4	0.999932 625528	ENSG00000157680	hsa:9162	9162 DGKI, DGK-IOTA	
Epstein-Barr virus infection	3	202	0.94993983666 1	0.999932 625528	ENSG00000082512 ENSG00000106211 ENSG00000197157	hsa:7188 hsa:3315 hsa:27044	7188 3315 27044	TRAF5, MGC:39780, RNF84 HSPB1, CMT2F, HEL-S-102, HMN2B, HS.76067, HSP27, HSP28, Hsp25, SRP27 SND1, TDRD11, p100
Jak-STAT signaling pathway	2	156	0.95450945470 2	0.999932 625528	ENSG00000115415 ENSG00000145623	hsa:6772 hsa:3977	6772 3977	STAT1, CANDF7, ISGF-3, STAT91 LIFR, CD118, LIF-R, SIS2, STWS, SWS
T cell receptor signaling pathway	1	104	0.96073469310 8	0.999932 625528	ENSG00000172575	hsa:10125	10125 RASGRP1, CALDAG-GEFI, CALDAG-GEFII, RASGRP, V, hRasGRP1	
Toll-like receptor signaling pathway	1	106	0.96308786698 1	0.999932 625528	ENSG00000115415	hsa:6772	6772 STAT1, CANDF7, ISGF-3, STAT91	
Alzheimer's disease	2	168	0.96663388333 6	0.999932 625528	ENSG00000182621 ENSG00000150995	hsa:23236 hsa:3708	23236 3708	PLCB1, EIEE12, PI-PLC, PLC-154, PLC-I, PLC154, PLCB1A, PLCB1B ITPR1, ACV, CLA4, INSP3R1, IP3R, IP3R1, PPP1R94, SCA15, SCA16, SCA29
Protein processing in endoplasmic reticulum	2	168	0.96663388333 6	0.999932 625528	ENSG00000102580 ENSG00000120725	hsa:5611 hsa:64374	5611 64374	DNAIC3, ERdj6, HPS8, P58, P58IPK, PRKRI SIL1, BAP, MSS, ULG5
Metabolic pathways	27	1213	0.97463189925 9	0.999932 625528	ENSG00000147224 ENSG00000206527 ENSG00000068383 ENSG00000130707 ENSG00000157680 ENSG00000166741 ENSG00000110328 ENSG00000079739 ENSG00000159267 ENSG00000160211 ENSG00000176928 ENSG00000198108 ENSG00000143641 ENSG00000135069 ENSG00000065833 ENSG00000182197 ENSG00000124212 ENSG00000183044 ENSG00000112893 ENSG00000164574 ENSG00000182621 ENSG00000052802 ENSG00000158008 ENSG00000070669 ENSG00000001084 ENSG00000114480 ENSG00000137124	hsa:5634 hsa:201562 hsa:3632 hsa:445 hsa:9162 hsa:4837 hsa:374378 hsa:5236 hsa:3141 hsa:2539 hsa:51301 hsa:337876 hsa:2590 hsa:29968 hsa:4199 hsa:2131 hsa:5740 hsa:18 hsa:4124 hsa:55568 hsa:23236 hsa:6307 hsa:2134 hsa:440 hsa:2729 hsa:2632 hsa:219	5634 201562 3632 445 9162 4837 374378 5236 3141 2539 51301 337876 2590 29968 4199 2131 5740 18 4124 55568 23236 6307 2134 440 2729 2632 219	PRPS2, PRSI PTPLB, HACD2 INPP5A, SPTASE AS51, AS5, CTLN1 DGKI, DGK-IOTA NNMT GALNT18, GALNACT18, GALNT15, GALNT4, GalNAc-T15, GalNAc-T18 PGM1, CDG1T, GSD14 HLC5, HCS G6PD, G6PD1 GCNT4, C2GNT3 CHS CSS3 GALNT2, GalNAc-T2 PSAT1, EPIP, PSA, PSAT ME1, HUMNDME, MES EXT1, EXT, LGCR, LGS, TRPS2, TTV PTGIS, CYP8, CYP8A1, PGIS, PTGI ABAT, GABA-AT, GABAT, NPD009 MAN2A1, AMan_II, GOLIM7, MANA2, MANII GALN GALNACT10, PPGALNACT10, PPGALNTASE10 PLCB1, EIEE12, PI-PLC, PLC-154, PLC-I, PLC154, PLCB1A, PLCB1B MSMO1, DESP4, ERG25, SC4MOL EXTL1, EXTL ASNS, ASNS0, TS11 GCLC, GCL, GCS, GLCI, GLCLC GBE1, APBD, GBE, GI ALDH5, ALDHX
Tuberculosis	2	179	0.97496852884 5	0.999932 625528	ENSG00000115415 ENSG00000092969	hsa:6772 hsa:7042	6772 7042	STAT1, CANDF7, ISGF-3, STAT91 TGFB2, LDS4, TGF-beta2
Alcoholism	2	180	0.97561765178	0.999932 625528	ENSG00000246705 ENSG00000146592	hsa:55766 hsa:9586	55766 9586	H2AFJ, H2AJ CREBS, CRE-BPA
Hepatitis C	1	133	0.98398178287 6	0.999932 625528	ENSG00000115415	hsa:6772	6772 STAT1, CANDF7, ISGF-3, STAT91	
Natural killer cell mediated cytotoxicity	1	134	0.98446974987 6	0.999932 625528	ENSG00000154229	hsa:5578	5578 PRKCA, AAG6, PKC-alpha, PKCA, PRKACA	
Non-alcoholic fatty liver disease (NAFLD)	1	151	0.99082330798 2	0.999954 288201	ENSG00000171105	hsa:3643	3643 INSR, CD220, HHF5	
Neuroactive ligand-receptor interaction	1	275	0.99980449255 9	0.999954 288201	ENSG00000151090	hsa:7068	7068 THRB, C-ERBA-2, C-ERBA-BETA, ERBA2, GRTH, NR1A2, PRTH, THR1, THRB1, THRB2	
Olfactory transduction	2	405	0.99995428820 1	0.999954 288201	ENSG00000154678 ENSG00000180785	hsa:5137 hsa:143503	5137 143503	PDE1C, Hcam3, cam-PDE_1C, hCam-3 OR51E1, D-GPCR, DGPCR, GPR136, GPR164, OR51E1P, OR52A3P, POGR, PSGR2